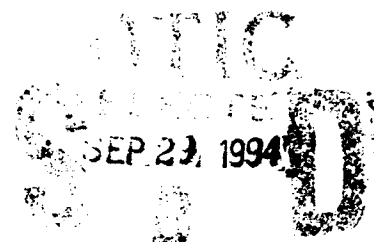# NAVAL POSTGRADUATE SCHOOL
Monterey, California

THESIS

SEP 21 1994

PERFORMANCE OF A FAST FREQUENCY-HOPPED
NONCOHERENT MFSK RECEIVER WITH NON-IDEAL NOISE
NORMALIZATION COMBINING OVER RICEAN FADING
CHANNELS WITH PARTIAL-BAND INTERFERENCE

by

Hidetoshi Iwasaki

September 1994

Thesis Advisor: R. Clark Robertson

Approved for public release; distribution is unlimited.

94 9 28 115

REPORT DOCUMENTATION PAGE

1.AGENCY USE ONLY *(Leave blank)*	2.REPORT DATE September 1994	3.REPORT TYPE AND DATES COVERED Master's Thesis

4.TITLE AND SUBTITLE
PERFORMANCE OF A FAST FREQUENCY-HOPPED NONCOHERENT MFSK RECEIVER WITH NON-IDEAL NOISE NORMALIZATION COMBINING OVER RICEAN FADING CHANNELS WITH PARTIAL-BAND INTERFERENCE

5.FUNDING NUMBERS

6.AUTHOR(S)
Iwasaki, Hidetoshi

7.PERFORMING ORGANIZATION NAME(S) AND ADDRESS(ES)
Naval Postgraduate School
Monterey CA 93943-5000

8.PERFORMING ORGANIZATION REPORT NUMBER

9.SPONSORING/MONITORING AGENCY NAME(S) AND ADDRESS(ES)

10.SPONSORING/MONITORING AGENCY REPORT NUMBER

11.SUPPLEMENTARY NOTES
The views expressed in this thesis are those of the author and do not reflect the official policy or position of the Department of Defense or the U.S. Government.

12a.DISTRIBUTION/AVAILABILITY STATEMENT
Approved for public release; distribution is unlimited.

12b. DISTRIBUTION CODE

A

13.ABSTRACT *(maximum 200 words)*

An error probability analysis is performed for a noncoherent M-ary orthogonal frequency-shift keying (MFSK) communication system employing fast frequency-hopped (FFH) spread spectrum. The signal is assumed to be transmitted through a frequency-nonselective, slowly fading channel with partial-band interference. The partial-band interference is modeled as a Gaussian process. The noise-normalized receiver is employed to minimize partial-band interference effects, and the effect of inaccurate noise measurement on the ability of the noise-normalized receiver to reject partial-band interference is examined. Each diversity reception is assumed to fade independently according to a Ricean process. Thermal noise is also included in the analysis. It is found that diversity dramatically reduces the degradation due to partial-band interference, and noise measurement error does not significantly degrade receiver performance. The robustness of the receiver with regard to noise measurement error is independent of the strength of channel fading.

14. SUBJECT TERMS communications,noise-normalized receiver,spread spectrum,FFH,M-ary FSK	15.NUMBER OF PAGES 86
	16.PRICE CODE

17. SECURITY CLASSIFICATION OF REPORT Unclassified	18. SECURITY CLASSIFICATION OF THIS PAGE Unclassified	19.SECURITY CLASSIFICATION OF ABSTRACT Unclassified	20.LIMITATION OF ABSTRACT UL

DTIC QUALITY INSPECTED 3

i

PERFORMANCE OF A FAST FREQUENCY-HOPPED NONCOHERENT MFSK RECEIVER WITH NON-IDEAL NOISE NORMALIZATION COMBINING OVER RICEAN FADING CHANNELS WITH PARTIAL-BAND INTERFERENCE

by

Hidetoshi Iwasaki
Lieutenant, Japanese Navy
B.S., National Defense Academy, 1986

Submitted in partial fulfillment of the requirements for the
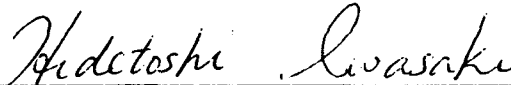degree of

MASTER OF SCIENCE IN ELECTRICAL ENGINEERING

MASTER OF SCIENCE IN SYSTEMS ENGINEERING

from the

NAVAL POSTGRADUATE SCHOOL
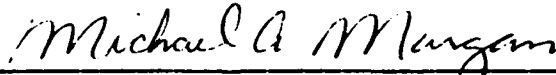September 1994

Author: _____

Hidetoshi Iwasaki

Approved by: _____

R. Clark Robertson, Thesis Advisor

_____

Donald v. Z. Wadsworth, Second Reader

_____

Michael A. Morgan, Chairman, Department of Electrical and
Computer Engineering

_____

Fred H. Levien, Chairman, Electronic Warfare Academic Group

ii

ABSTRACT

An error probability analysis is performed for a noncoherent M-ary orthogonal frequency-shift keying (MFSK) communication system employing fast frequency-hopped (FFH) spread spectrum. The signal is assumed to be transmitted through a frequency-nonselective, slowly fading channel with partial-band interference. The partial-band interference is modeled as a Gaussian process. The noise-normalized receiver is employed to minimize partial-band interference effects, and the effect of inaccurate noise measurement on the ability of the noise-normalized receiver to reject partial-band interference is examined. Each diversity reception is assumed to fade independently according to a Ricean process. Thermal noise is also included in the analysis. It is found that diversity dramatically reduces the degradation due to partial-band interference, and noise measurement error does not significantly degrade receiver performance. The robustness of the receiver with regard to noise measurement error is independent of the strength of channel fading.

iii

TABLE OF CONTENTS

LIST OF FIGURES

ACKNOWLEDGMENTS

I. INTRODUCTION

A. BACKGROUND

A spread spectrum system is a type of communication system that produces a signal with a bandwidth much wider than the message bandwidth. Spread spectrum systems are useful for secure communications since they can suppress the effect of intentional interference, make it difficult for an opponent to detect the transmitted waveform, extract the message, or jam the intended receiver. There are three major types of spread spectrum systems: direct-sequence, frequency-hopping, and time-hopping systems. Hybrids of such systems can also be obtained[1].

One of the applications of frequency-hopped spread spectrum signals is to reduce receiver performance degradation due to narrowband interference (either intentional or otherwise). A frequency-hopped spread spectrum system is one where each data symbol is transmitted at a different carrier frequency according to some apparently random pattern known only by the transmitter and receiver. The bandwidth of the frequency-hopped signal is generally much larger than the signal bandwidth in the absence of frequency-hopping. Consequently, in order to interfere with the entire spread spectrum band, given a fixed total interference power, the available noise power spectral density of the narrowband interference is reduced in comparison with that for a non-hopping signal. Rather than interfere simultaneously with the entire spread spectrum bandwidth, with the consequent reduction in noise power spectral density, the narrowband interference can be designed to affect only a portion of the total spread spectrum bandwidth at any one time. This portion can be shifted over the total spread spectrum bandwidth in

an apparently random manner. This is referred to as partial-band interference. In the case of partial-band interference, only some of the transmitted symbols will be affected by narrowband interference. In this case, receiver performance may be improved by implementing diversity in the form of fast frequency-hopping; that is, each information symbol is transmitted multiple times, and each transmission is at a different, apparently random, carrier frequency within the overall spread spectrum bandwidth.

B. OBJECTIVE

In this thesis, the performance of a fast frequency-hopped M-ary orthogonal frequency-shift keying system (FFH/MFSK) with noncoherent, non-ideal noise-normalized detection is investigated. The channel is modeled as a Ricean fading channel, and partial-band noise interference is assumed. The FFH/MFSK transmitter is assumed to perform L ($L \geq 1$) hops per data symbol where the noise normalization is a method of minimizing the effects of partial-band jamming. This system is described in Chapter II. An accurate measurement of the noise power present in each hop is a challenging problem in fast frequency-hopped spread spectrum systems. The performance of the FFH/MFSK noncoherent noise-normalized receiver in a Ricean fading channel with partial band jamming has been previously investigated [2]. In [2] the noise power is assumed to be estimated without error; hence, the performance obtained for the noise-normalized receiver is in this sense ideal. This thesis presents an evaluation of the effect of inaccurate measurement of jamming noise power at the receiver on the ability of the receiver to reject partial-band jamming. This is accomplished by introducing non-ideal noise normalization into the model.

II. DESCRIPTION OF SYSTEM

The fast frequency-hopped M-ary orthogonal frequency-shift keying (FFH/MFSK) transmitter is assumed to perform L hops per data symbol where L is an integer greater than one. This is equivalent to an L-fold frequency diversity. A block diagram of the FFH/MFSK receiver with noise-normalization combining is shown in Fig. 1. At the receiver the FFH signals are first dehopped. For eachM-ary signal waveform the dehopped signal is then quadratically detected. The detector demodulates the signal by means of two correlators in phase quadrature. The two correlator outputs are sampled every T seconds where T is the hop duration. Since the carrier phases are not recovered, the sampled outputs of each correlator pair are squared and summed to form L detector outputs, X_{1k} through X_{Mk}. These outputs are then divided by the noise normalization factor σ_k^2. Next, these L normalized diversity receptions, Z_{1k} through Z_{Mk}, are combined in each branch to form M decision statistics. These M outputs, Z_1 through Z_M, are then compared with each other, and the largest is chosen as the transmitted symbol. This problem was initially investigated for ideal noise-normalized MFSK demodulators in [2].

In this thesis, the previous work [2] is extended to include non-ideal noise normalization combining (also referred to as adaptive gain control) [4]-[5]. Noise normalization has the advantage of minimizing receiver performance degradation due to partial-band noise jamming. The goal of this thesis is to evaluate the effect of significant error in the noise power estimator on the noise-normalized receiver. This is an important problem since accurate, real-time noise estimation is difficult to implement for a FFH system.
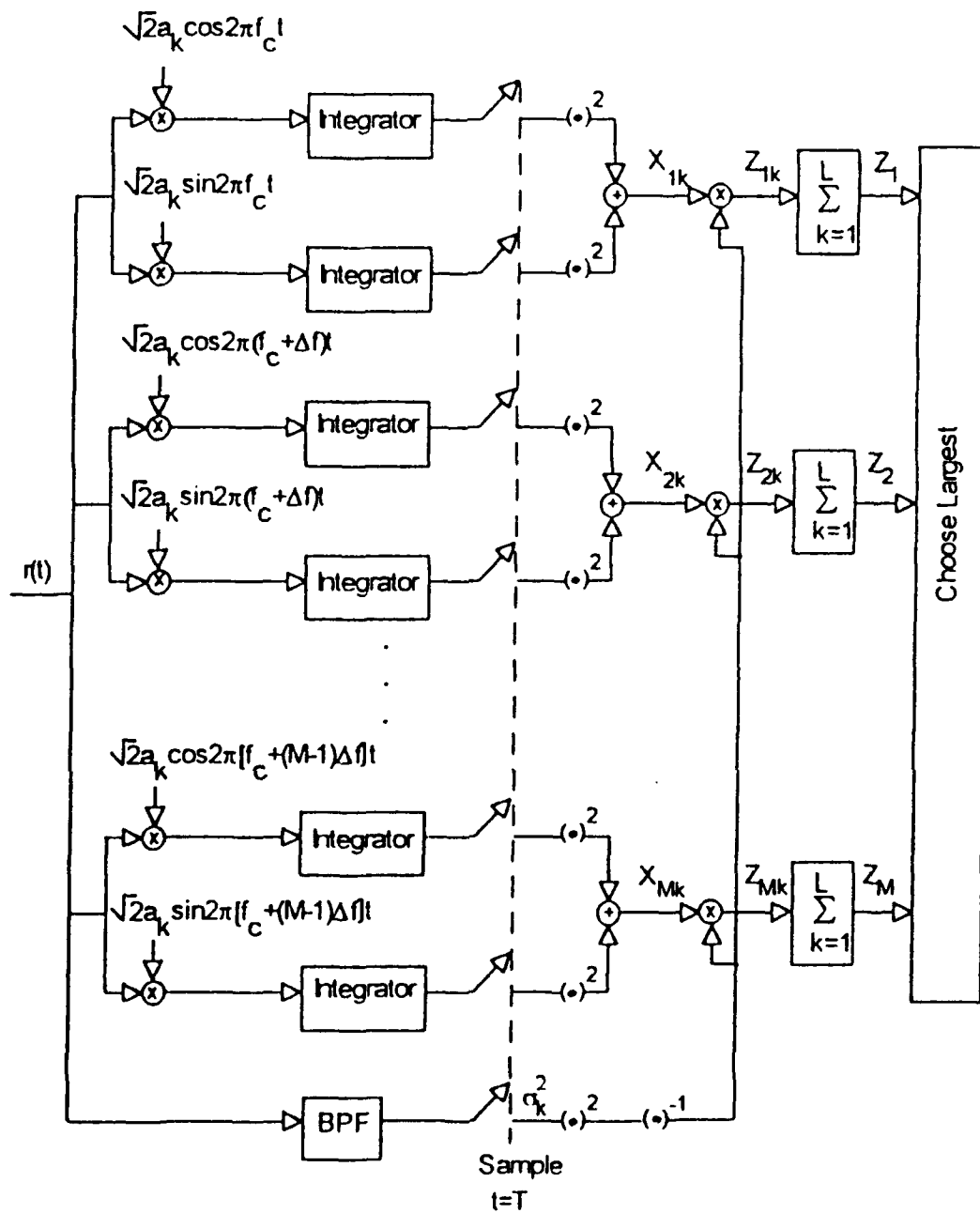
Figure 1. FFH/MFSK noise-normalized receiver

4

By modeling the fading channel as Ricean, in which the signal consists of a direct signal component and a diffuse signal component, a general result is obtained that is valid in the limit of large direct-to-diffuse signal power ratios for Gaussian channels and in the limit of small direct-to-diffuse signal power ratios for Rayleigh fading channels as well as the general case where the effects of both the direct and diffuse components of the signal must be included in the analysis. The effect of partial-band interference on communication systems was initially investigated for standard noncoherent MFSK demodulators in [3]; and the effect of both partial-band interference and channel fading on noise-normalized FFH/MFSK receiver has been investigated in [2].

Each dehopped signal is assumed to fade independently; that is, the smallest spacing between frequency hop slots is assumed to be larger than the coherence bandwidth of the channel [6]-[8]. The channel for each hop is also modeled as a frequency-nonselective, slowly fading Ricean process. Hence, the signal bandwidth is assumed to be much smaller than the coherence bandwidth of the channel and the hop duration is much smaller than the coherence time of the channel [6]-[7]. The latter assumption is equivalent to requiring the hop rate to be large compared to the Doppler spread of the channe1 As a result, the dehopped signal amplitude is a Ricean random variable, and the dehopped signal can be considered as the sum of two components, a nonfaded(direct) component and a Rayleigh-faded(diffuse) component.

The interference that is considered in this thesis is partial-band interference which may due to either a partial-band jammer or some unintended narrowband interference. The interference is modeled as additive Gaussian noise and is assumed to be present in each branch of the MFSK demodulator for any

5

reception of the dehopped signal with probability γ. Thus, γ represents the fraction of the spread bandwidth being jammed, and the probability that narrowband interference is not present in all M detectors is $1-\gamma$. If $N_I/2$ is the average power spectral density of interference over the entire spread bandwidth, then $\gamma^{-1}N_I/2$ is the power spectral density of partial-band interference when it is present. In addition to partial-band interference, the signal is also assumed to be corrupted by thermal noise and other wideband interferences which are modeled as additive white Gaussian noise. The wideband noise is assumed to be unaffected by the fading channel. The power spectral density of this wideband noise is defined as $N_0/2$. Thus, the power spectral density of the total noise is $\gamma^{-1}N_I/2 + N_0/2$ when interference is present and $N_0/2$ otherwise. If the equivalent noise bandwidth of each branch in the noise-normalized MFSK demodulator is B Hz, then for each hop the signal is received with noise of power N_0B with probability $1-\gamma$ when interference is not present and with noise of power $(\gamma^{-1}N_I + N_0)B$ with probability γ when interference is present in each branch of the MFSK demodulator.

The bit rate is designated R_b. Thus, the corresponding symbol rate is $R_s = R_b/\log_2 M$ where M is the order of the MFSK modulation. The MFSK signal is assumed to perform L hops per symbol where $L \geq 1$. Therefore, the hop rate is $R_h = LR_s$. Clearly, when $L = 1$ there is no diversity and noise normalization has no effect. The equivalent noise bandwidth of each branch in the noise-normalized MFSK demodulator must be at least as wide as the hop rate, and in this thesis is taken to be $B = R_h$. This is equivalent to noncoherent matched filter detection. Matched filter detection is optimum for AWGN (additive white Gaussian noise) but may not be for colored noise such as partial-band interference. The overall

system bandwidth is assumed to be very large compared to the hop rate. Note that for a fixed symbol rate that the hop rate increases as the number of the hops per symbol increases. As the result, the required minimum equivalent noise bandwidth of each branch of the MFSK demodulator also increases as the number of the hops per symbol increases. Hence, as the number of the hops per symbol increases, the assumption that the channel is frequency non-selective becomes more restrictive. On the other hand, the assumption that the channel is slowly fading becomes stronger. Obviously, for a fixed hop rate system, this is not a concern. Only fixed symbol rate systems are investigated in this thesis.

III. PERFORMANCE ANALYSIS

The performance of the noise-normalized receiver is evaluated in this thesis by obtaining the bit error probability versus the bit energy-to-interference density for the receiver in Fig. 1 given the model of the channel as Ricean. The analysis requires the statistics of the sampled outputs $x_{ik}, i = 1,2,...,M$ of the quadratic detectors for each hop k of a symbol as well as the normalized samples $z_{ik}, i = 1,2,...,M$ that are combined to provide the decision samples $z_i, i = 1,2,...,M$. The analysis assumes perfect dehopping. For orthogonal MFSK the bit error probability can be related to the symbol error probability by

$$P_b = \frac{M}{2(M-1)} P_s \tag{1}$$

The energy per bit E_b is related to the energy per symbol E_s by

$$E_b = \frac{E_s}{\log_2 M} \tag{2}$$

and the energy per bit E_b is related to the energy per symbol E_h by

$$E_b = L E_h \tag{3}$$

A. NOISE POWER ESTIMATOR

Let σ_k^2 represent the noise power in a given hop k of a symbol. An accurate measurement of σ_k^2 is a challenging problem in fast frequency-hopped spread spectrum systems. In order to perform a complete evaluation of the noise normalized receiver, σ_k^2 is modeled as a random variable. In this thesis, $\hat{\sigma}_k^2$ is an

estimate of σ_k^2 ; hence, the performance obtained for the noise-normalized receiver is in this sense non-ideal.

From the noise power spectral density and the equivalent noise bandwidth of each detector branch as discussed in the previous chapter, for each hop each correlator output has noise power $\sigma_k^2 = N_0 B$ with probability $1 - \gamma$ when interference is not present and noise power $\sigma_k^2 = (\gamma^{-1} N_I + N_0) B$ with probability γ when interference is present. The output of the noise power estimator is assumed to be σ_k^2 with probability $1 - \gamma$; that is, $\hat{\sigma}_k^2$ is determined with no error when only thermal noise is present. This seems reasonable since wideband thermal noise is essentially the same for all hops. Hence, the noise power in a given hop k of a symbol is defined

$$\hat{\sigma}_k^2 = \begin{cases} \sigma_T^2 + \hat{\sigma}_I^2 & with \quad probability \quad \gamma \\ \sigma_T^2 & with \quad probability \quad 1 - \gamma \end{cases} \tag{4}$$

where $\sigma_T^2 = N_0 B$, $\sigma_I^2 = \gamma^{-1} N_I B$ and $\hat{\sigma}_I^2$ is the estimate of the σ_I^2. The estimate $\hat{\sigma}_I^2$ is modeled as a uniform random variable. This model is chosen since it represents a worst case noise power estimation error.

B. PROBABILITY DENSITY FUNCTION OF THE DECISION VARIABLES

The signal is assumed to be present in branch 1 of the MFSK demodulator without loss of generality due to demodulator symmetry. Then the conditional probability density function of the random variable X_{1k} at the output of the branch 1 before normalization or diversity combining, given a signal amplitude $\sqrt{2}a_k$, is [9]

$$f_{X_{1k}}(x_{1k} \mid a_k) = \frac{1}{2\sigma_k^2}\exp\left(-\frac{x_{1k}+2a_k^2}{2\sigma_k^2}\right)I_0\left(\frac{a_k\sqrt{2x_{1k}}}{\sigma_k^2}\right)u(x_{1k}) \qquad (5)$$

where $u(\bullet)$ is the unit step function and $I_0(\bullet)$ represents the modified Bessel function of order zero. The average received signal power of hop k is $\overline{a_k^2}$, and channel fading is modeled by assuming a_k to be a Ricean random variable. The probability density function of the Ricean random variable a_k is [9]

$$f_{A_k}(a_k) = \frac{a_k}{\sigma^2}\exp\left(-\frac{a_k^2+\alpha^2}{2\sigma^2}\right)I_0\left(\frac{a_k\alpha}{\sigma^2}\right)u(a_k) \qquad (6)$$

where α^2 is the average power of the nonfaded (direct) component of the signal and $2\sigma^2$ is the average power of the Rayleigh-faded (diffuse) component of the signal. The total average received signal power of hop k is $\overline{a_k^2}=\alpha^2+2\sigma^2$ and is assumed to remain constant from hop to hop. Note that if $\alpha^2=0$ the channel model is a Rayleigh fading model, and if $2\sigma^2=0$ there is no fading.

The conditional probability density function of the noise-normalized random variable $Z_{1k}=X_{1k}/\hat{\sigma}_k^2$ is given by

$$f_{Z_{1k}}(z_{1k} \mid a_k,\hat{\sigma}_k^2) = \frac{1}{2(\sigma_k^2/\hat{\sigma}_k^2)}\exp\left(-\frac{z_{1k}+2a_k^2/\hat{\sigma}_k^2}{2(\sigma_k^2/\hat{\sigma}_k^2)}\right)I_0\left(\frac{a_k\sqrt{2(\hat{\sigma}_k^2/\sigma_k^2)z_{1k}}}{\sigma_k}\right)u(z_{1k}) \qquad (7)$$

The probability density function of Z_{1k} conditioned only on $\hat{\sigma}_k^2$ is found by integrating (7) with respect to a_k

$$f_{Z_{1k}}(z_{1k} \mid \hat{\sigma}_k^2) = \int_0^\infty f_{Z_{1k}}(z_{1k} \mid a_k,\hat{\sigma}_k^2)f_{A_k}(a_k)\,da_k \qquad (8)$$

11

Substituting (6) and (7) into (8) and integrating, we obtain [11]

$$f_{Z_{1k}}(z_{1k} \mid \hat{\sigma}_k^2) = \frac{1}{2(1+\xi_k)(\sigma_k^2/\hat{\sigma}_k^2)} \exp\left(-\frac{\rho_k}{1+\xi_k}\right) \exp\left(-\frac{z_{1k}}{2(1+\xi_k)(\sigma_k^2/\hat{\sigma}_k^2)}\right)$$
$$\bullet I_0\left(\frac{\sqrt{2(\hat{\sigma}_k^2/\sigma_k^2)\rho_k z_{1k}}}{1+\xi_k}\right) u(z_{1k}) \tag{9}$$

where $\rho_k = \alpha^2/\sigma_k^2$ is the signal-to-noise ratio of the direct component of hop k of a symbol and $\xi_k = 2\sigma^2/\sigma_k^2$ is the signal-to-noise ratio of the diffuse component of hop k of a symbol.

The probability density function of the noise-normalized random variable Z_{mk}, $m = 2,3,...,M$ of hop k of a symbol that corresponds to the noise-normalized sampled outputs of the branches m of the demodulator (Fig. 1) that contain no signal is obtained from (9) by letting $\rho_k = \xi_k = 0$ to yield

$$f_{Z_{mk}}(z_{mk} \mid \hat{\sigma}_k^2) = \frac{1}{2(\sigma_k^2/\hat{\sigma}_k^2)} \exp\left(-\frac{z_{mk}}{2(\sigma_k^2/\hat{\sigma}_k^2)}\right) u(z_{mk}), m = 2,3,....M. \tag{10}$$

As a special case, the ideal estimator has $\hat{\sigma}_k^2 = \sigma_k^2$ which yields

$$f_{Z_{1k}}(z_{1k}) = \frac{1}{2(1+\xi_k)} \exp\left(-\frac{\rho_k}{1+\xi_k}\right) \exp\left(-\frac{z_{1k}}{2(1+\xi_k)}\right) I_0\left(\frac{\sqrt{2\rho_k z_{1k}}}{1+\xi_k}\right) u(z_{1k}) \tag{11}$$

and

$$f_{Z_{mk}}(z_{mk}) = \frac{1}{2}\exp\left(-\frac{z_{mk}}{2}\right) u(z_{mk}), m = 2,3,....M. \tag{12}$$

12

Let $Z_{1k}^{(1)}$ and $Z_{1k}^{(2)}$ denote the random variable Z_{1k} when hop k of a symbol has interference and no interference, respectively. Let i be the number of hops of a symbol that have interference. Then the decision random variable $Z_1(\hat{\sigma}_k^2)$ after L independent hops are combined is given by

$$Z_1(\hat{\sigma}_k^2) = \sum_{k=1}^{L} Z_{1k}(\hat{\sigma}_k^2) = \sum_{k=1}^{i} Z_{1k}^{(1)}(\hat{\sigma}_{k1}^2) + \sum_{k=i+1}^{L} Z_{1k}^{(2)}(\hat{\sigma}_{k2}^2 = \sigma_T^2) \tag{13}$$

Let $f_{Z_{1k}^{(n)}}(z_{1k}^{(n)} \mid \hat{\sigma}_{kn}^2), n = 1,2$ denote the probability density function of the random variable $Z_{1k}^{(n)}(\hat{\sigma}_{kn}^2), n = 1,2$ which is obtained from (9) by replacing ρ_k and ξ_k with $\rho_k^{(n)}$ and $\xi_k^{(n)}$, respectively. Thus , $\rho_k^{(n)}$ is the signal-to-noise ratio of the direct component of hop k of a symbol with interference ($n = 1$) and without interference ($n = 2$), respectively, and $\xi_k^{(n)}$ is the signal-to-noise ratio of the diffuse component of hop k of a symbol with interference ($n = 1$) and without interference ($n = 2$), respectively.

Now the Laplace transform of $f_{Z_{1k}^{(n)}}(z_{1k}^{(n)} \mid \hat{\sigma}_{kn}^2), n = 1,2$ is

$$F_{Z_{1k}^{(n)}}(s \mid \hat{\sigma}_{kn}^2) = \int_0^\infty f_{Z_{1k}^{(n)}}(z_{1k}^{(n)} \mid \hat{\sigma}_{kn}^2) \exp\left[-s z_{1k}^{(n)}\right] dz_{1k}^{(n)}, n = 1,2 \tag{14}$$

Substituting (9) into (14), we obtain

$$F_{Z_{1k}^{(n)}}(s \mid \hat{\sigma}_{kn}^2) = \frac{1}{2(1 + \xi_k^{(n)})(\sigma_{kn}^2 / \hat{\sigma}_{kn}^2)} \exp\left(-\frac{\rho_k^{(n)}}{1 + \xi_k^{(n)}}\right)$$
$$\bullet \int_0^\infty \exp\left\{-z_{1k}\left[s + \frac{1}{2(1 + \xi_k^{(n)})(\sigma_{kn}^2 / \hat{\sigma}_{kn}^2)}\right]\right\}$$

13

$$\bullet I_0\left(\frac{\sqrt{2(\hat{\sigma}_{kn}^2/\sigma_{kn}^2)\rho_k^{(n)}}z_{1k}}{1+\xi_k^{(n)}}\right)dz_{1k} \qquad (15)$$

The above integral can be evaluated as [10],[11]

$$F_{Z_{1k}^{(n)}}(s\,|\,\hat{\sigma}_{kn}^2) = \frac{1}{2(1+\xi_k^{(n)})(\sigma_{kn}^2/\hat{\sigma}_{kn}^2)}\exp\left(-\frac{\rho_k^{(n)}}{1+\xi_k^{(n)}}\right)$$

$$\bullet\left(\frac{1}{s+\dfrac{1}{2(1+\xi_k^{(n)})(\sigma_{kn}^2/\hat{\sigma}_{kn}^2)}}\right)$$

$$\bullet\exp\left(\frac{\rho_k^{(n)}}{2(1+\xi_k^{(n)})^2(\sigma_{kn}^2/\hat{\sigma}_{kn}^2)}\bullet\frac{1}{s+\dfrac{1}{2(1+\xi_k^{(n)})(\sigma_{kn}^2/\hat{\sigma}_{kn}^2)}}\right) \qquad (16)$$

where $n=1,2$.

Since all L hops are independent, we obtain the conditional probability density function for the decision variable Z_1 given i hops of a bit have interference from (13) as

$$f_{Z_1}(z_1\,|\,i,\hat{\sigma}_k^2) = [f_{Z_{1k}^{(1)}}(z_{1k}^{(1)}\,|\,\hat{\sigma}_{k1}^2)]^{\otimes i}\otimes[f_{Z_{1k}^{(n)}}(z_{1k}^{(2)}\,|\,\hat{\sigma}_{k2}^2)]^{\otimes(L-i)} \qquad (17)$$

where $\otimes N$ represents a N-fold convolution and $[f_{Z_{1k}^{(n)}}(z_{1k}^{(n)}\,|\,\hat{\sigma}_{kn}^2)]^{\otimes N}$ is obtained as the inverse Laplace transform of $[F_{Z_{1k}^{(n)}}(s\,|\,\hat{\sigma}_{kn}^2)]^N$ which is given by

$$[f_{Z_{1k}^{(n)}}(z_{1k}^{(n)}\,|\,\hat{\sigma}_{kn}^2)]^{\otimes N} = \frac{z_{1k}^{(n)\frac{N-1}{2}}}{(2(\sigma_{kn}^2/\hat{\sigma}_{kn}^2))^{\frac{N+1}{N}}(1+\xi_k^{(n)})(N\rho_k^{(n)})^{\frac{N-1}{N}}}\exp\left(-\frac{N\rho_k^{(n)}}{1+\xi_k^{(n)}}\right)$$

$$\bullet\exp\left(-\frac{z_{1k}^{(n)}}{2(1+\xi_k^{(n)})(\sigma_{kn}^2/\hat{\sigma}_{kn}^2)}\right)\bullet I_{N-1}\left(\frac{\sqrt{2(\hat{\sigma}_{kn}^2/\sigma_{kn}^2)\rho_k^{(n)}}z_{1k}^{(n)}}{1+\xi_k^{(n)}}\right)u\left(z_{1k}^{(n)}\right) \qquad (18)$$

14

From (17), the Laplace transform of $f_{Z_1}(z_1 \mid i, \hat{\sigma}_k^2)$ is

$$F_{Z_1}(s \mid i, \hat{\sigma}_{k1}^2) = [F_{Z_{1k}^{(1)}}(s \mid \hat{\sigma}_k^2)]^i [F_{Z_{1k}^{(2)}}(s)]^{(L-i)} \tag{19}$$

since $\hat{\sigma}_{k2}^2 = \sigma_{k2}^2 = \sigma_T^2$ is assumed to be known without error. Substituting (16) into (19), we get

$$F_{Z_1}(s \mid i, \hat{\sigma}_{k1}^2) = \frac{1}{2^L (\sigma_{k1}^2 / \hat{\sigma}_{k1}^2)^i (1 + \xi_{k1})^i} \exp\left(-\frac{i\rho_{k1}}{1 + \xi_{k1}}\right)$$

$$\bullet \left(\frac{1}{s + \dfrac{1}{2(1 + \xi_{k1})(\sigma_{k1}^2 / \hat{\sigma}_{k1}^2)}}\right)^i$$

$$\bullet \exp\left(\frac{i\rho_{k1}}{2(1 + \xi_{k1})^2 (\sigma_{k1}^2 / \hat{\sigma}_{k1}^2)} \bullet \frac{1}{s + \dfrac{1}{2(1 + \xi_{k1})(\sigma_{k1}^2 / \hat{\sigma}_{k1}^2)}}\right)$$

$$\bullet \frac{1}{(1 + \xi_{k2})^{(L-i)}} \exp\left(-\frac{(L-i)\rho_{k2}}{1 + \xi_{k2}}\right) \bullet \left(\frac{1}{s + \dfrac{1}{2(1 + \xi_{k2})}}\right)^{(L-i)}$$

$$\bullet \exp\left(\frac{(L-i)\rho_{k2}}{2(1 + \xi_{k2})^2} \bullet \frac{1}{s + \dfrac{1}{2(1 + \xi_{k2})}}\right) \tag{20}$$

In general, except for the special case of all hops jammed $(i = L)$ and no hops jammed $(i = 0)$, $f_{Z_1}(z_1 \mid i, \hat{\sigma}_k^2)$ must be obtained from (20) by numerical inversion. For the two special case mentioned, (18) may be used.

The probability density functions of $Z_{mk}, m = 2, 3, ..., M$ of hop k of a symbol for the branches that do not contain the signal are a special case of $f_{Z_1}(z_1 \mid i, \hat{\sigma}_k^2)$

15

with $\rho_k^{(n)} = 0$ and $\xi_k^{(n)} = 0$. The Laplace transform of $F_{Z_m}(s \mid i, \hat{\sigma}_{k1}^2)$ is obtained from (20) with $\rho_k^{(n)} = \xi_k^{(n)} = 0$ as

$$F_{Z_m}(s \mid i, \hat{\sigma}_{k1}^2) = \left(\frac{\alpha}{s+\alpha} \right)^i \left(\frac{1/2}{s+1/2} \right)^{L-i} \tag{21}$$

where

$$\alpha = \frac{\hat{\sigma}_{k1}^2 / \sigma_{k1}^2}{2} \tag{22}$$

Equation (21) can be inverted analytically, but the computational complexity of the result leads to problems with round-off error. Consequently, when needed, (21) is inverted numerically.

C. PROBABILITY OF BIT ERROR

The symbol error probability for the receiver in Fig. 1 in the presence of partial-band interference is [1]

$$P_s(\hat{\sigma}_k^2) = \sum_{i=0}^{L} \binom{L}{i} \gamma^i (1-\gamma)^{L-i} P_s(i, \hat{\sigma}_k^2) \tag{23}$$

where $P_s(i, \hat{\sigma}_k^2)$ is the conditional symbol error probability given that i hops of a symbol have interference and given the estimated noise power for each hop. It is well known that $P_s(i, \hat{\sigma}_k^2)$ is obtained from [7]

$$P_s(i, \hat{\sigma}_k^2) = 1 - \int_0^\infty f_{Z_1}(z_1 \mid i, \hat{\sigma}_k^2) \left[\int_0^{Z_1} f_{Z_m}(z_m \mid i, \hat{\sigma}_k^2) dz_m \right]^{M-1} dz_1 \tag{24}$$

16

which results from the independence of the decision statistics $Z_j, j = 1, 2, ..., M$ and the fact that the decision statistics for the non-signal branches are identical random variables. For the general case of some hops jammed and others free of interference, (24) must be evaluated numerically. For perfect noise estimation, $\hat{\sigma}_k^2 = \sigma_k^2$, and the integral in the bracket of (24) can be evaluated to yield

$$P_s(i) = 1 - \int_0^\infty f_{Z_1}(z_1 \mid i) \left[1 - \exp\left(-\frac{z_1}{2} \right) \sum_{k=0}^{L-1} \frac{(z_1/2)^k}{k} \right]^{M-1} dz_1 \qquad (25)$$

By using first the binomial theorem and the multinomial theorem, we can express the $[\bullet]^{M-1}$ term in (25) as a double summation of powers of Z_1. Then, for the special cases of either all hops jammed or all hops free of interference, (17) reduces to (18), and replacing the modified Bessel function in (18) with a series representation, we can integrate (25) analytically term by term [12]. The result is in the form of a double summation of the product of powers of rational functions, exponentials, and confluent hypergeometric functions with arguments depending on both summation indices. As a result, it is more straightforward to evaluate (25) numerically for all cases even though an analytic expression is available in two special cases. For a numerical evaluation of (25), it is preferable to use $[\bullet]^{M-1}$ rather than its expression as a double summation in powers of Z_1.

The numerical evaluation of both (24) and (25) is made substantially easier by nothing that

$$\lim_{z_1 \to \infty} \left[\int_0^{z_1} f_{Z_m}(z_m \mid i, \hat{\sigma}_k^2) dz_m \right]^{M-1} = 1 \qquad (26)$$

17

Hence, by adding and subtracting

$$\int_0^\infty f_{Z_1}(z_1 \mid i, \hat{\sigma}_k^2) dz_1 = 1 \qquad (27)$$

on the right-hand side of (24), we obtain a computationally efficient expression for the conditional probability of symbol error given that i hops of a symbol have interference as

$$P_s(i, \hat{\sigma}_k^2) = \int_0^\infty f_{Z_1}(z_1 \mid i, \hat{\sigma}_k^2) \left\{ 1 - \left[\int_0^{Z_1} f_{Z_m}(z_m \mid i, \hat{\sigma}_k^2) dz_m \right]^{M-1} \right\} dz_1 \qquad (28)$$

since the $\{\bullet\}$ term in (28) approaches zero as $z_1 \to \infty$. Note that $f_{Z_1}(z_1 \mid i, \hat{\sigma}_k^2)$ and $f_{Z_m}(z_m \mid i, \hat{\sigma}_k^2)$ are obtained by numerical inversion of (20) and (21), respectively. The $[\bullet]$ term in (28) is evaluated by $\dfrac{F_{Z_m}(s \mid i, \hat{\sigma}_{k1}^2)}{s}$.

The remaining analysis problem is to remove the conditioning of $P_s(i, \hat{\sigma}_k^2)$ on $\hat{\sigma}_k^2$. In the numerical results chapter, $\hat{\sigma}_k^2$ is used both as a parameter and modeled as a random variable. When modeled as a random variable, $\hat{\sigma}_k^2$ is taken to be a uniform random variable which is the least favorable a priori density function under the circumstances. A uniform probability density function over $(0.5\sigma_k^2, 1.5\sigma_k^2)$ and $(0, 2.0\sigma_k^2)$, allowing up to $\pm 50\%$ and $\pm 100\%$ noise power estimation error, respectively, are used. The conditioning on $\hat{\sigma}_k^2$ is removed by

$$P_s = \int_{\sigma_{k-}^2}^{\sigma_{k+}^2} P_s(\hat{\sigma}_k^2) f(\hat{\sigma}_k^2) d\hat{\sigma}_k^2 \qquad (29)$$

where σ_{k-}^2 and σ_{k+}^2 represent the lower and upper limit of the uniform probability density function $f(\hat{\sigma}_k^2)$, respectively. Equation (29) is evaluated numerically.

18

IV. NUMERICAL PROCEDURE AND RESULTS

A. NUMERICAL PROCEDURE

Computation of the probability of bit error involves a numerical evaluation of (28) for each of the possible combinations of jammed and unjammed hops given L hops per symbol and noise power estimator. In addition, except for the special cases of either all hops jammed or all hops free of interference, the probability density function of Z_1 given that i hops of a bit have interference $f_{Z_1}(z_1 \mid i, \hat{\sigma}_k^2)$ must be evaluated numerically. Using (20), we have the analytic expression for $F_{Z_1}(s \mid i, \hat{\sigma}_k^2)$, the Laplace transform of $f_{Z_1}(z_1 \mid i, \hat{\sigma}_k^2)$. Hence, the most efficient way to evaluate $f_{Z_1}(z_1 \mid i, \hat{\sigma}_k^2)$ is to invert $F_{Z_1}(s \mid i, \hat{\sigma}_k^2)$ numerically. This is accomplished using a variation of the method detailed in [13] where

$$f_{Z_1}(z_1 \mid i, \hat{\sigma}_k^2) = \frac{\exp(az_1)}{2z_1}$$

$$\bullet \left[F_{Z_1}(s \mid i, \hat{\sigma}_k^2) + 2 \sum_{k=1}^{\infty} (-1)^k \operatorname{Re}\left\{ F_{Z_1}(a + jk\pi / z_1 \mid i, \hat{\sigma}_k^2) \right\} \right]$$

$$+ Error \tag{30}$$

The variable a in (29) is related to the exponential order β of $F_{Z_1}(s \mid i, \hat{\sigma}_k^2)$ and the upper bound of the relative error E by

$$a = \frac{3}{2}\beta - \frac{\ln E}{2z_1} \tag{31}$$

The magnitude of the error term in (30) is controlled by the choice of the maximum relative error E .

19

To obtain worst case partial-band jamming, the jamming fraction γ which maximizes the probability of bit error is found for various values of diversity, fading conditions, signal-to-noise power density ratios, and order of modulation. This investigation does not include coding. All results presented in this thesis are obtained by assuming that the ratio of direct-to-diffuse signal energy $\alpha^2/2\sigma^2$ is the same for each hop k of a symbol.

B. NUMERICAL RESULTS

1. Ideal Noise Normalization Case

Receiver performance for specific fractions of partial-band interference are compared to worst case performance for a relatively strong direct signal $(\alpha^2/2\sigma^2 = 10$) given ideal noise power estimation in Figs. 2-5 for M = 4 and diversities of L = 2, 3 ,4 and 6, respectively. In each of these figures, the ratio of bit energy-to-thermal noise density is $E_b/N_0 = 13.35$ dB. This value of E_b/N_0 corresponds to $P_b = 10^{-5}$ when there is no fading or interference, M = 2, and L = 1. This corresponds to the signal-to-thermal noise density ratio used in [4] and allows our results to be compared directly to the nonfaded results presented in [4].

As can be seen in Fig. 2, partial band interference results in significant degradation in performance over a broad range of bit energy-to-interference noise density ratios. As a general rule, as ratio of bit energy-to-interference noise density increases, the degradation due to the partial-band interference increases as the fraction of the spread bandwidth being jammed γ decreases; although, for both very large and very small bit energy-to-interference noise density ratios, there is very little degradation due to partial-band interference. As can be seen in Figs. 3-5, the degradation due to partial-band interference is progressively

reduced as diversity increases. At this value of E_b/N_0, a diversity of four is sufficient to virtually eliminate any degradation due to partial-band interference. Hence, for the case of a strong direct component, diversity is capable of completely eliminating the degradation introduced by partial-band interference. It is also interesting to note that for bit energy-to-interference noise density ratios less than about 15 dB, receiver performance improves dramatically when the interference is partial-band rather than uniform. This is particularly true for L > 2. Overall worst case receiver performance for various values of diversity with modulation order fixed is illustrated in Fig. 6. For bit energy-to-interference noise density ratios less than about 12 dB, fewer diversity receptions gives slightly better performance, although increasing diversity has significant improvement for bit energy-to-interference noise density ratios greater than about 12 dB. This behavior is a consequence of noncoherent combining losses which are greater for small bit energy-to-interference noise density ratios. This negates performance improvement due to diversity for bit energy-to-interference noise density ratios less than about 12 dB. Noncoherent combing losses also account for the diminishing amount of improvement for increasing diversity when $E_b/N_I >12$ dB. Receiver performance for specific fractions of partial-band interference are compared to worst case performance for a very strong direct signal ($\alpha^2/2\sigma^2 = 100$) in Figs. 7-9 for M = 4 and diversities L = 2, 3, 4, respectively. The ratio of bit energy-to-thermal noise density is also $E_b/N_0 = 13.35$ dB. As can be seen in Fig. 7, partial-band interference significantly degrades performance. From Figs. 8 and 9, increasing diversity is seen to dramatically reduce the effect of partial-band interference. Overall worst case receiver performance for various values of diversity with modulation order fixed is illustrated in Fig. 10. It is

interesting to note that noncoherent combining losses again negates performance improvement due to diversity for $E_b / N_I > 30$ dB.

When there is not a strong direct component to the signal, partial-band interference results in virtually no degradation of receiver performance. In this case, the worst case performance is virtually identical to the performance when interference is uniform. A representative example is shown in Fig. 11 for M = 4 and diversity L = 3.

Receiver performance for specific fractions of partial-band interference are compared to worst case performance for a relatively strong signal ($\alpha^2 / 2\sigma^2 = 10$) in Fig. 12, Fig. 5, and Fig. 13 for L = 4 and modulation orders of M= 2, 4, 8, respectively. The ratio of bit energy-to-thermal noise density is again taken to be $E_b / N_0 = 13.35$ dB. As the order of modulation increases partial-band interference becomes more effective in degrading relative receiver performance; however, for each increase in modulation order there is a significant improvement in overall receiver performance that for outweigths any degradation that is introduced by partial-band interference.

2. Non-ideal Noise Normalization Case

Receiver performance for specific fractions of partial-band interference are compared to worst case performance for a relatively strong direct signal ($\alpha^2 / 2\sigma^2 = 10$) with a noise power estimator error of as much as ±50% in Figs. 14-17 for M = 4 and diversities of L = 2, 3 ,4 and 6, respectively. Figs. 18-21 illustrate receiver performance under the same conditions except using a noise power esimator error of as much as ±100%. In each of these figures, the ratio of

22

bit energy-to-thermal noise density is $E_b / N_0 = 13.35$ dB. As mentioned in the last chapter, the noise power estimator error is modeled a uniform random variable.

The worst case performance for non-ideal noise normalization with ±50% noise power estimator error is basically the same as for the ideal noise normalization case. Comparing the results obtained with ±50% estimator error with those obtained with ±100% estimator error, the performance of receiver with ±100% estimator error is only slightly worse than that with ±50% estimator error. The difference between the two cases due to the partial-band interference increases as the fraction of the spread bandwidth being jammed γ decreases. It is also found that there is a distinct difference around 25 dB of bit energy-to-interference noise density ratio due to the degradation of performance with ±100% estimator error at small fraction of γ and that this difference disappears as diversity increases. These facts are shown in Figs. 22-24.

Non-ideal noise-normalized receiver performance for a fixed fraction of partial-band interference ($\gamma = 0.25$) are compared to the ideal noise normalization case performance for a relatively strong direct signal ($\alpha^2 / 2\sigma^2 = 10$) with ±50% noise power estimator error in Figs. 25-28 for M = 4 and diversities of L = 2, 3 ,4 and 6, respectively. Here, in addition to modeling the noise power estimate as a random variable, the noise power estimate is also used as a parameter where a -50% means that the noise power is underestimated by 50% and +50% means that the noise power is overestimated by 50%. Figs. 29-30 illustrate the performance of the non-ideal noise-normalized receiver with ±50% estimator error for L = 4 and modulation order of M = 2, 8, respectively ($\gamma = 0.25$). As can be seen, differences between ideal and non-ideal noise normalization are found for bit energy-to-interference noise density ratios less than about 20 dB and the

23

performance curves are identical above that particular bit energy-to-interference noise density ratio. As expected, the poorest receiver performance is obtained when the noise jamming power is underestimated. When the fraction of partial-band interference is $\gamma = 0.01$, receiver performance is shown in Figs. 31-33 for L = 4 and modulation orders of M = 2, 4, 8, respectively. It is interesting to note that the effect of the noise normalization error becomes smaller as bit energy-to-interference noise density ratios increase, and at 35 dB receiver performance is the same as for the ideal noise normalization case when $\gamma = 0.01$. This behavior is a consequence of the assumption that wideband noise can be accurately measured. Comparing Figs. 31-33, we see that the difference between overestimated noise power and underestimated noise power increases as modulation order increases; although, the increase in modulation order gives significant improvement in performance in spite of increased sensitivity to normalization error.

As previously noted, the sensitivity of the receiver to normalization error increases as diversity increases. This is not surprising since noise normalization has no effect on either the all hops jammed case or the all hops free from interference case. For L=2, for example, this leaves only one case, the one hop jammed and one not, that is affected by the normalization. As L increases, there are a greater number of cases affected by the normalization; hence, as L increases there is greater sensitivity to normalization error. Nevertheless, as can be seen by examining Figs. 23-33, the difference between ideal performance and non-ideal performance when the noise power estimate error is modeled as a random variable is not great. Consequently, we conclude that the noise-normalized receiver is relatively insensitive to noise power measurement error. In this sense, the noise-

normalized receiver is very robust in worst case partial-band jamming environment.

Figs. 34-36 illustrate the performance for a very strong direct signal ($\alpha^2/2\sigma^2 = 100$) for M = 4 and diversities of L = 2, 3, 4, respectively. Fig. 37-39 display the performance comparison between ideal and non-ideal noise-normalized case. As was found for a relatively strong direct signal ($\alpha^2/2\sigma^2 = 10$), the worst case performance for non-ideal noise normalization with ±50% noise power estimator error is basically the same as that obtained for ideal noise normalization. There is a distinct performance degradation around 25-30 dB of bit energy-to-interference noise density ratio with ±100% estimator error. Non-ideal noise-normalized receiver performance for a fixed fraction of partial-band interference ($\gamma = 0.25$) is compared to the ideal noise normalization case performance for a strong direct signal ($\alpha^2/2\sigma^2 = 100$) with ±50% noise power estimator error in Figs. 40-42 for M = 4 and diversities of L = 2, 3, 4, respectively. Here, as previously, in addition to modeling the noise power estimate error as a random variable, it is also used a parameter. As can be seen, noise normalization error does not significantly degrade performance as compared to ideal noise normalization. As before for $\alpha^2/2\sigma^2 = 10$, the primary effect of normalization error is for bit energy-to-interference noise density ratios less than about 20 dB with essentially no difference in performance above that particular bit energy-to-interference noise density ratio.

Finally, when there is not a strong direct component to the signal, partial-band interference results in virtually no degradation of receiver performance. In this case, the worst case performance is virtually identical to the performance when interference is uniform. As a example, Figs. 43-44 show the

25

receiver performance for M = 4 and diversity L = 3. Since noise normalization has no effect on broadband jamming ($\gamma = 1$), non-ideal noise normalization has no effect on worst case performance. This is shown in Fig. 45.

From the above observations, it can be concluded that the noise-normalized receiver is very robust with regard to noise measurement error independent of the strength of channel fading.
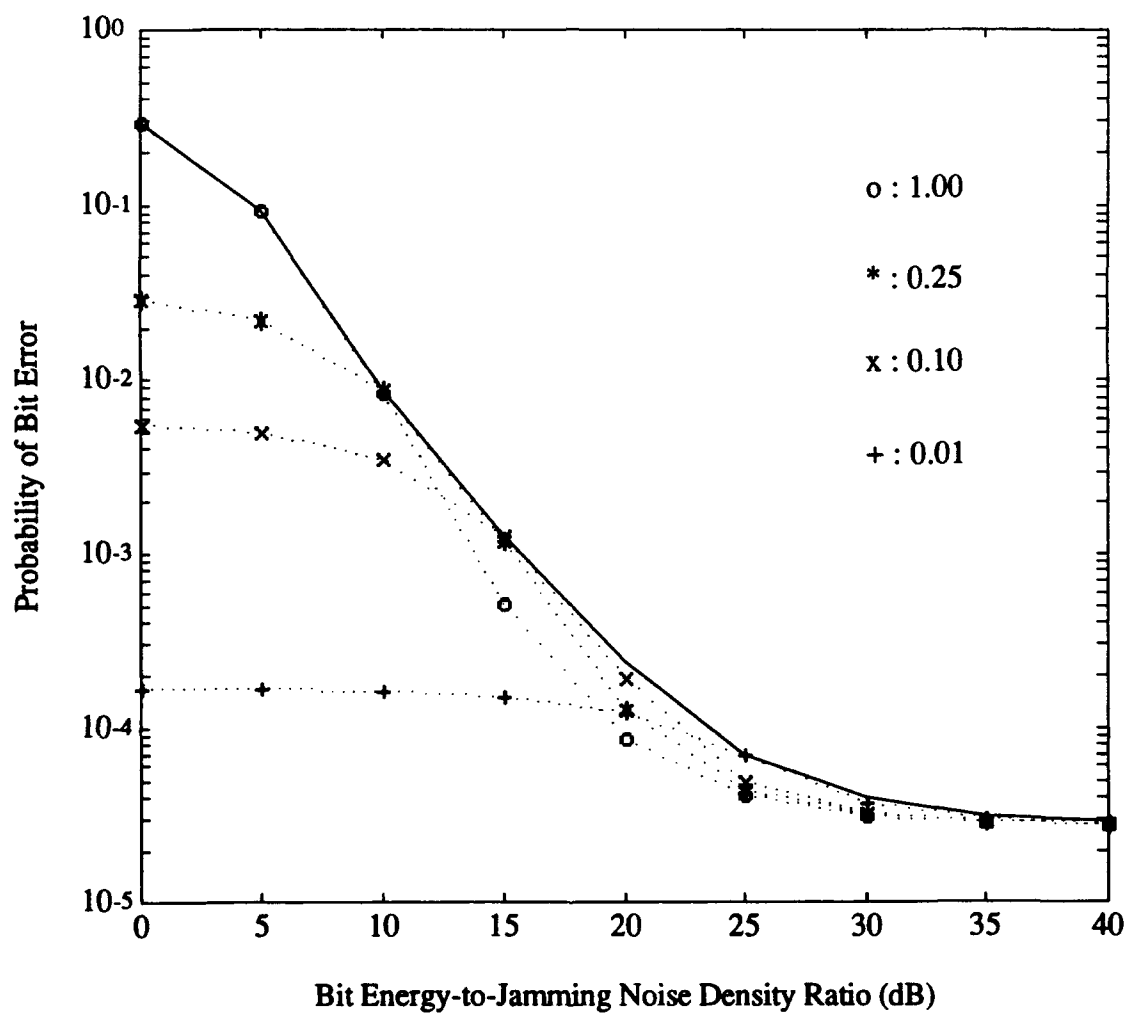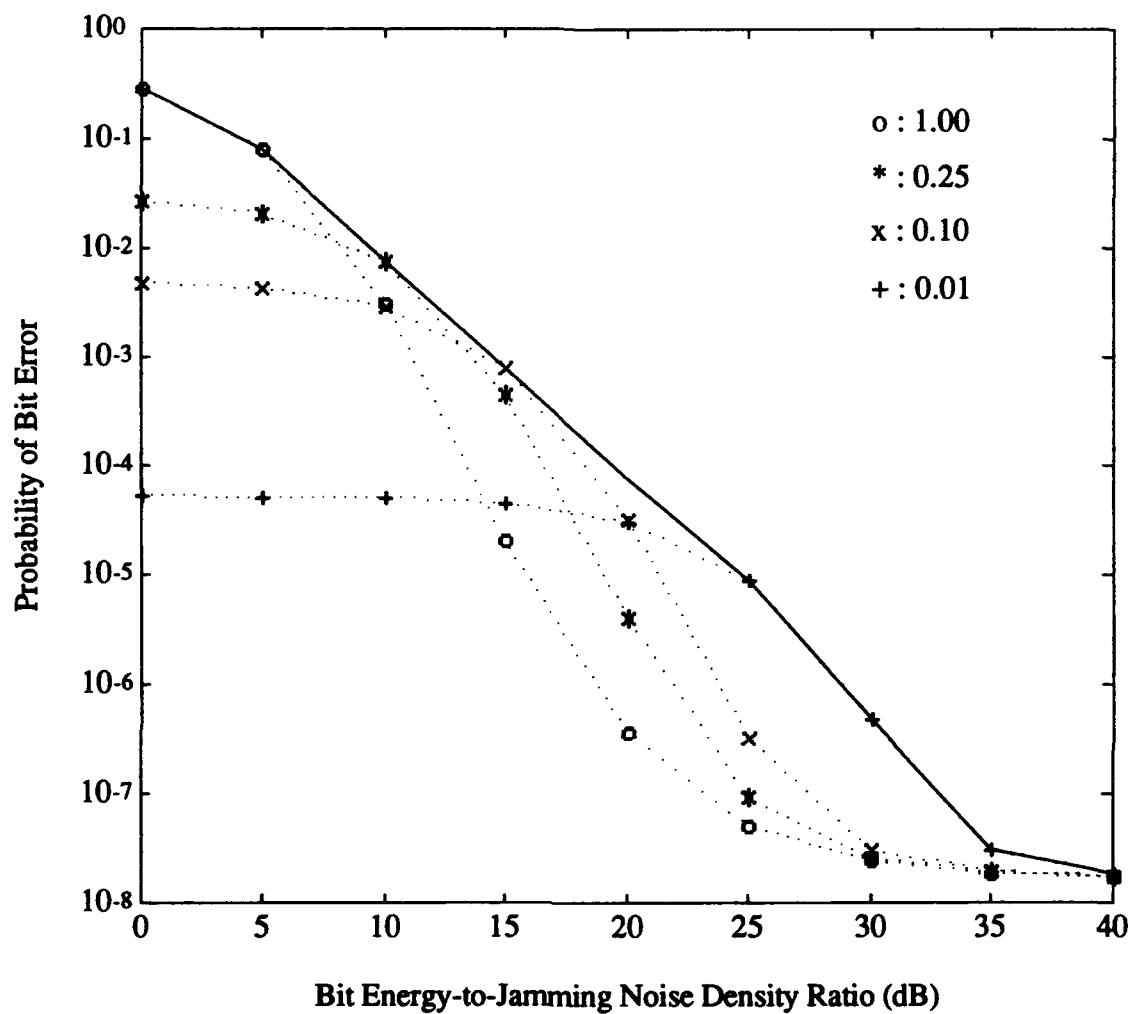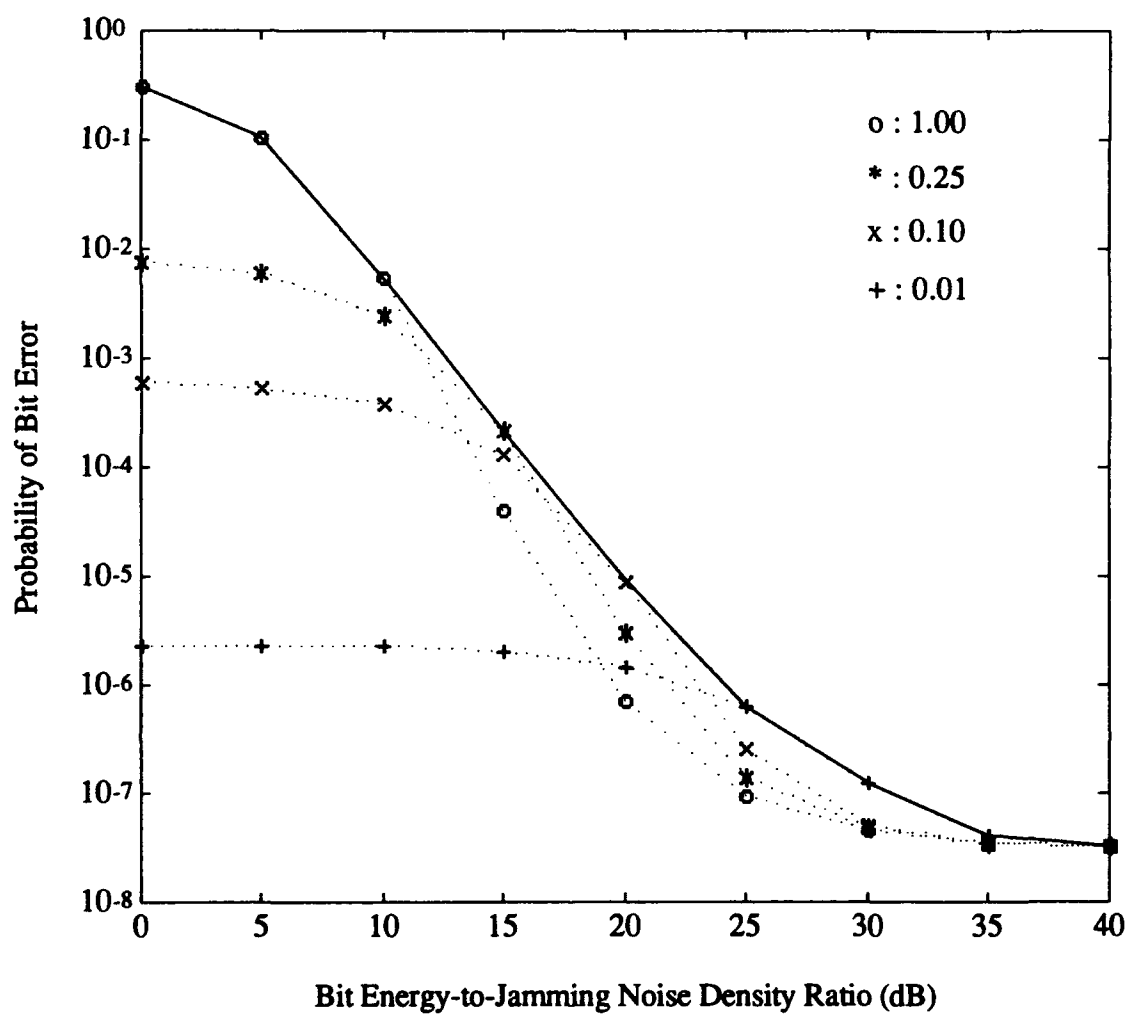
Figure 2.   Ideal receiver performance for a Ricean faded signal with M=4, L=2, E_b / N_0 =13.35 dB and direct-to-diffuse power ratio=10.
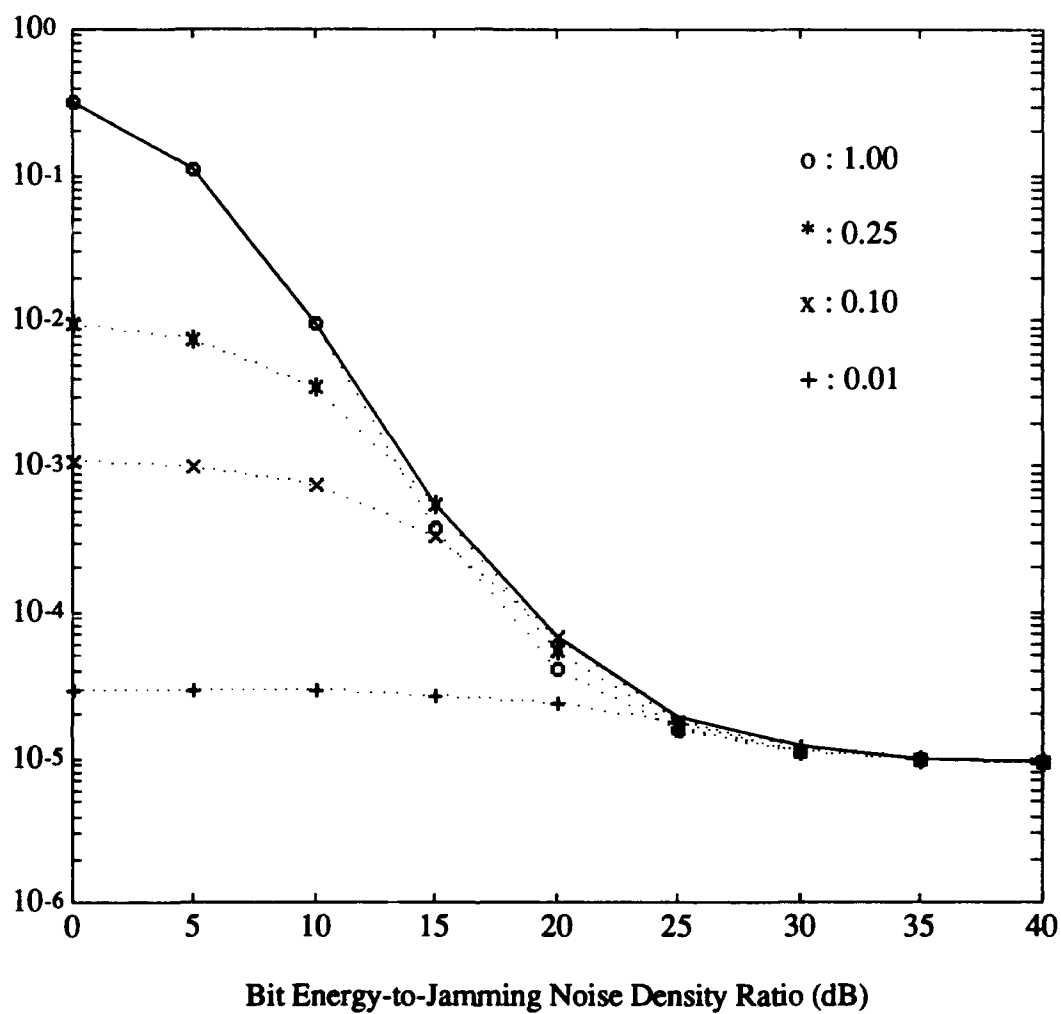
Figure 3.   Ideal receiver performance for a Ricean faded signal with M=4,
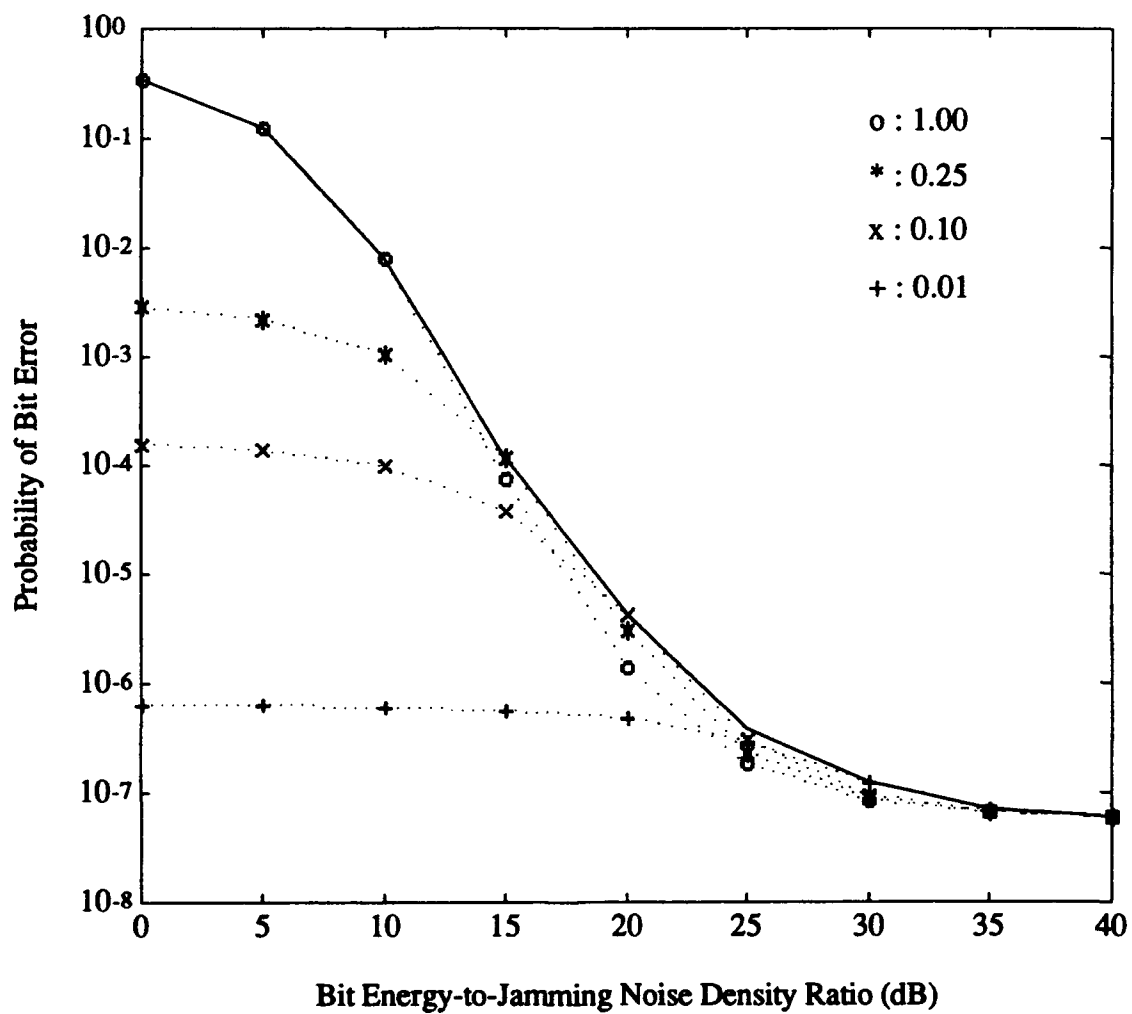L=3, E_b/N_0 =13.35 dB and direct-to-dffuse power ratio=10.
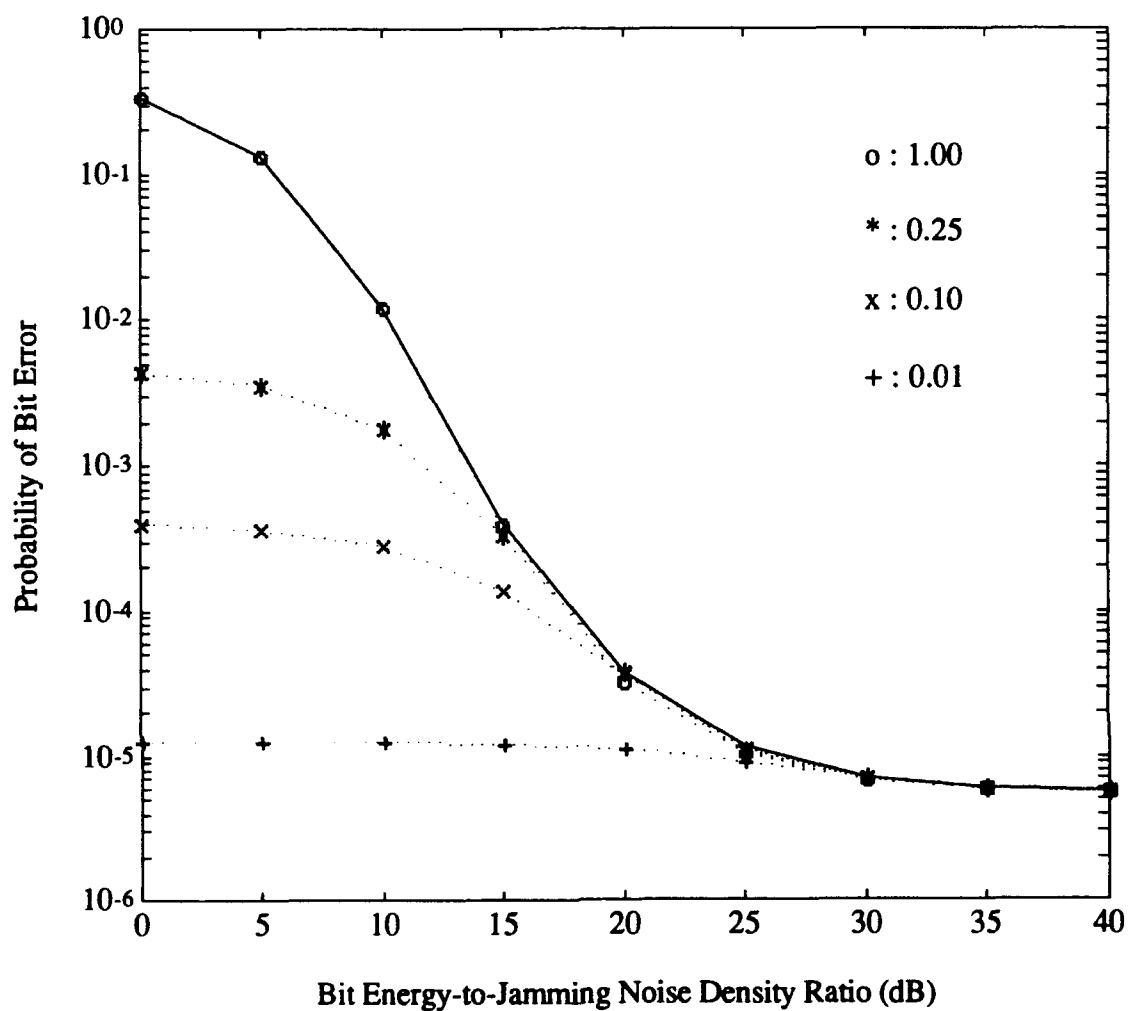
Figure 4.   Ideal receiver performance for a Ricean faded signal with M=4,
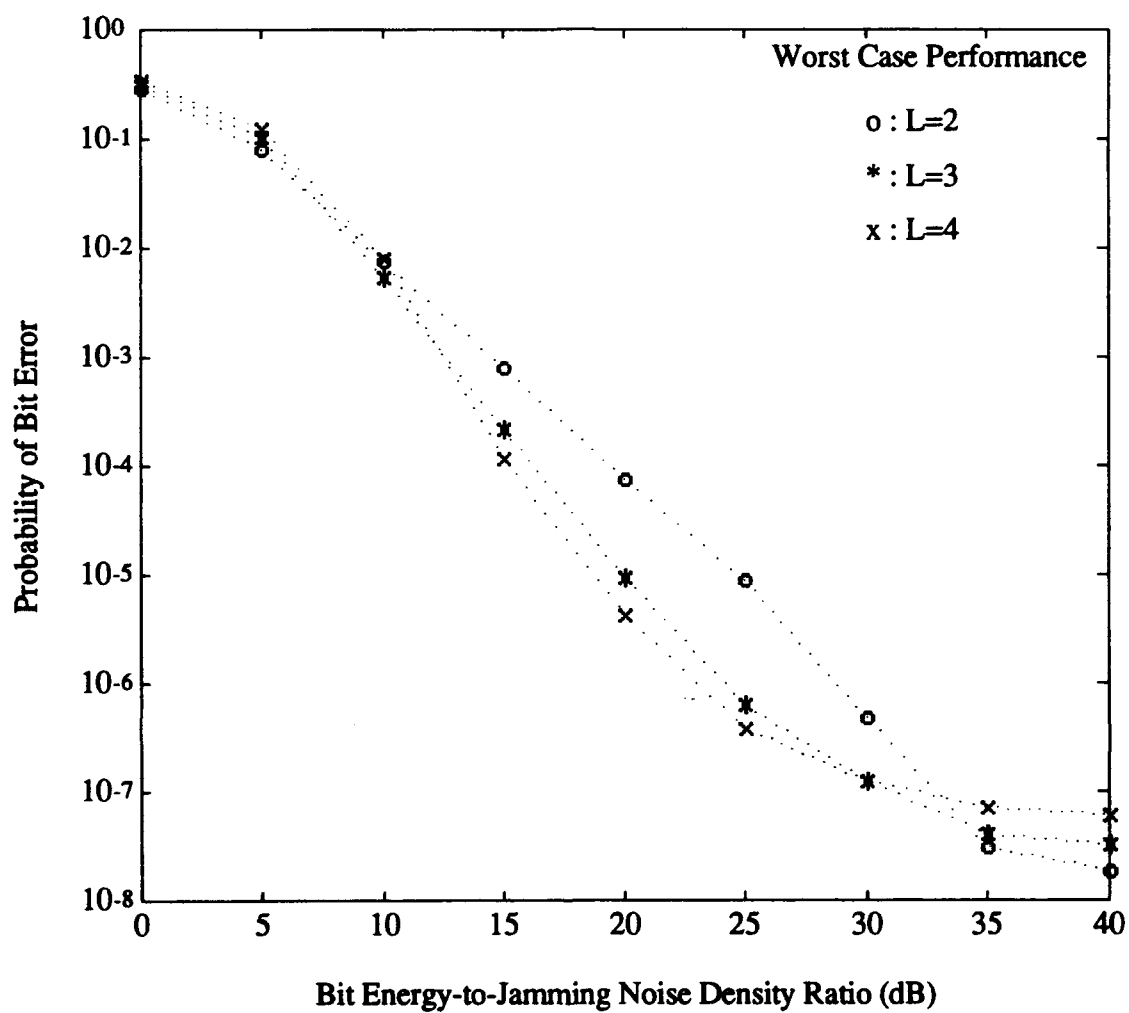L=4, E_b / N_0 =13.35 dB and direct-to-diffuse power ratio=10.

29
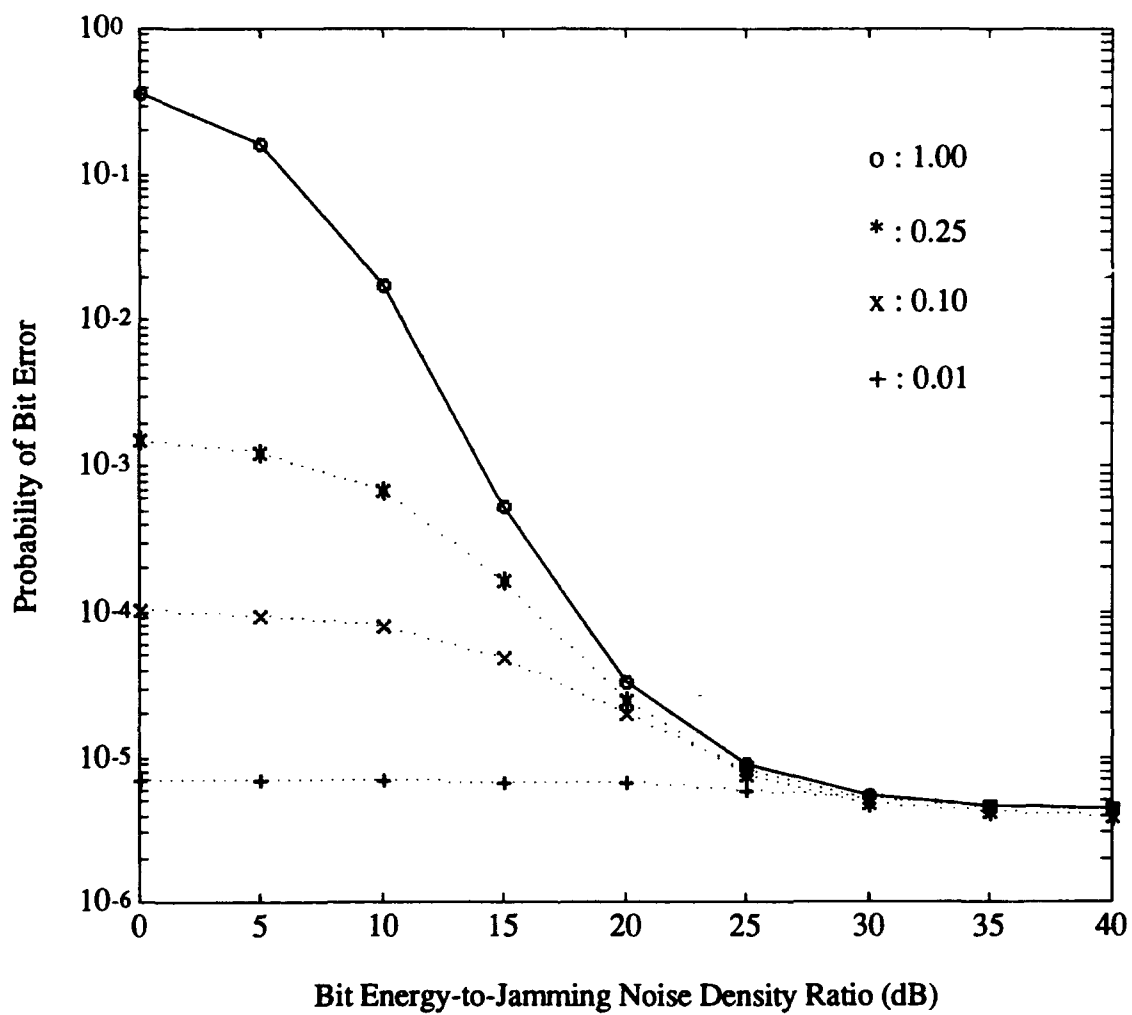
Figure 5. Ideal receiver performance for a Ricean faded signal with M=4, L=6, E_b / N_0 =13.35 dB and direct-to-diffuse power ratio=10.

30
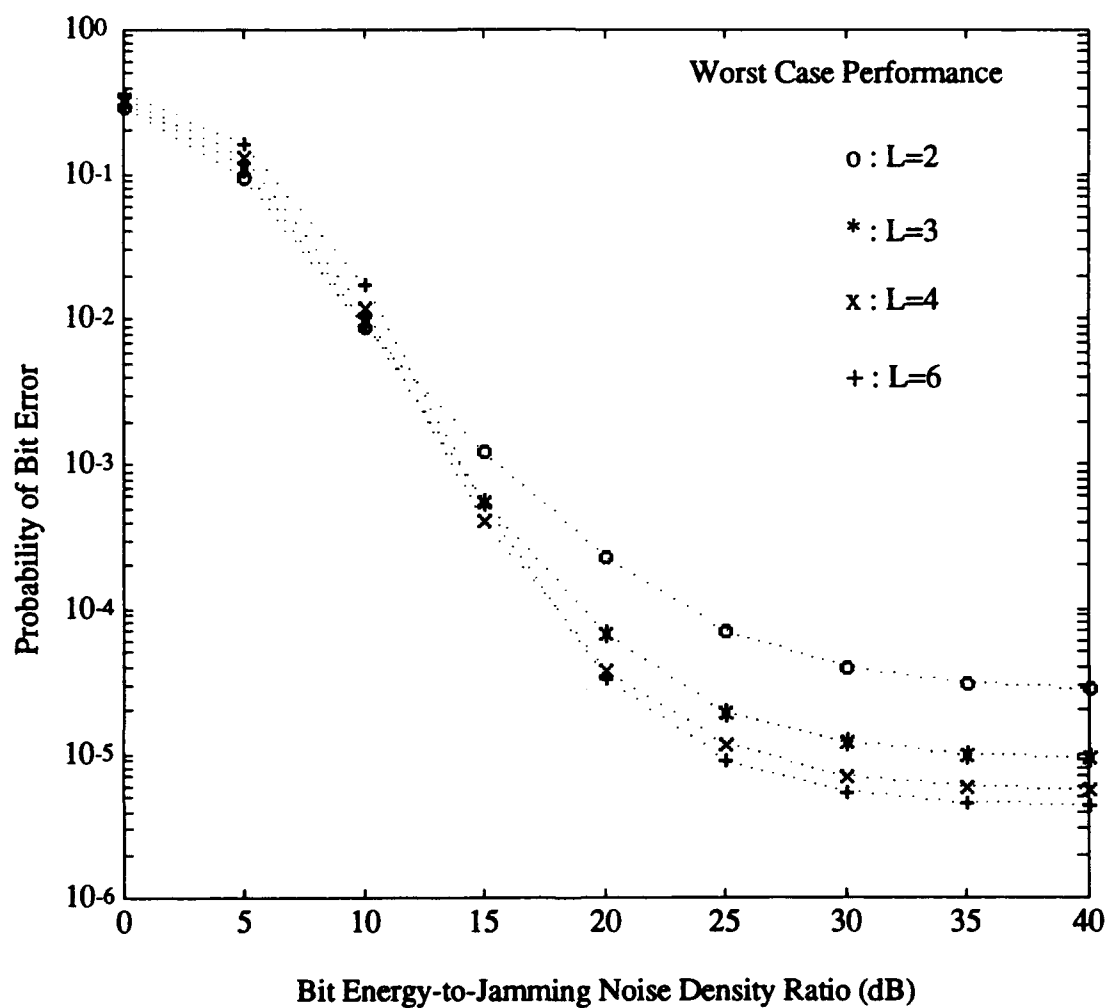
Figure 6.   Ideal worst case receiver performance comparison for a Ricean
             faded signal with M=4, diversities of L=2, 3, 4 and 6,
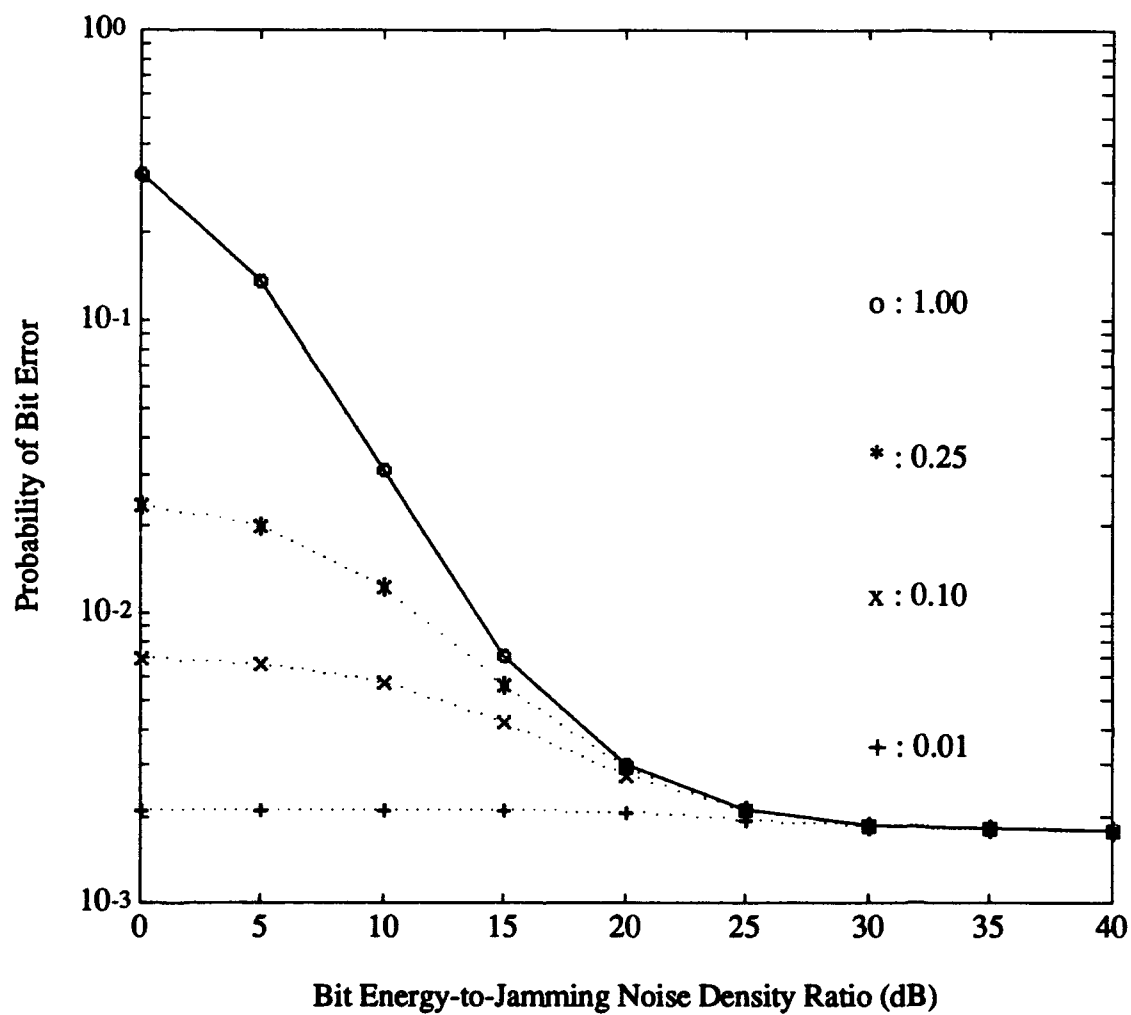 E_b / N_0 =13.35 dB and direct-to-diffuse power ratio=10.

31

Figure 7.   Ideal receiver performance for a Ricean faded signal with M=4,
L=2, E_b / N_0 =13.35 dB and direct-to-diffuse power ratio=100.

Figure 8.   Ideal receiver performance for a Ricean faded signal with M=4,
L=3, E_b / N_0 =13.35 dB and direct-to-diffuse power ratio=100.
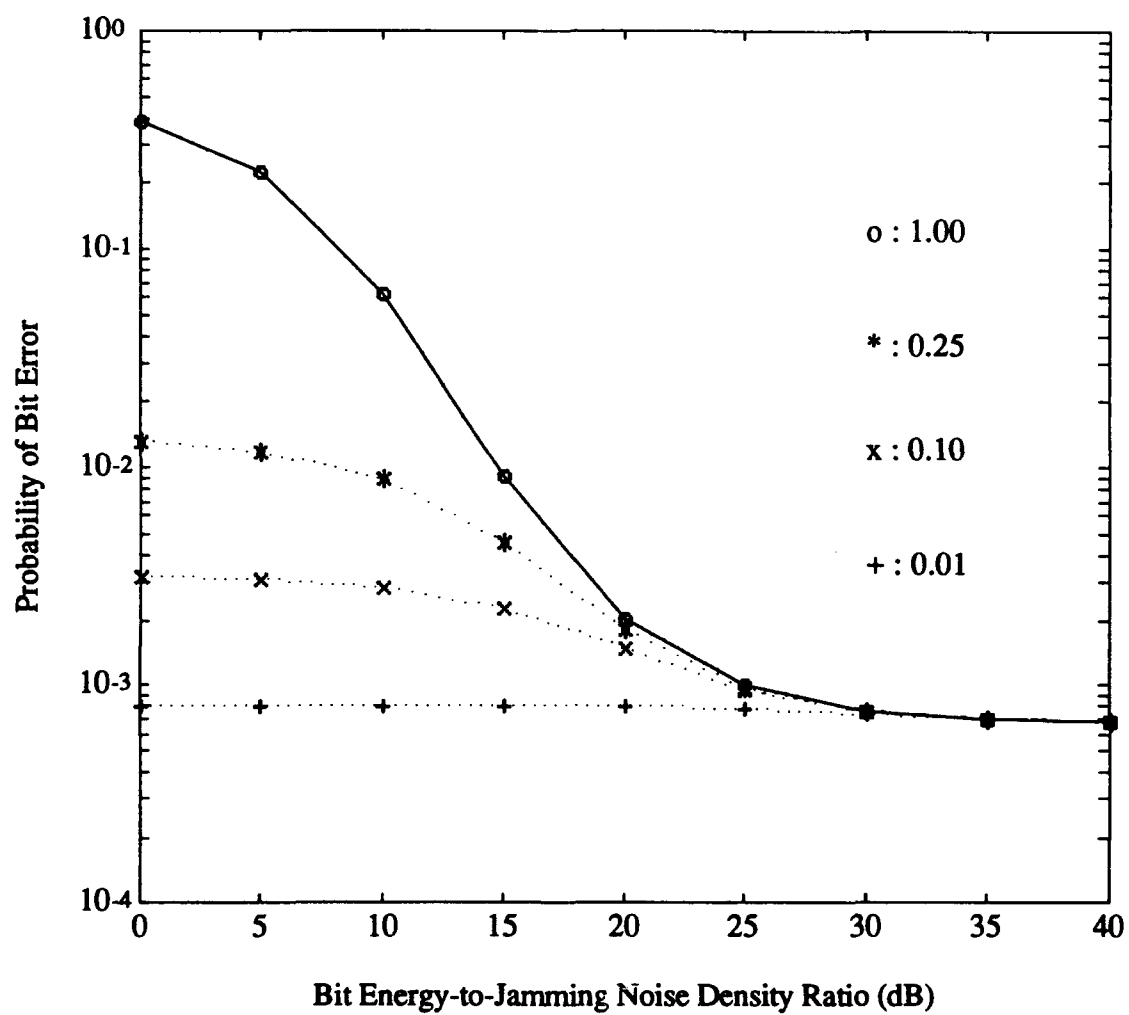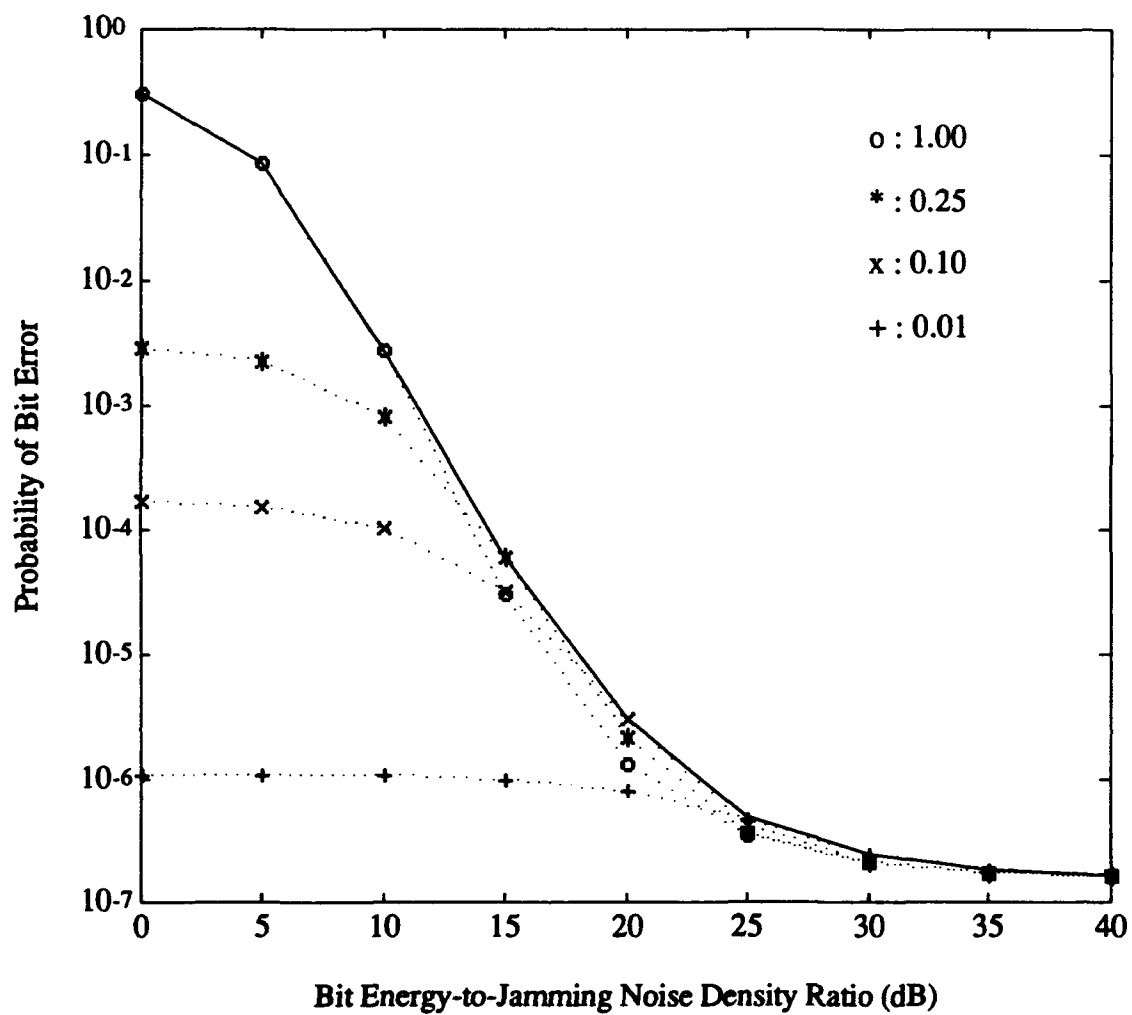
Figure 9.   Ideal receiver performance for a Ricean faded signal with M=4,
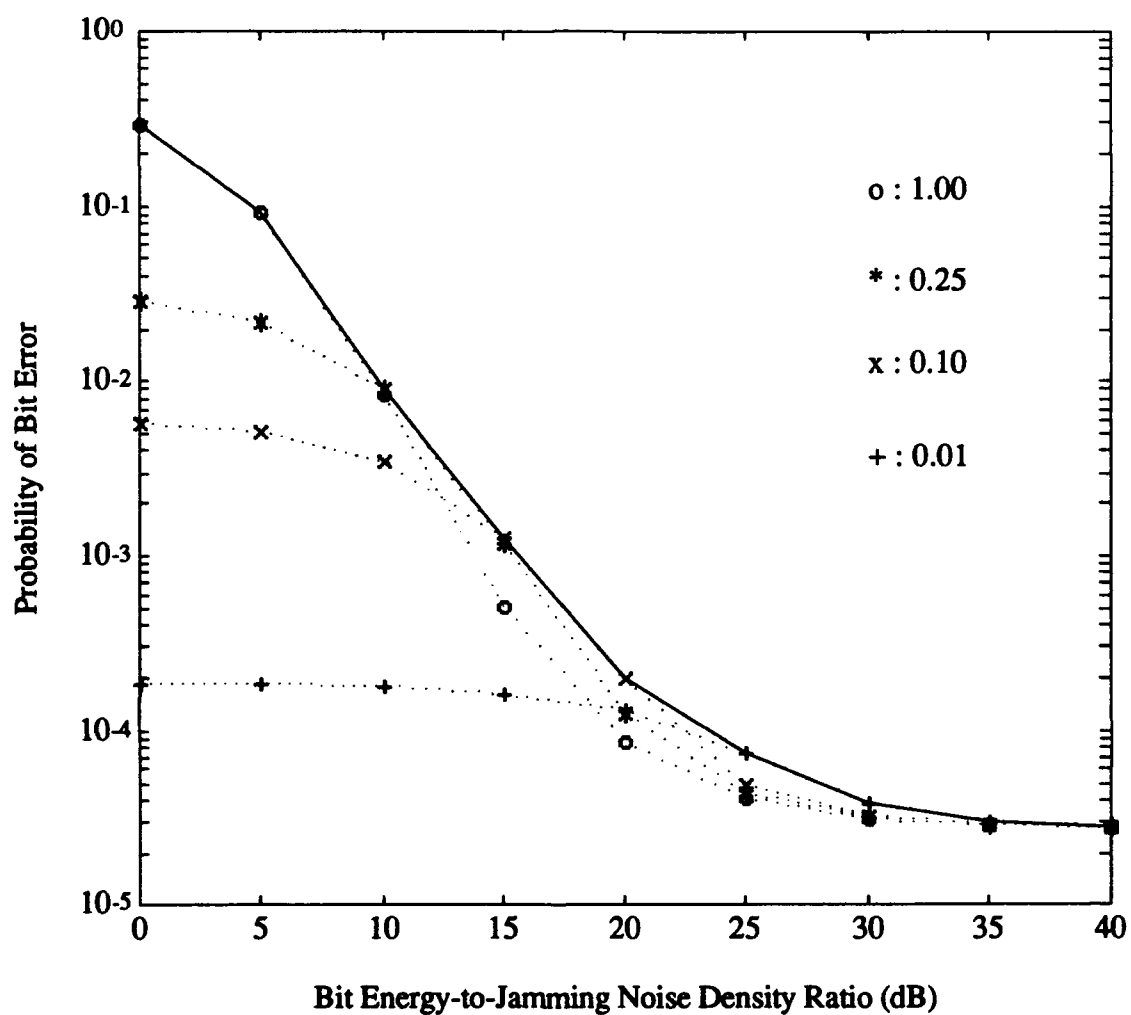L=4, E_b/N_0 =13.35 dB and direct-to-diffuse power ratio=100.

Figure 10. Ideal worst case receiver performance comparison for a Ricean faded signal with M=4, diversities of L=2, 3 and 4, E_b / N_0 =13.35 dB and direct-to-diffuse power ratio=100.

35

Figure 11. Ideal receiver performance for a Ricean faded signal with M=4, L=3, E_b / N_0 =13.35 dB and direct-to-diffuse power ratio=1.

36

Figure 12. Ideal receiver performance for a Ricean faded signal with M=2, L=4, E_b / N_0 =13.35 dB and direct-to-diffuse power ratio=10.

37

Figure 13. Ideal receiver performance for a Ricean faded signal with M=8,
L=4, E_b/N_0 =13.35 dB and direct-to-diffuse power ratio=10.

Figure 14. Receiver performance for a Ricean faded signal with M=4, L=2, $E_b / N_0 = 13.35$ dB, direct-to-diffuse power ratio=10 and ±50% estimate error with $\hat{\sigma}_k^2$ a random variable.
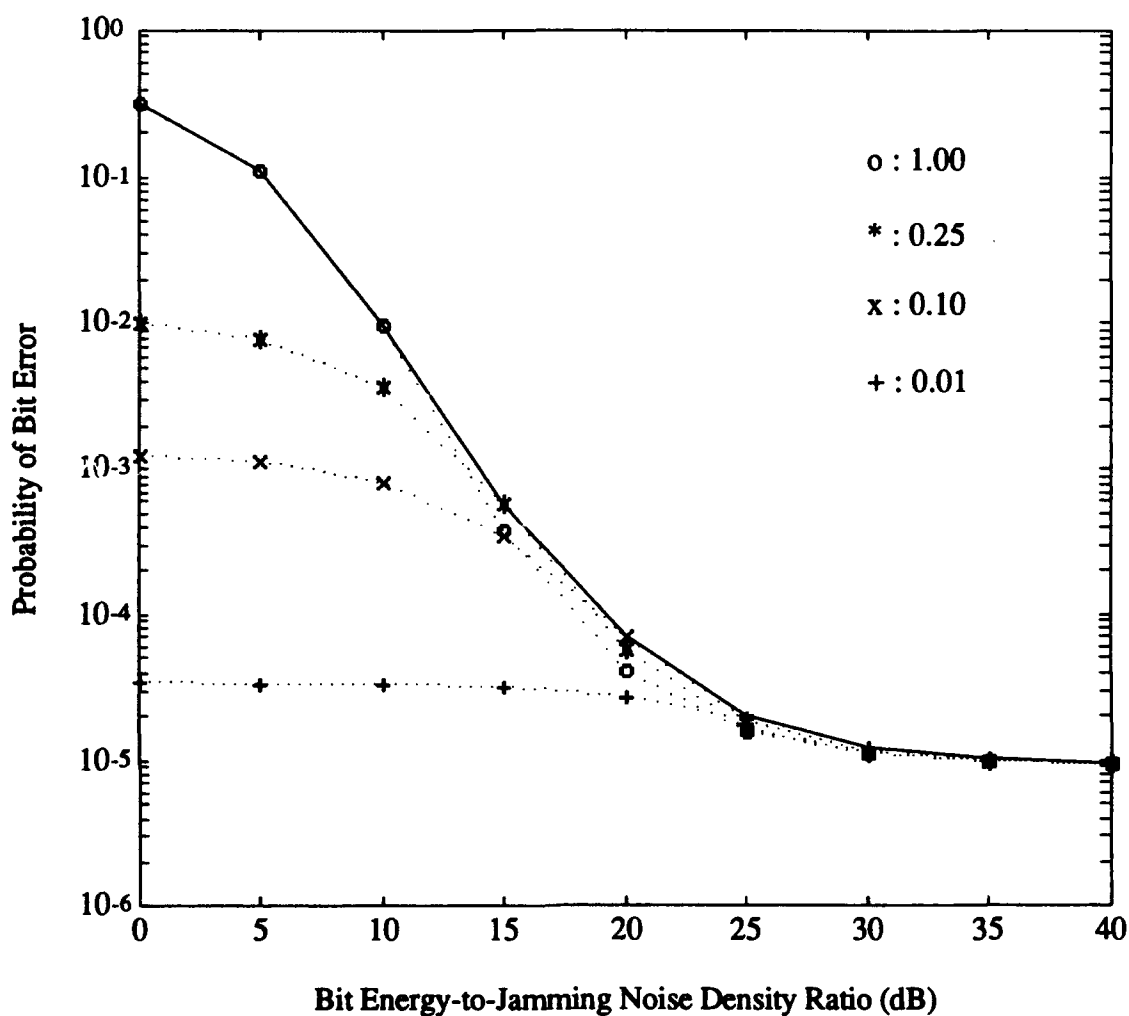
Figure 15. Receiver performance for a Ricean faded signal with M=4, L=3, E_b / N_0 =13.35 dB, direct-to-diffuse power ratio=10 and ±50% estimate error with $\hat{\sigma}_k^2$ a random variable.
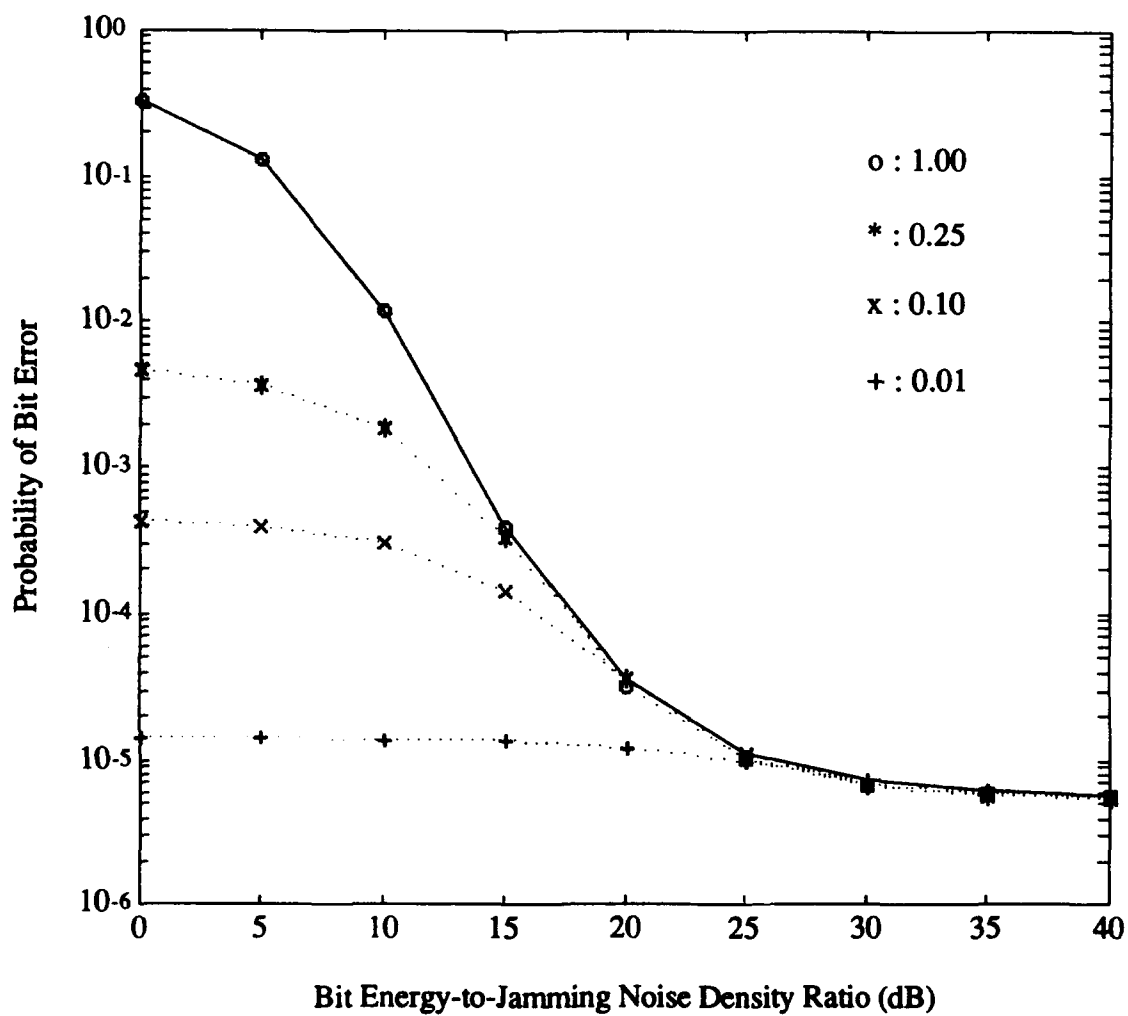
40

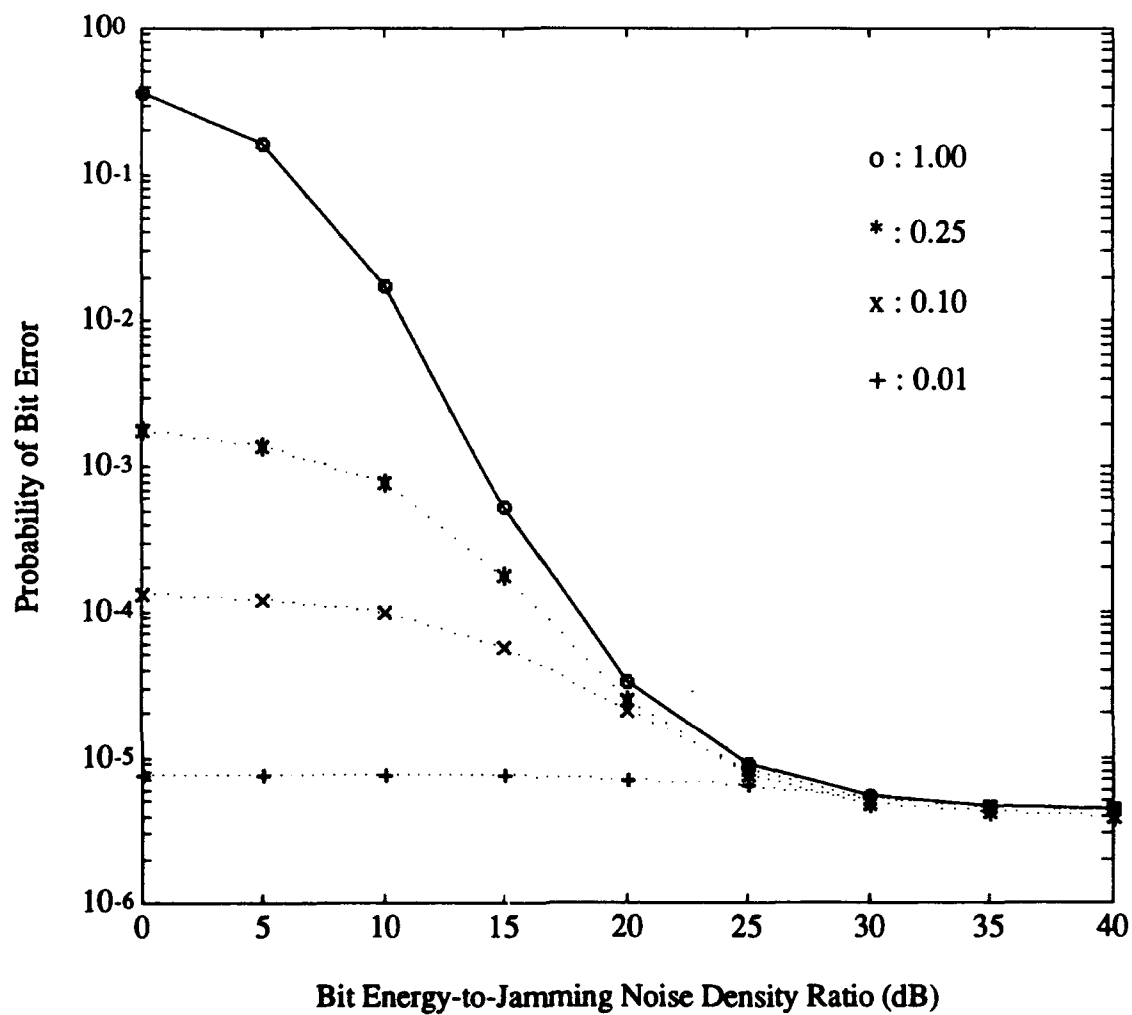Figure 16. Receiver performance for a Ricean faded signal with M=4, L=4, E_b / N_0 =13.35 dB, direct-to-diffuse power ratio=10 and ±50% estimate error with $\hat{\sigma}_k^2$ a random variable.

Figure 17. Receiver performance for a Ricean faded signal with M=4, L=6, E_b/N_0 =13.35 dB, direct-to-diffuse power ratio=10 and ±50% estimate error with $\hat{\sigma}_k^2$ a random variable.
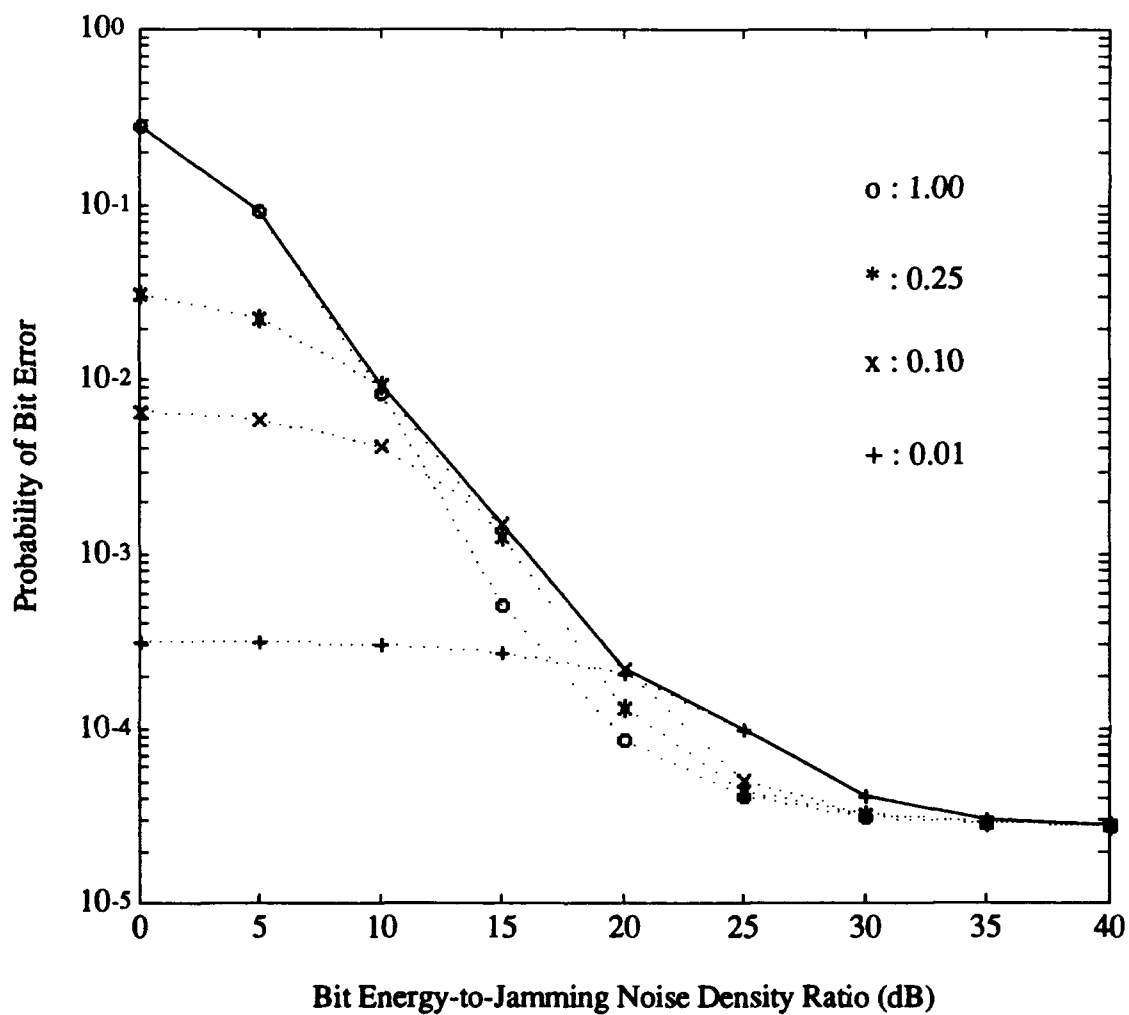
Figure 18.   Receiver performance for a Ricean faded signal with M=4, L=2,
             E_b/N_0 =13.35 dB, direct-to-diffuse power ratio=10 and
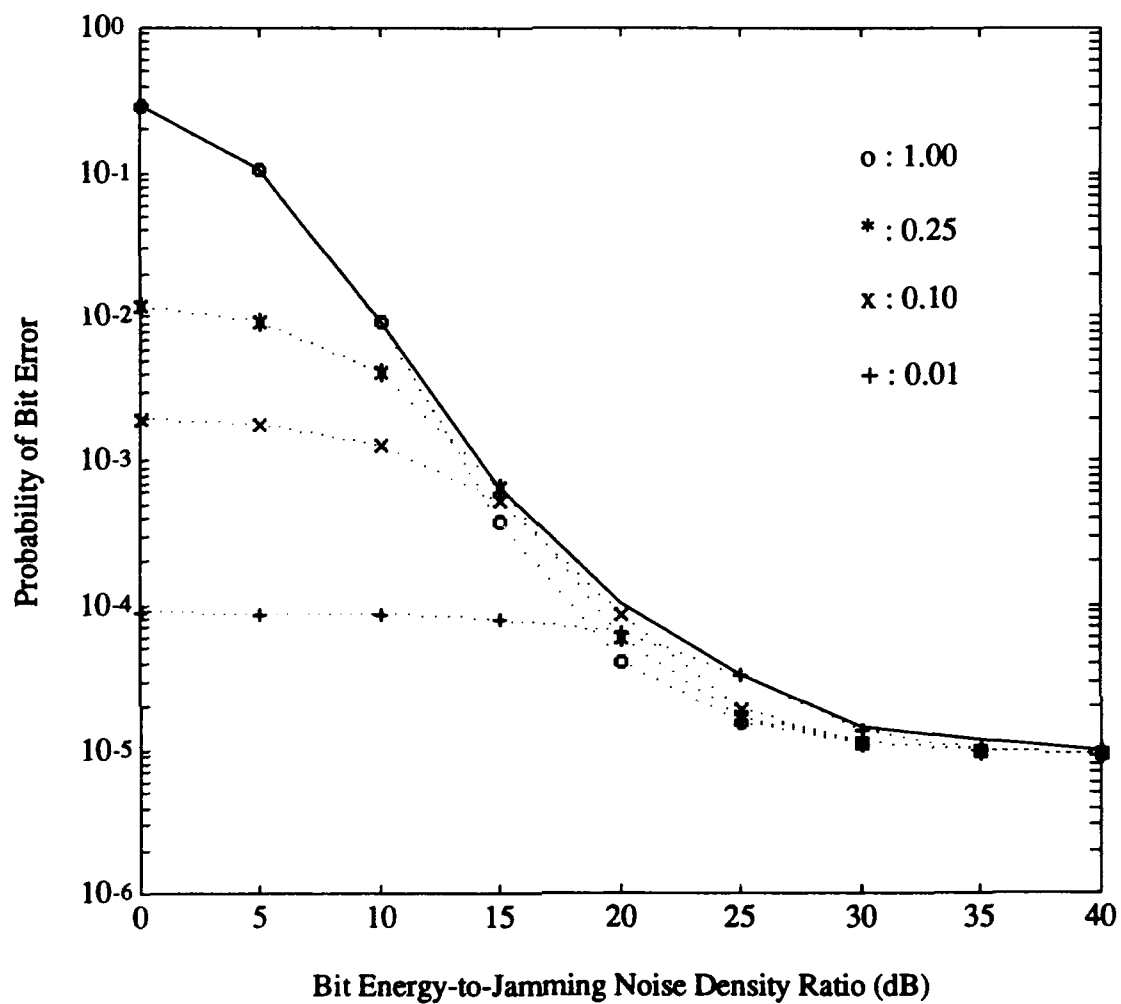   ±100% estimate error with $\hat{\sigma}_k^2$ a random variable.

43

Figure 19. Receiver performance for a Ricean faded signal with M=4, L=3, $E_b/N_0 =13.35$ dB, direct-to-diffuse power ratio=10 and $\pm 100\%$ estimate error with $\hat{\sigma}_k^2$ a random variable.
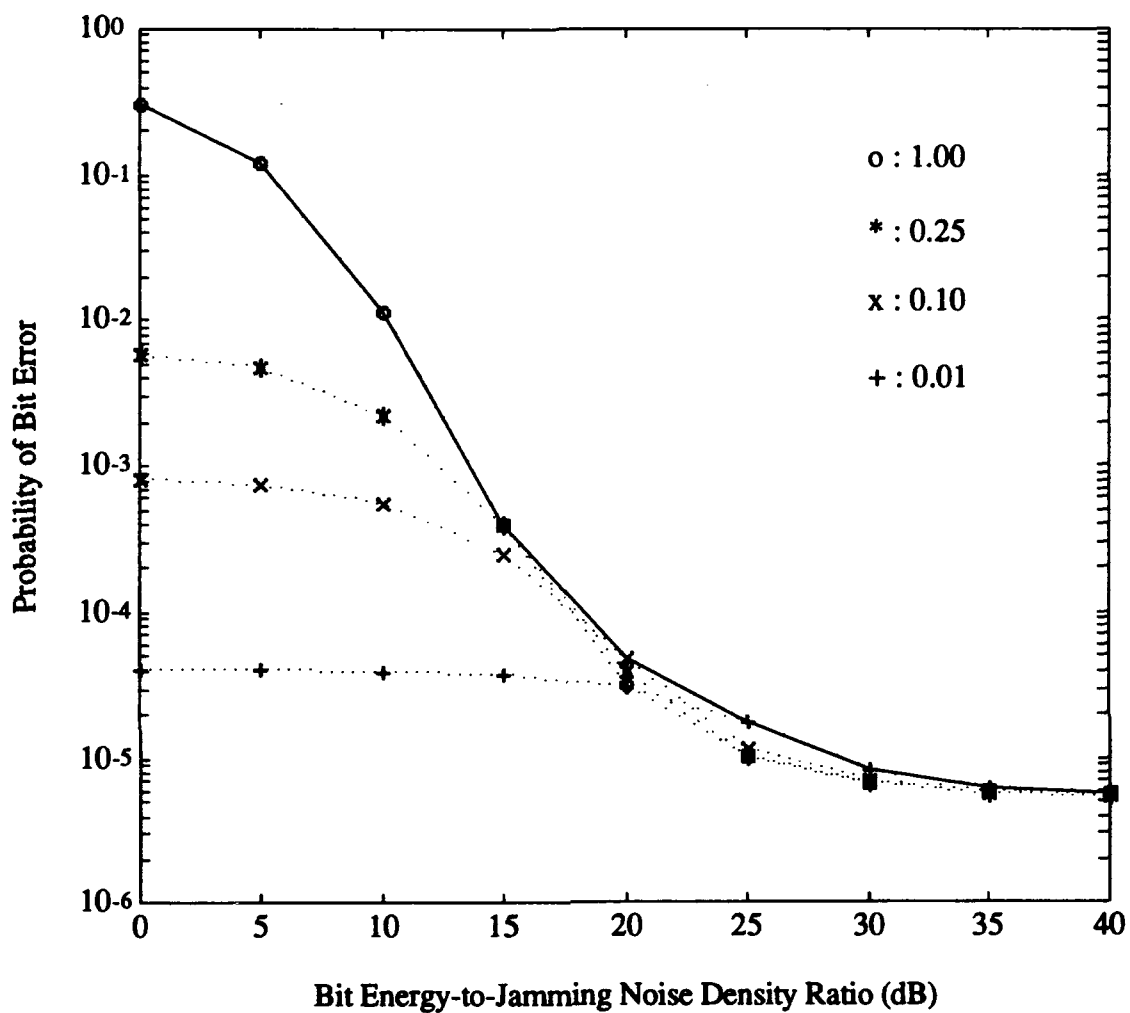
Figure 20. Receiver performance for a Ricean faded signal with M=4, L=4, E_b/N_0 =13.35 dB, direct-to-diffuse power ratio=10 and ±100% estimate error with $\hat{\sigma}_k^2$ a random variable.
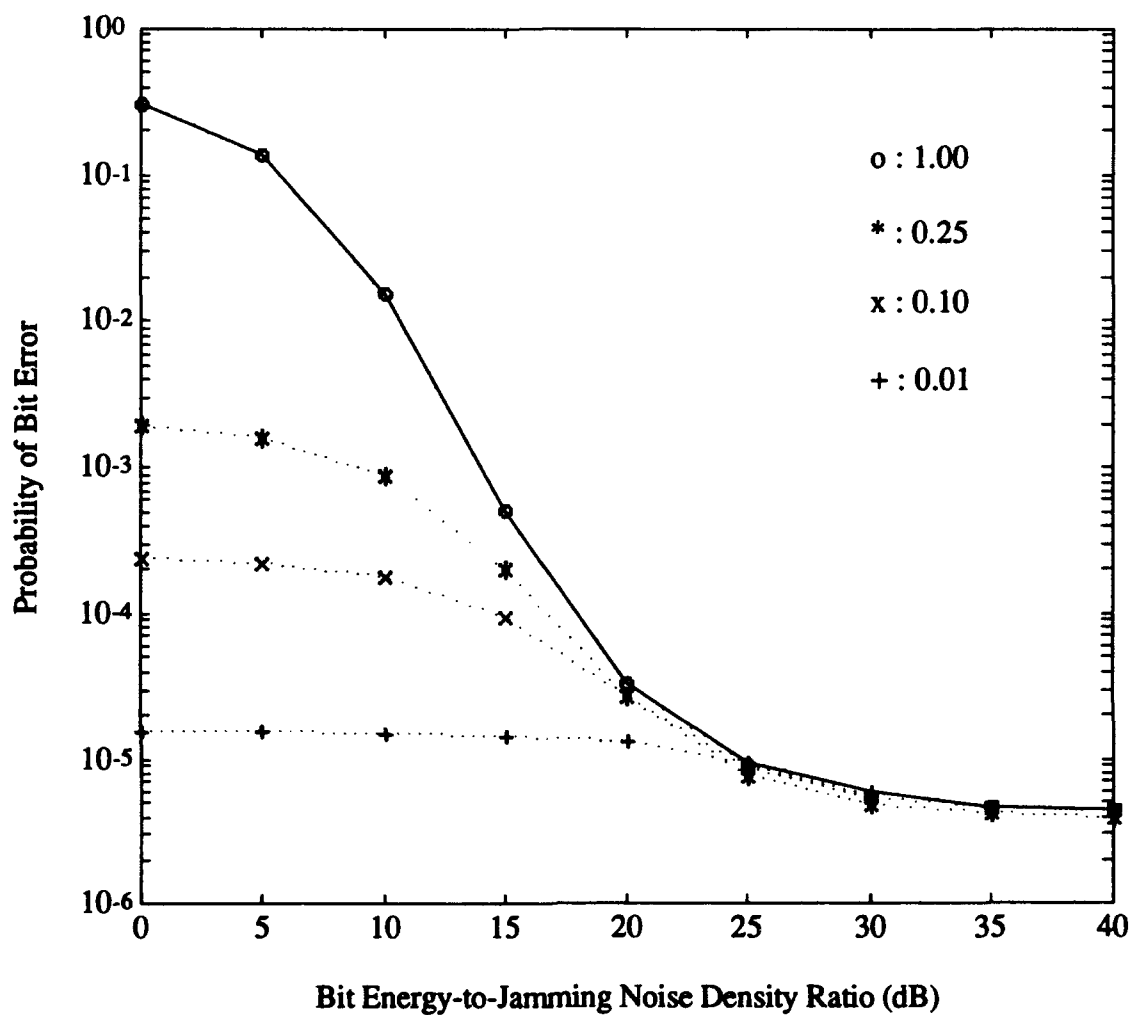
Figure 21. Receiver performance for a Ricean faded signal with M=4, L=6, E_b/N_0 =13.35 dB, direct-to-diffuse power ratio=10 and ±100% estimate error with $\hat{\sigma}_k^2$ a random variable.
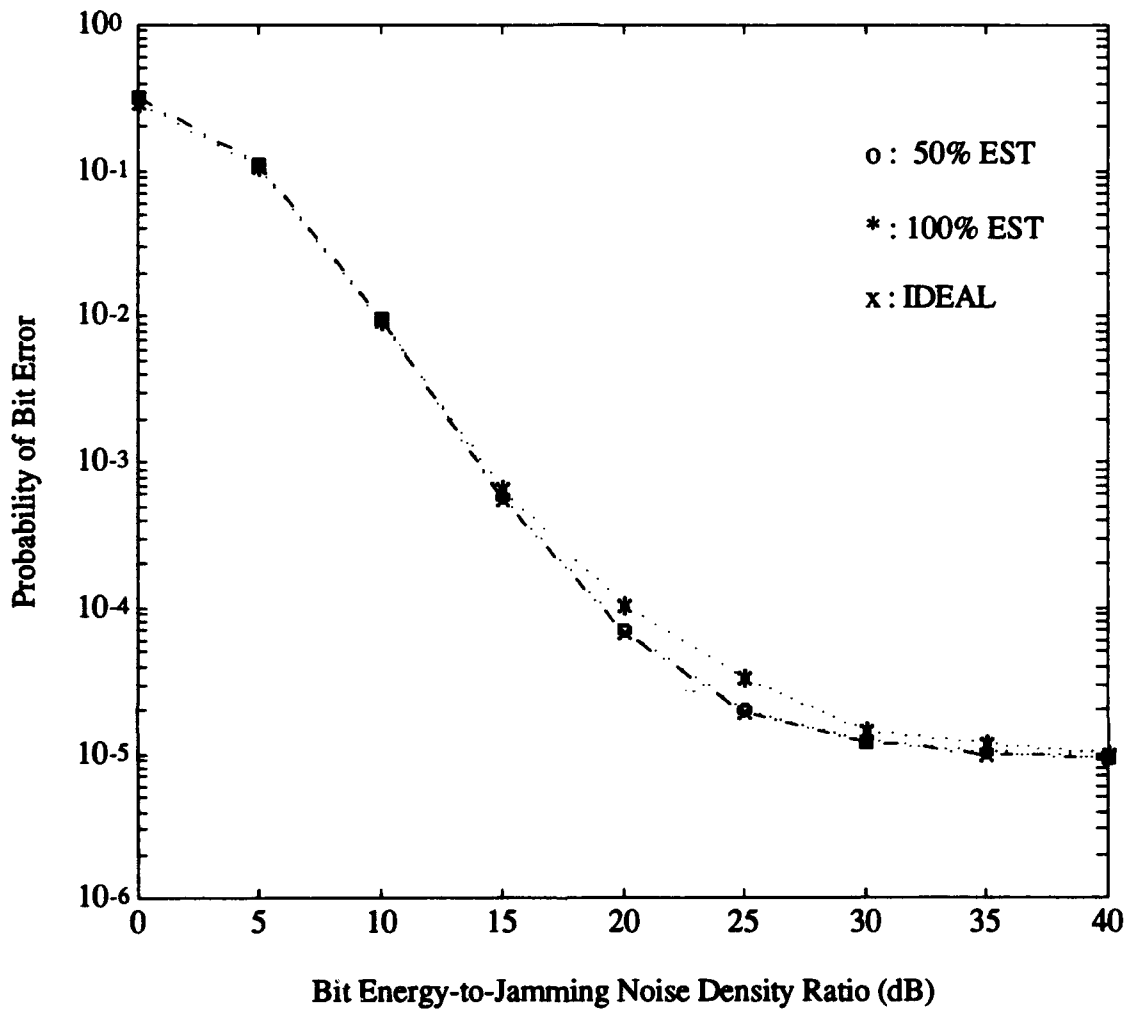
Figure 22. Worst case receiver performance comparison for a Ricean faded signal with M=4, L=3, E_b/N_0 =13.35 dB and direct-to-diffuse power ratio=10 with $\hat{\sigma}_k^2$ a random variable.

47

Figure 23. Worst case receiver performance comparison for a Ricean faded signal with M=4, L=4, E_b/N_0 =13.35 dB and direct-to-diffuse power ratio=10 with $\hat{\sigma}_k^2$ a random variable.

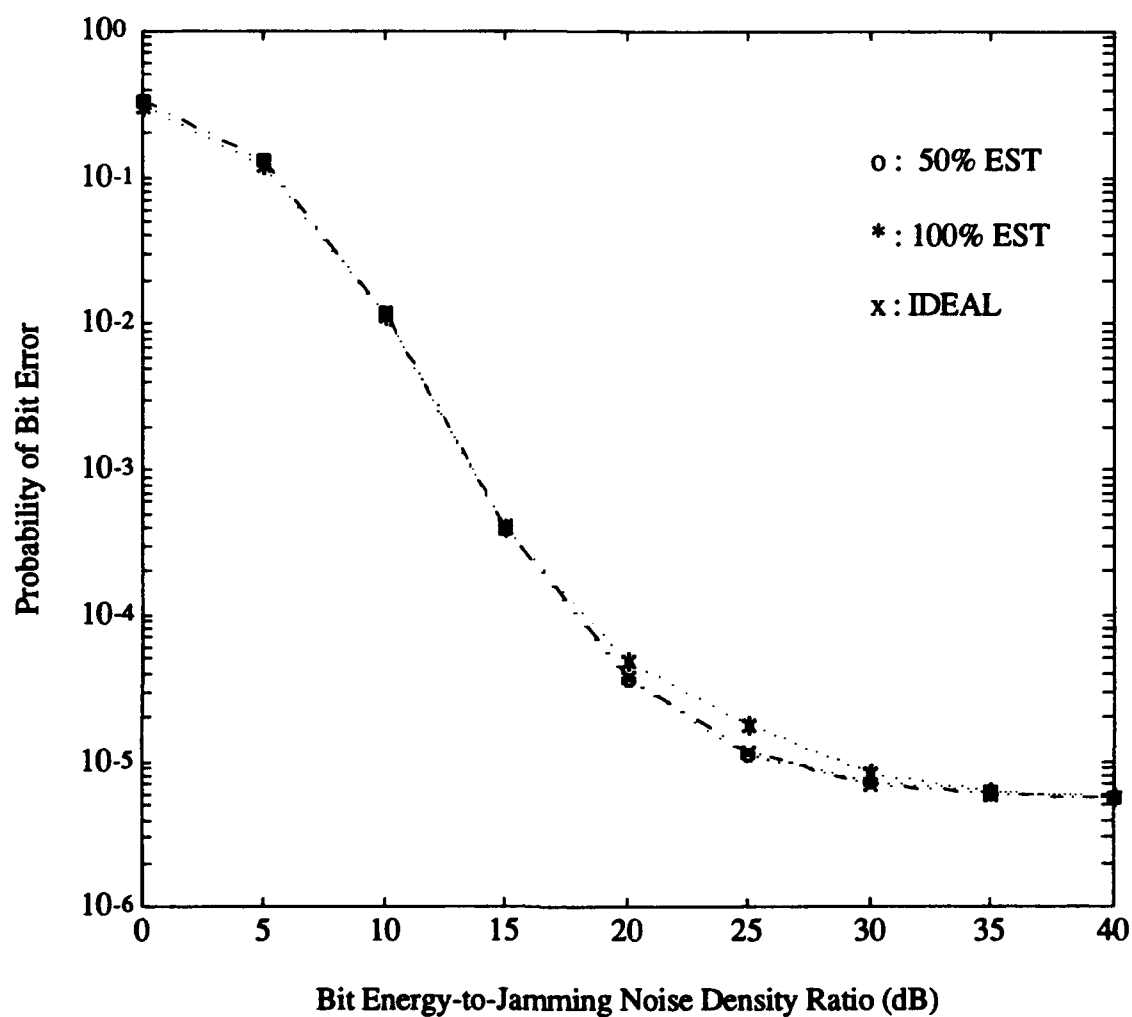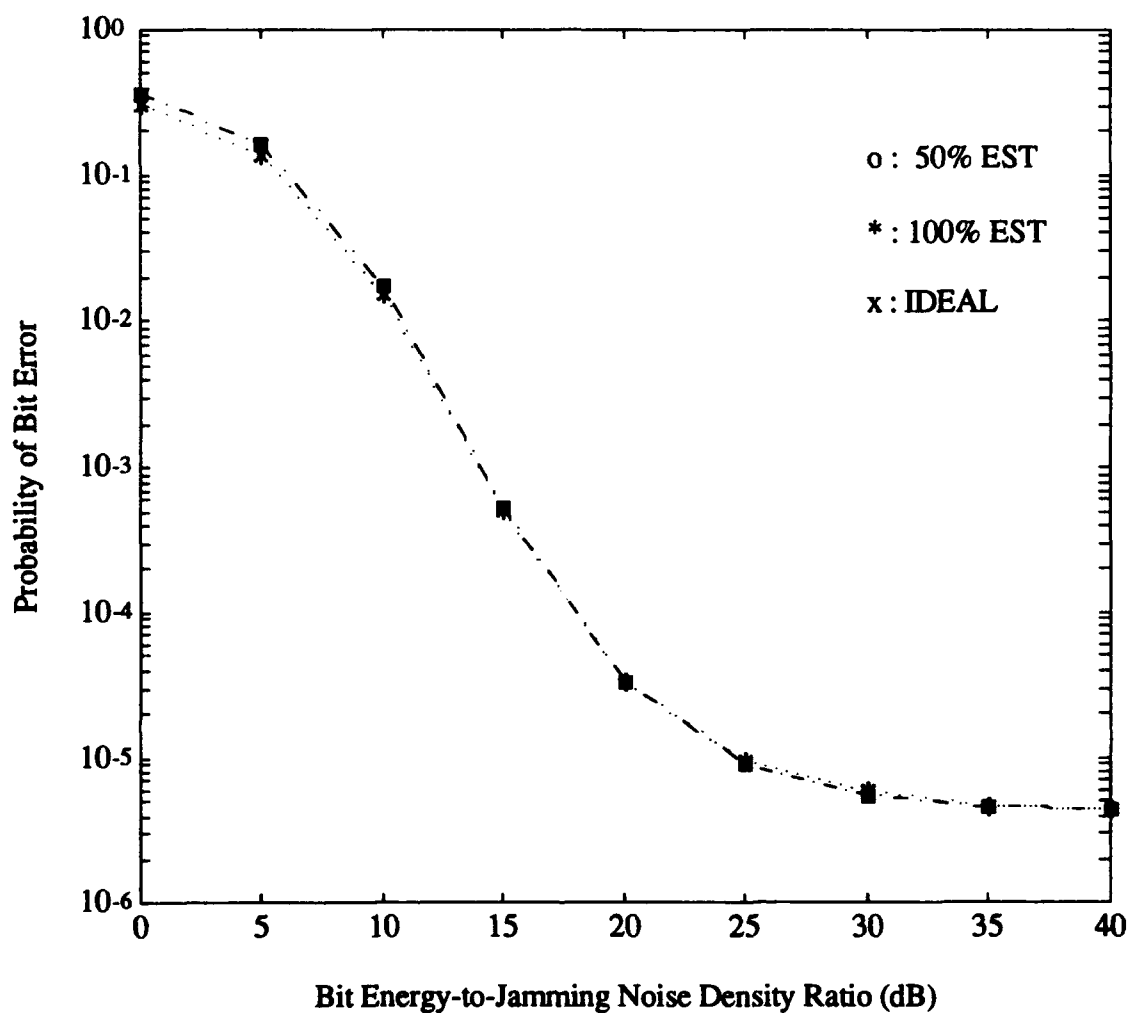Figure 24. Worst case receiver performance comparison for a Ricean faded signal with M=4, L=6, E_b/N_0 =13.35 dB and direct-to-diffuse power ratio=10 with $\hat{\sigma}_k^2$ a random variable.
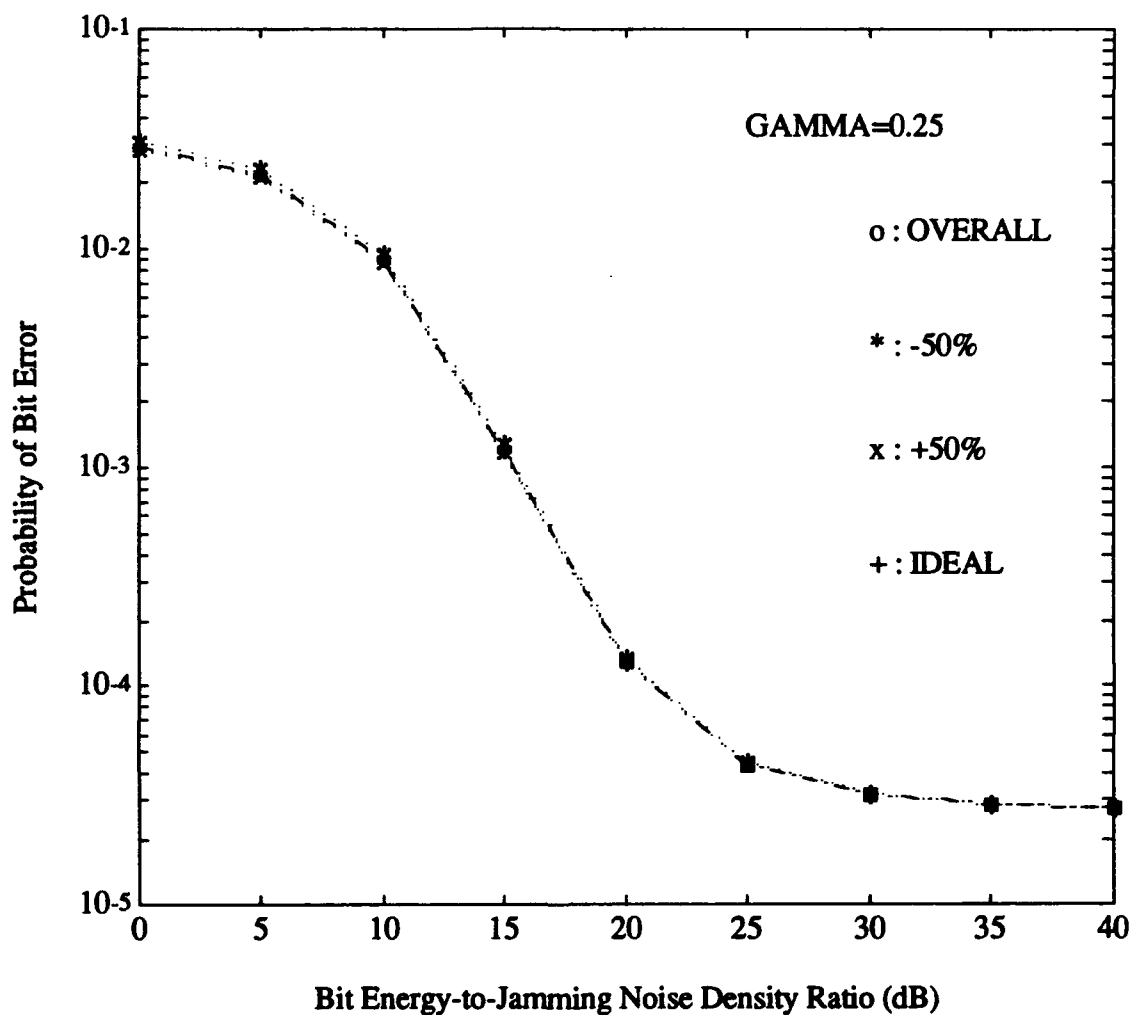
Figure 25. Receiver performance for a Ricean faded signal with M=4, L=2, E_b/N_0 =13.35 dB and direct-to-diffuse power ratio=10 with $\gamma = 0.25$ and ±50% estimate error with $\hat{\sigma}_k^2$ a parameter. For comparison, the performance with $\hat{\sigma}_k^2$ modeled as a random variable is also shown (labeled "overall").

50

Figure 26. Receiver performance for a Ricean faded signal with M=4, L=3, $E_b/N_0 = 13.35$ dB and direct-to-diffuse power ratio=10 with $\gamma = 0.25$ and ±50% estimate error with $\hat{\sigma}_k^2$ a parameter. For comparison, the performance with $\hat{\sigma}_k^2$ modeled as a random variable is also shown (labeled "overall").

51

Figure 27. Receiver performance for a Ricean faded signal with M=4, L=4, E_b/N_0 =13.35 dB and direct-to-diffuse power ratio=10 with $\gamma = 0.25$ and ±50% estimate error with $\hat{\sigma}_k^2$ a parameter. For comparison, the performance with $\hat{\sigma}_k^2$ modeled as a random variable is also shown (labeled "overall").
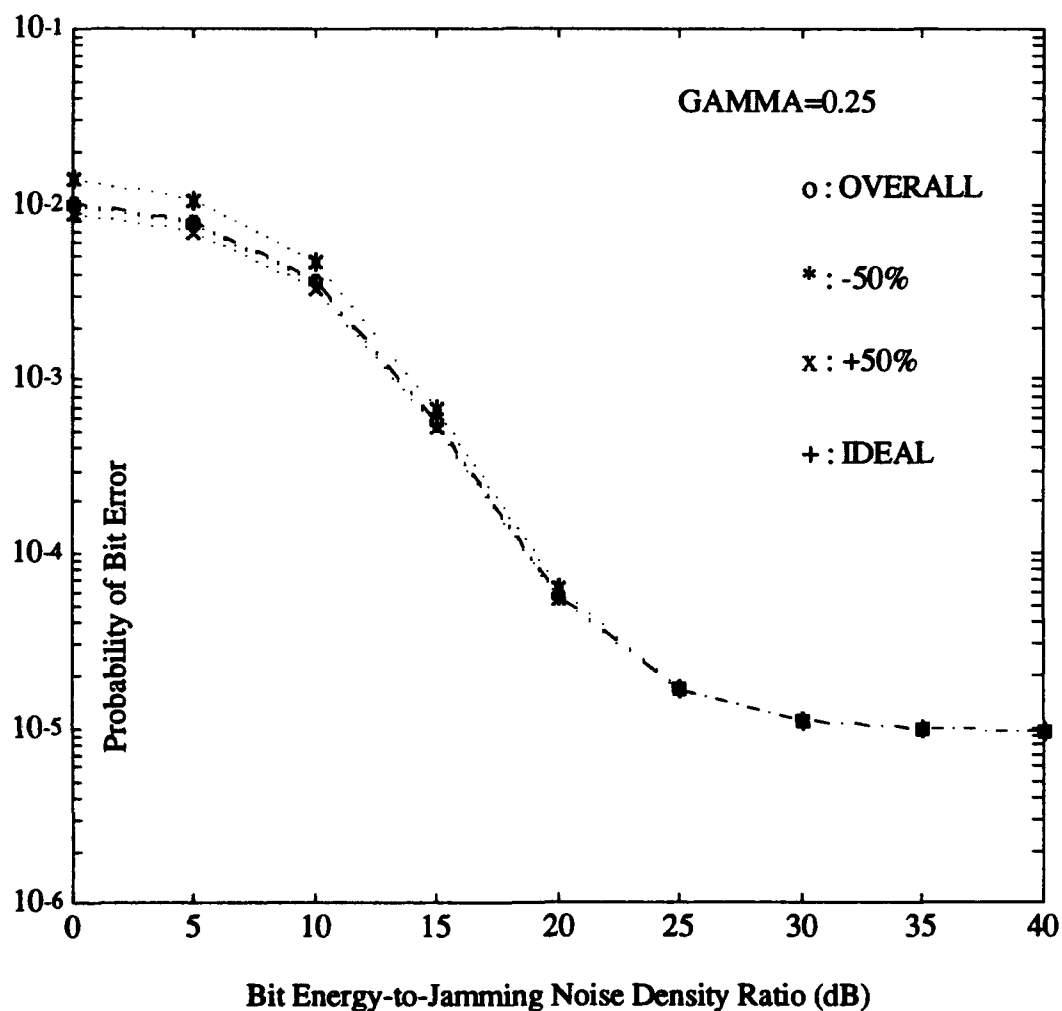
Figure 28. Receiver performance for a Ricean faded signal with M=4, L=6, E_b/N_0 =13.35 dB and direct-to-diffuse power ratio=10 with γ = 0.25 and ±50% estimate error with $\hat{\sigma}_k^2$ a parameter. For comparison, the performance with $\hat{\sigma}_k^2$ modeled as a random variable is also shown (labeled "overall").
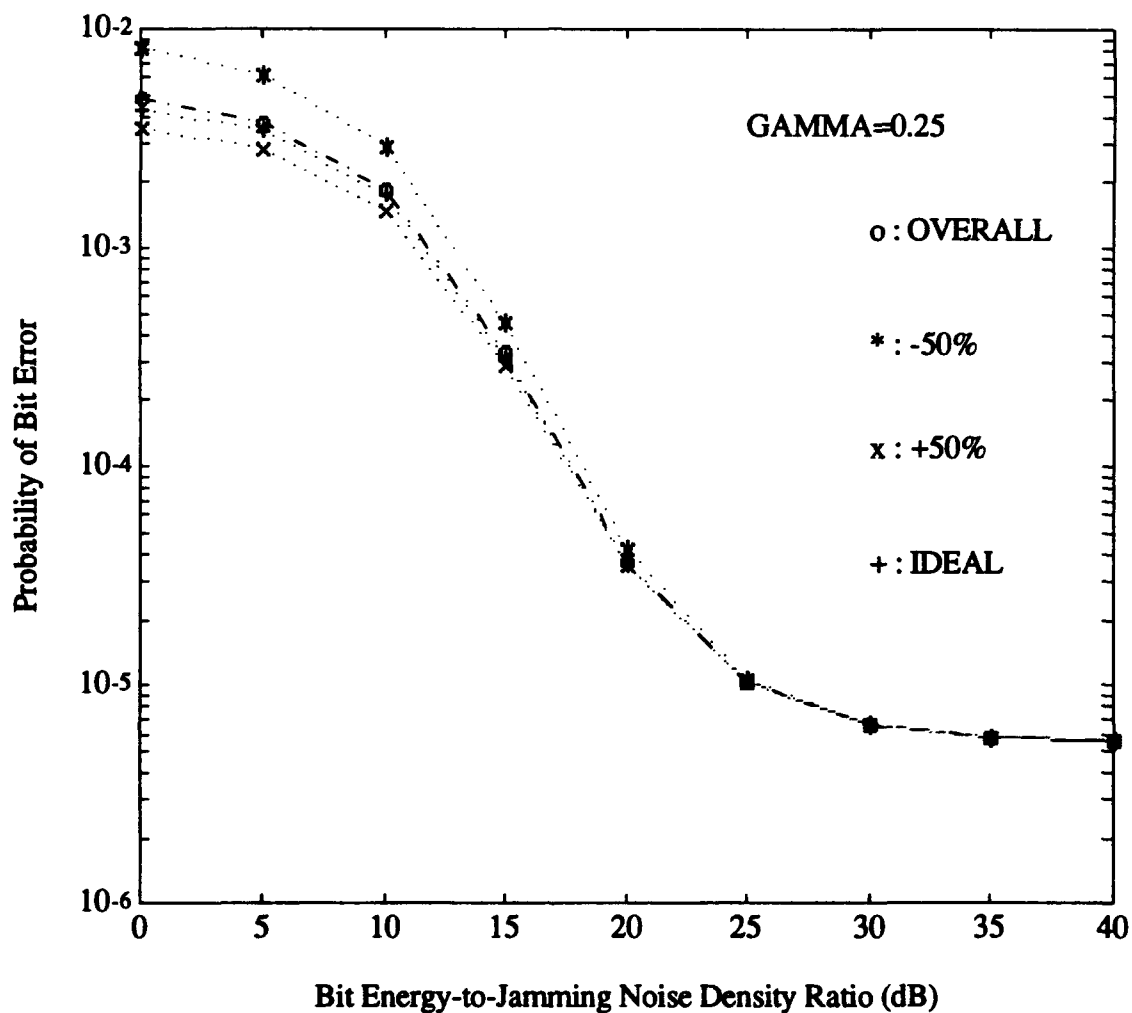
Figure 29. Receiver performance for a Ricean faded signal with M=2, L=4, E_b/N_0 =13.35 dB and direct-to-diffuse power ratio=10 with $\gamma = 0.25$ and ±50% estimate error with $\hat{\sigma}_k^2$ a parameter. For comparison, the performance with $\hat{\sigma}_k^2$ modeled as a random variable is also shown (labeled "overall").
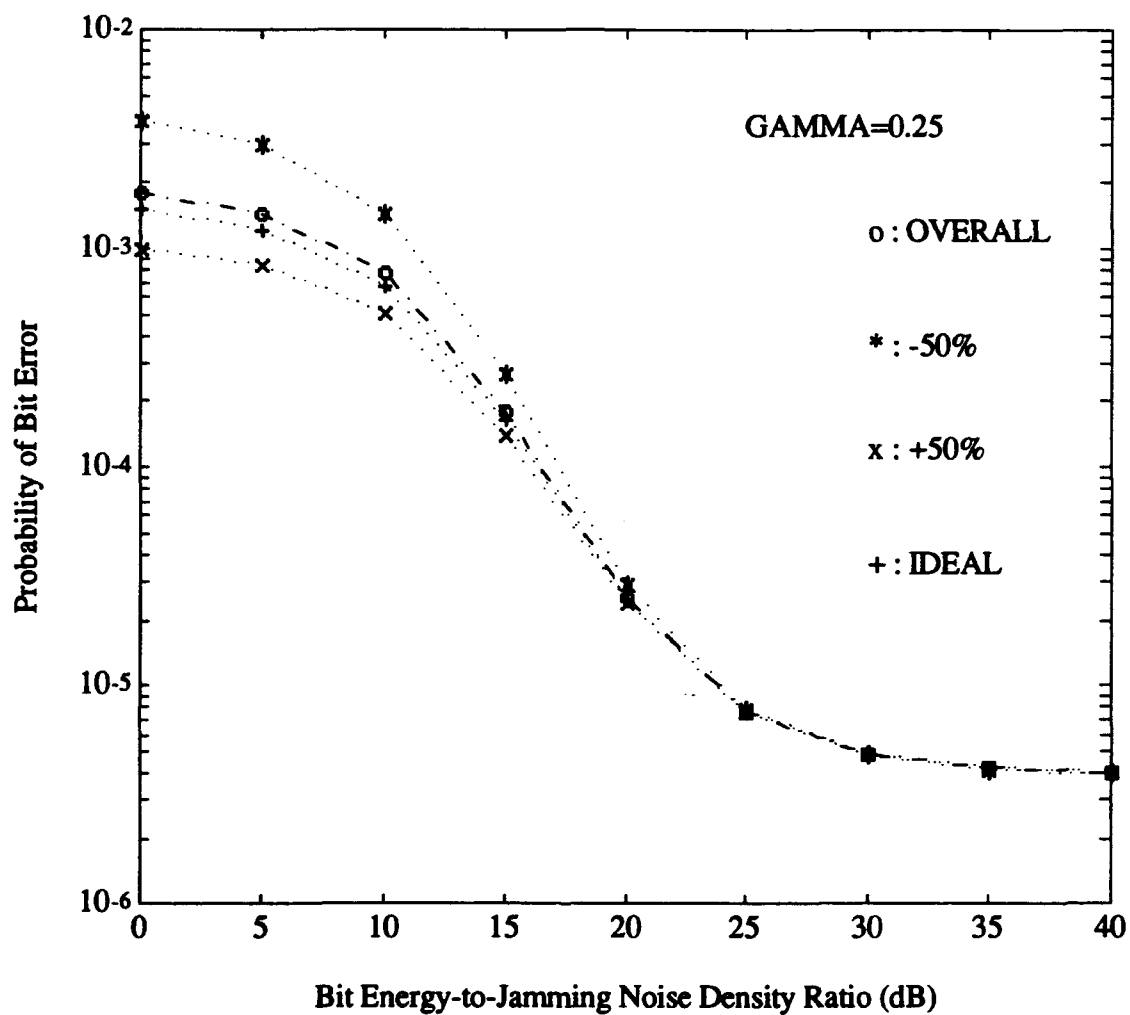
Figure 30. Receiver performance for a Ricean faded signal with M=8, L=4,
E_b/N_0 =13.35 dB and direct-to-diffuse power ratio=10 with
$\gamma = 0.25$ and ±50% estimate error with $\hat{\sigma}_k^2$ a parameter. For
comparison, the performance with $\hat{\sigma}_k^2$ modeled as a random
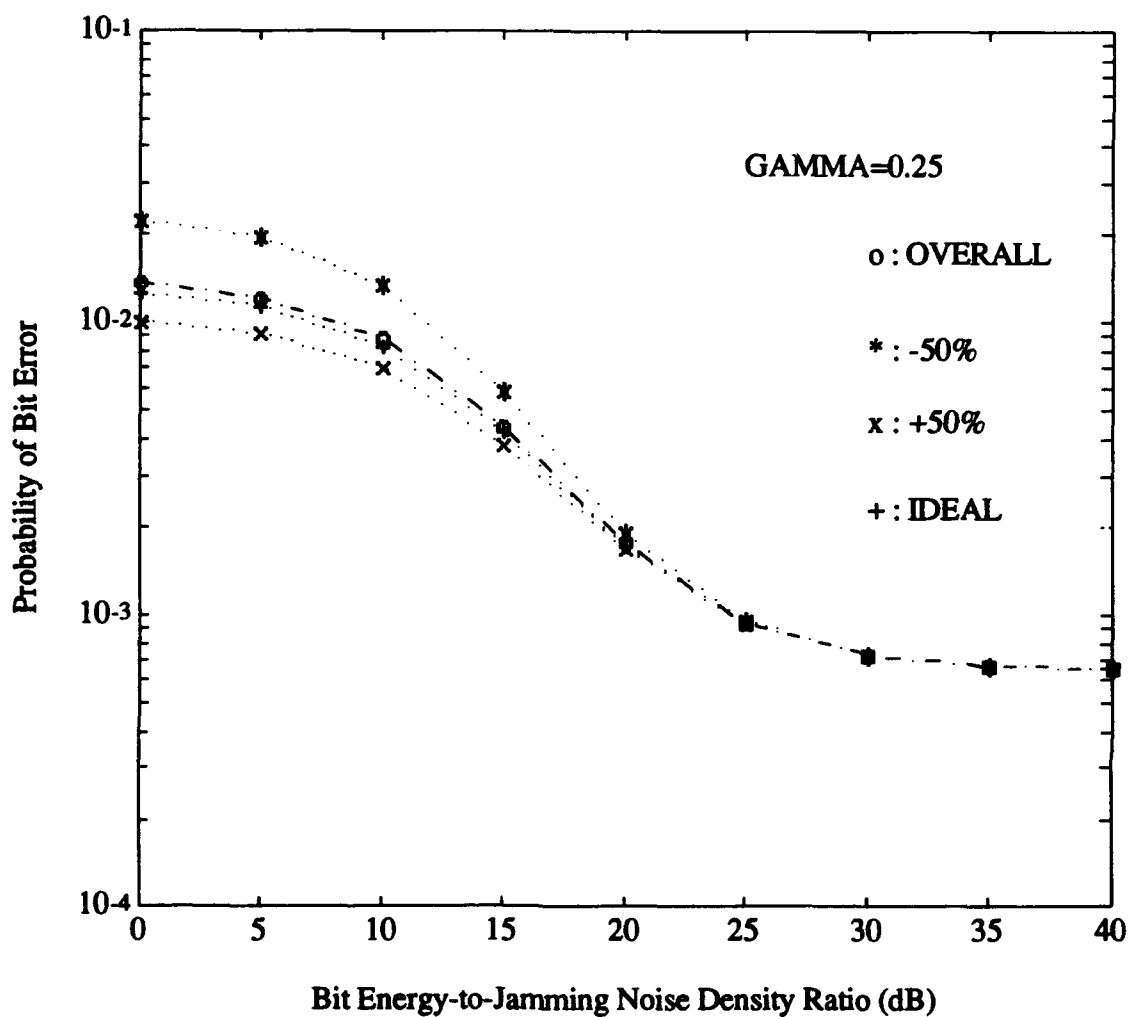variable is also shown (labeled "overall").

55

Figure 31. Receiver performance for a Ricean faded signal with M=2, L=4, $E_b/N_0 = 13.35$ dB and direct-to-diffuse power ratio=10 with $\gamma = 0.01$ and $\pm 50\%$ estimate error with $\hat{\sigma}_k^2$ a parameter. For comparison, the performance with $\hat{\sigma}_k^2$ modeled as a random variable is also shown (labeled "overall").
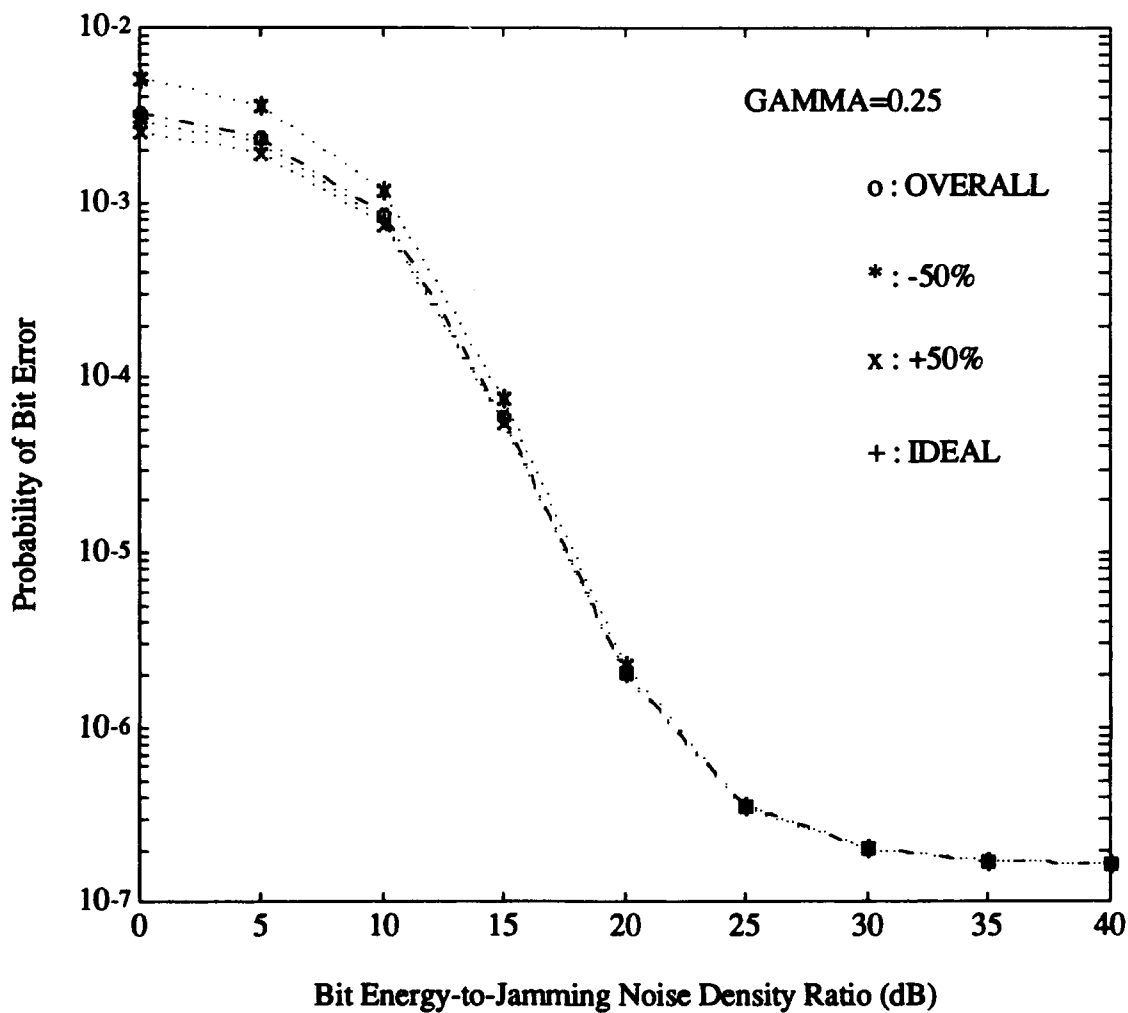
56

Figure 32. Receiver performance for a Ricean faded signal with M=4, L=4, E_b/N_0 =13.35 dB and direct-to-diffuse power ratio=10 with γ = 0.01 and ±50% estimate error with $\hat{\sigma}_k^2$ a parameter. For comparison, the performance with $\hat{\sigma}_k^2$ modeled as a random variable is also shown (labeled "overall").
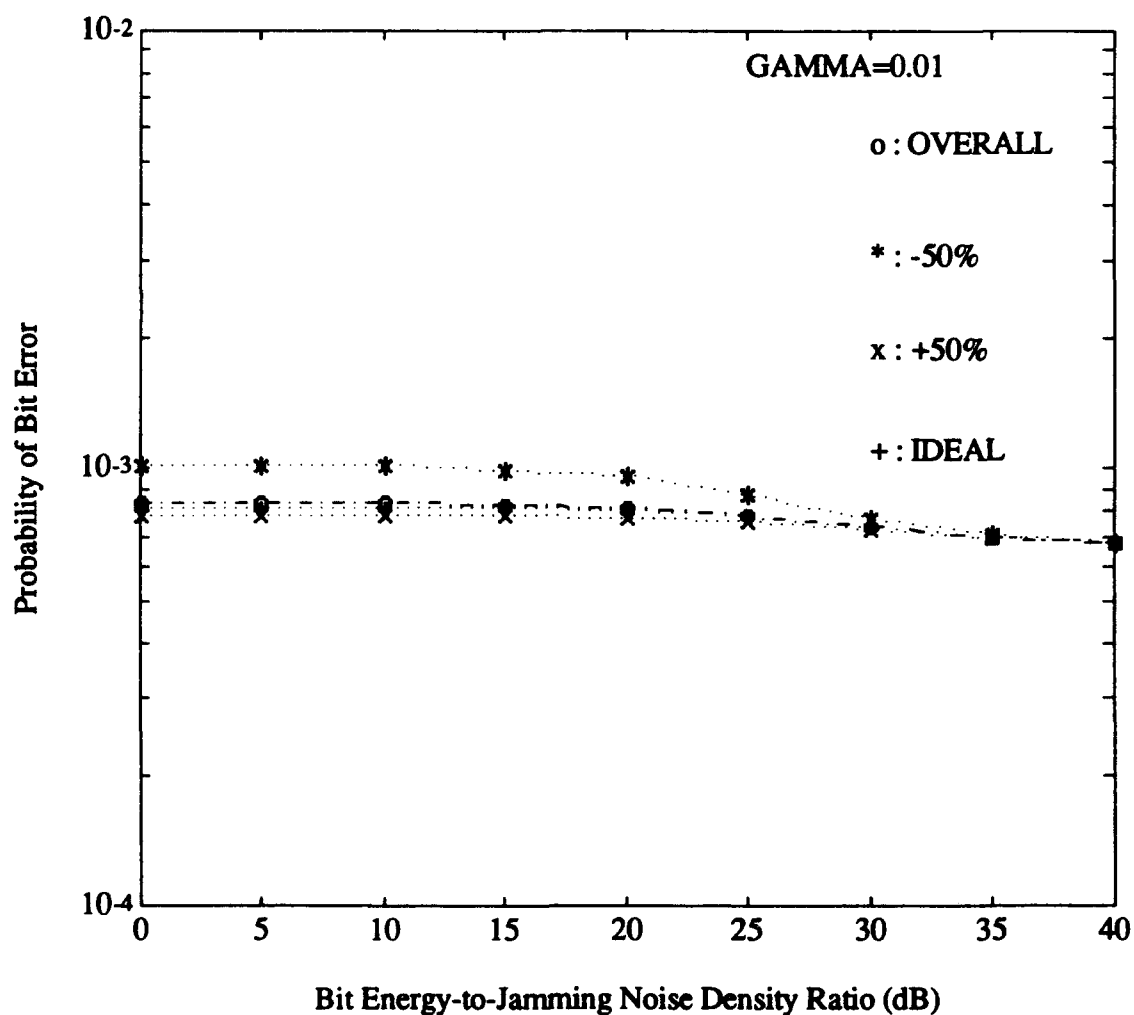
57

Figure 33. Receiver performance for a Ricean faded signal with M=8, L=4,
E_b/N_0 =13.35 dB and direct-to-diffuse power ratio=10 with
$\gamma = 0.01$ and ±50% estimate error with $\hat{\sigma}_k^2$ a parameter. For
comparison, the performance with $\hat{\sigma}_k^2$ modeled as a random
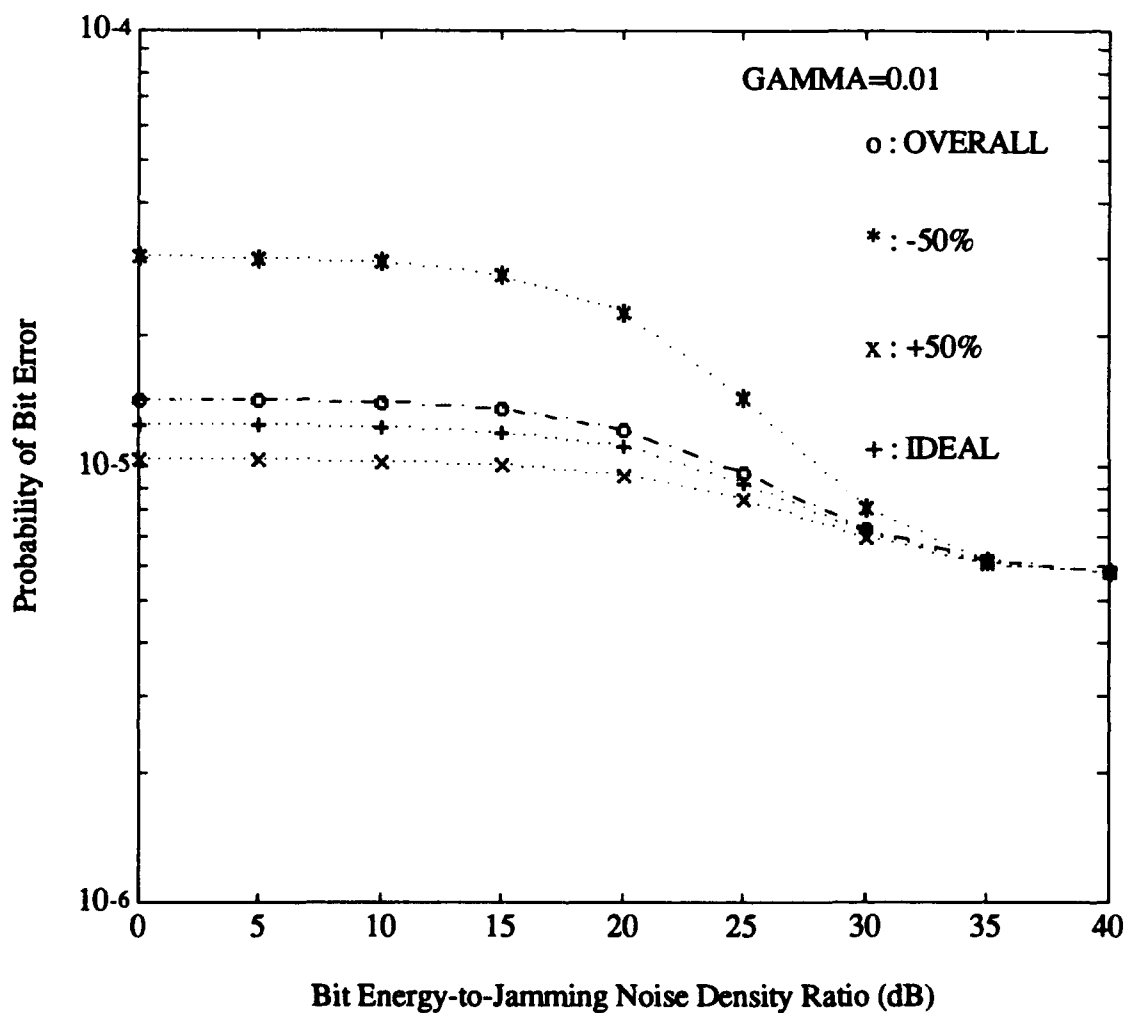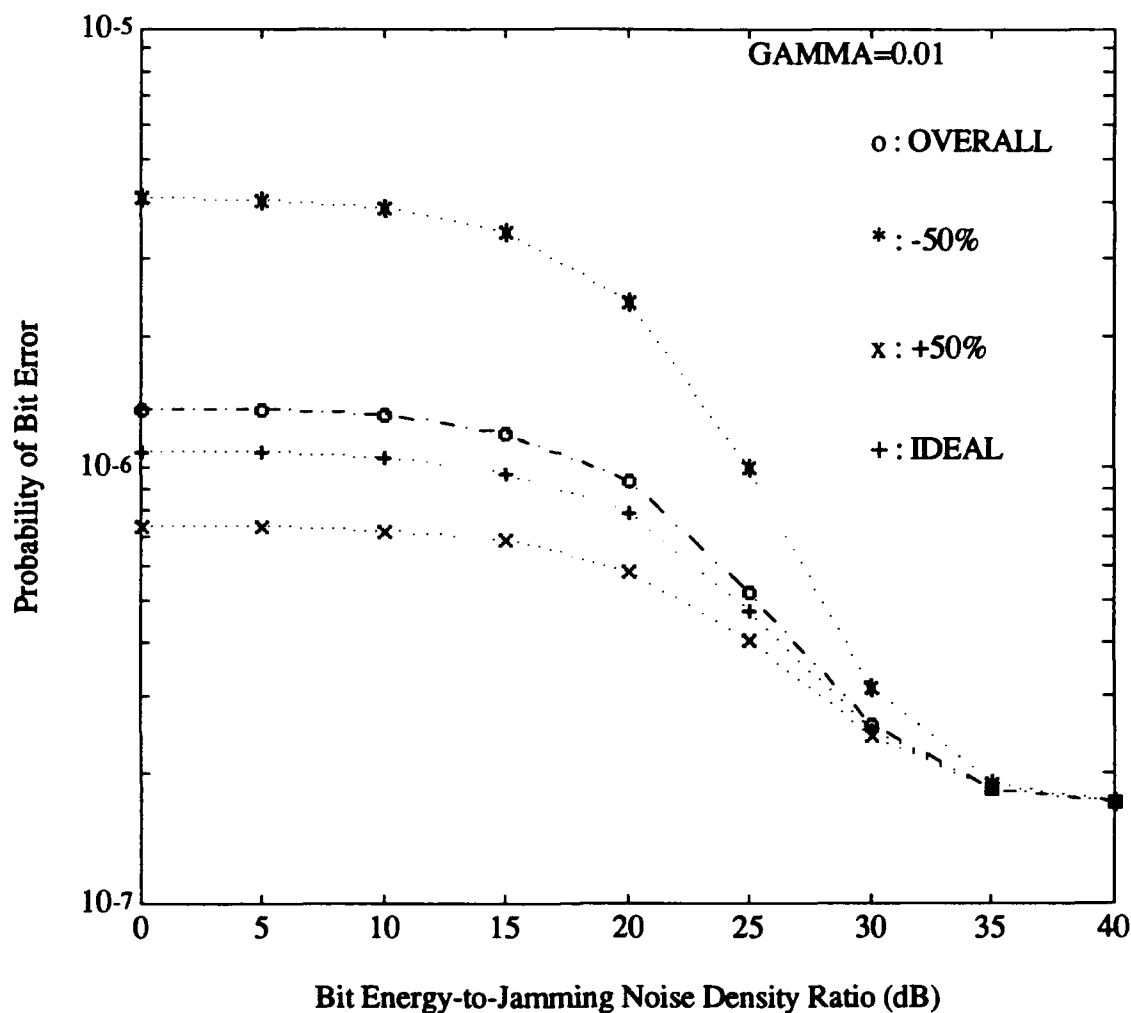variable is also shown (labeled "overall").

58

Figure 34. Receiver performance for a Ricean faded signal with M=4, L=2, E_b/N_0 =13.35 dB, direct-to-diffuse power ratio=100 and ±50% estimate error with $\hat{\sigma}_k^2$ a random variable.

Figure 35. Receiver performance for a Ricean faded signal with M=4, L=3, E_b/N_0 =13.35 dB, direct-to-diffuse power ratio=100 and ±50% estimate error with $\hat{\sigma}_k^2$ a random variable.
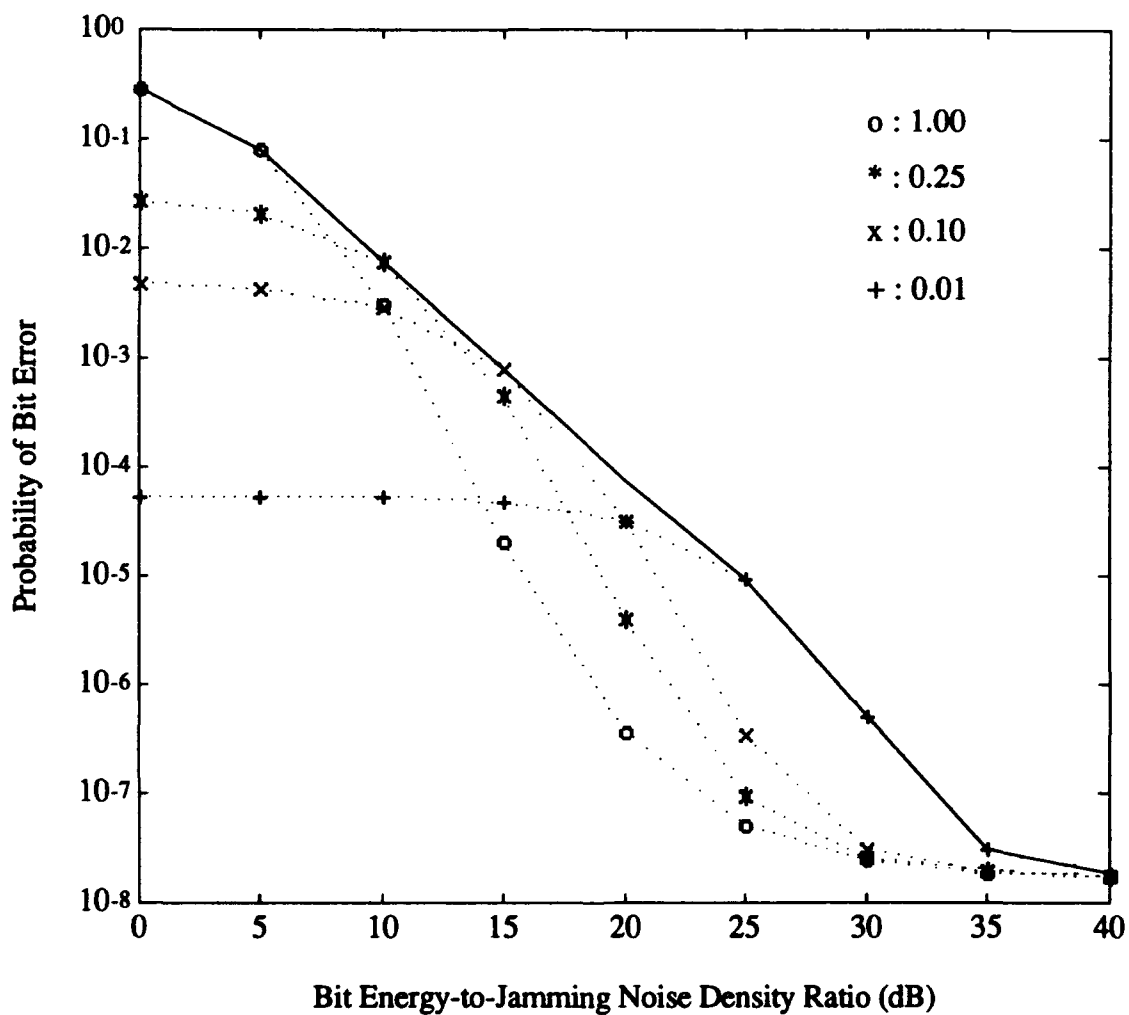
Figure 36. Receiver performance for a Ricean faded signal with M=4, L=4, E_b/N_0 =13.35 dB, direct-to-diffuse power ratio=100 and ±50% estimate error with $\hat{\sigma}_k^2$ a random variable.

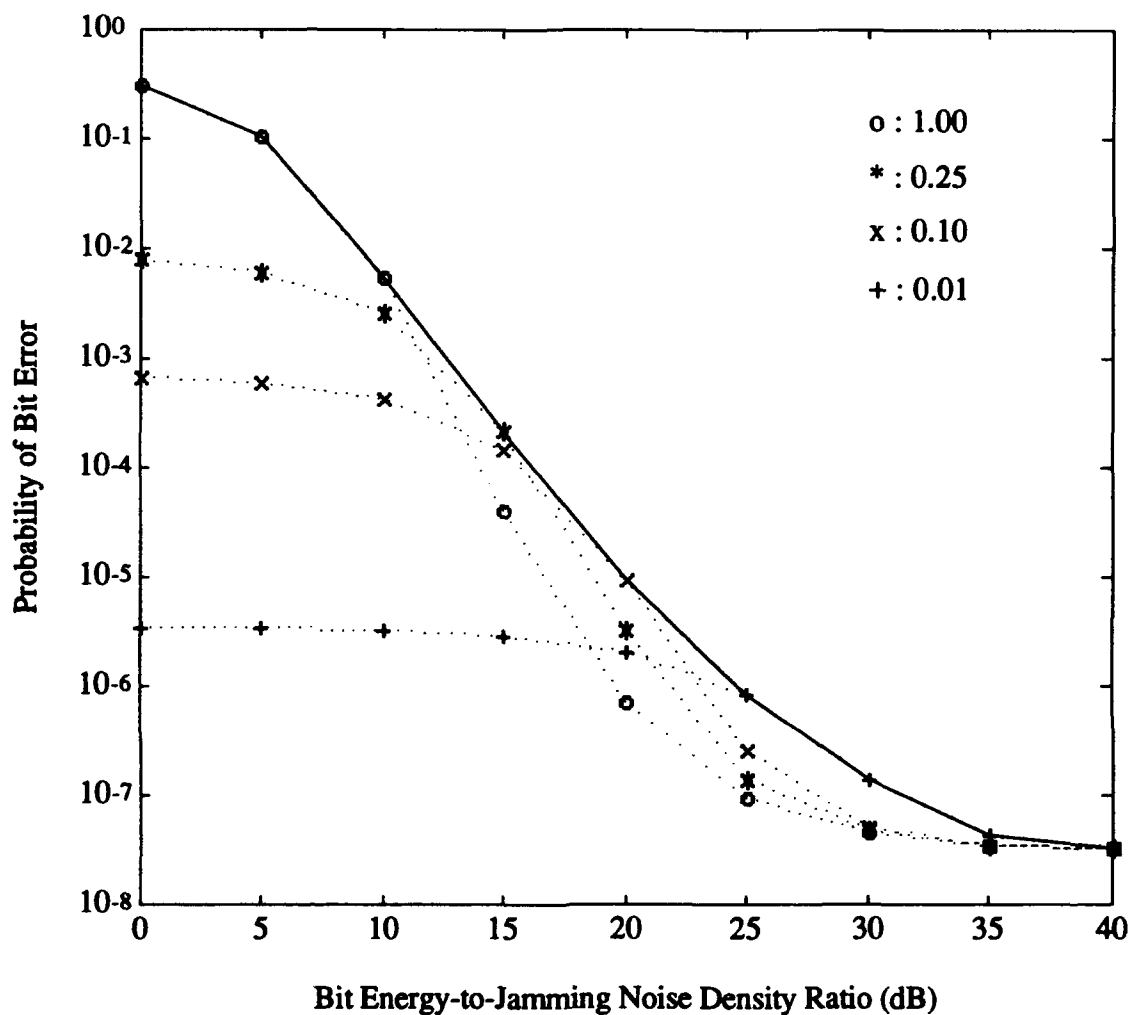Figure 37. Worst case receiver performance comparison for a Ricean faded signal with M=4, L=2, E_b/N_0 =13.35 dB and direct-to-diffuse power ratio=100 with $\hat{\sigma}_k^2$ a random variable.

Figure 38. Worst case receiver performance comparison for a Ricean faded signal with M=4, L=3, E_b/N_0 =13.35 dB and direct-to-diffuse power ratio=100 with $\hat{\sigma}_k^2$ a random variable.

Figure 39. Worst case receiver performance comparison for a Ricean faded signal with M=4, L=4, E_b/N_0 =13.35 dB and direct-to-diffuse power ratio=100 with $\hat{\sigma}_k^2$ a random variable.
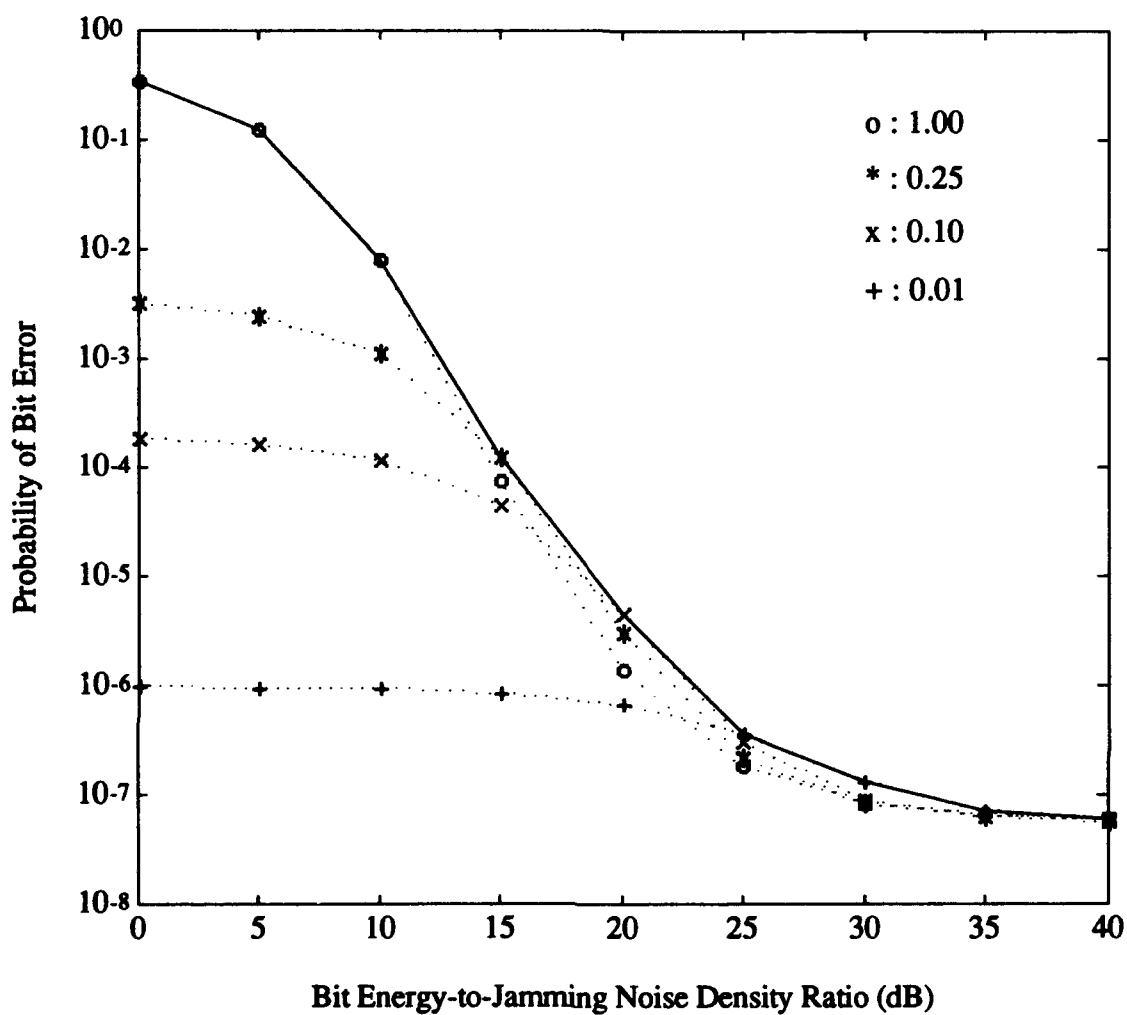
Figure 40. Receiver performance for a Ricean faded signal with M=4, L=2, $E_b/N_0 = 13.35$ dB and direct-to-diffuse power ratio=100 with $\gamma = 0.25$ and ±50% estimate error with $\hat{\sigma}_k^2$ a parameter. For comparison, the performance with $\hat{\sigma}_k^2$ modeled as a random variable is also shown (labeled "overall").
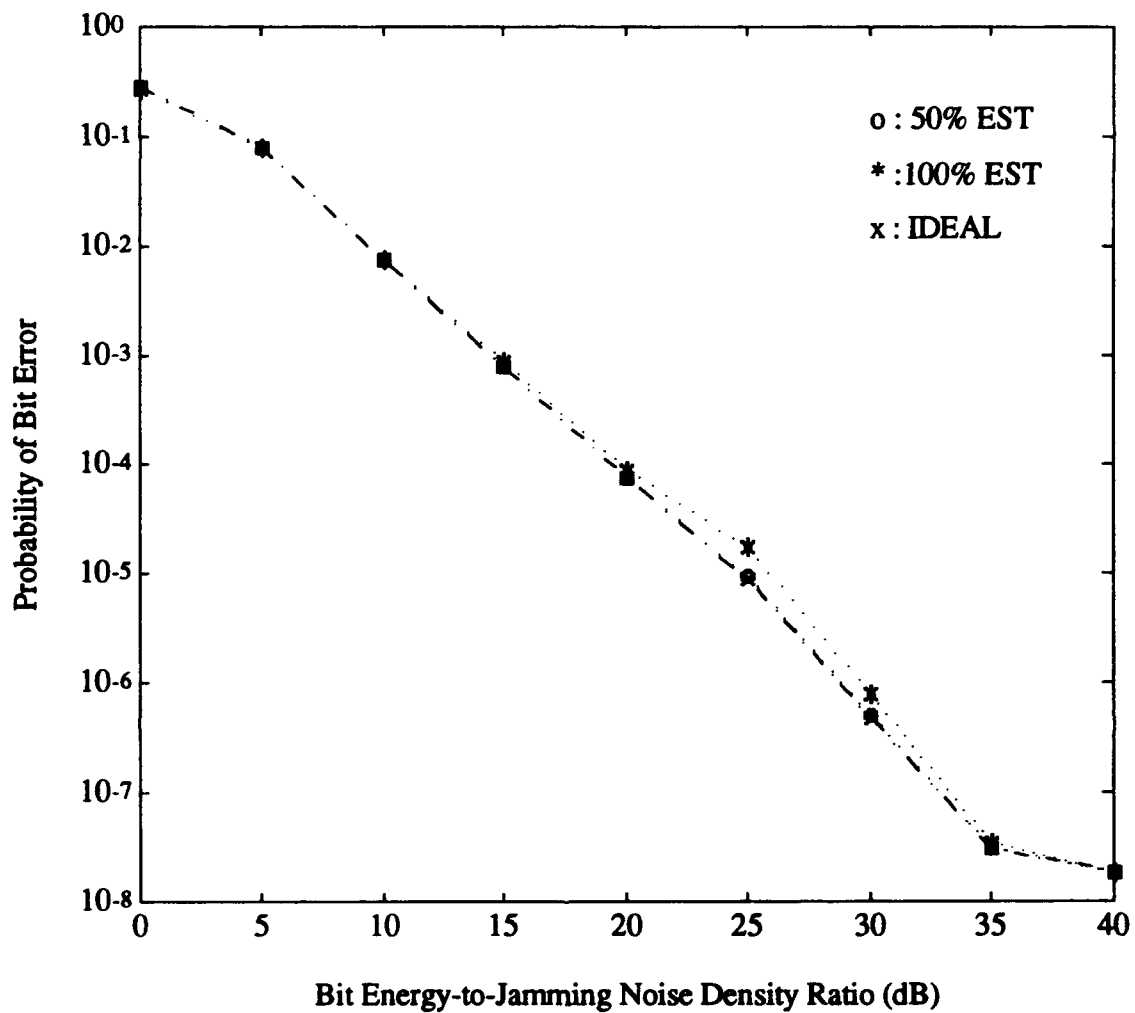
Figure 41. Receiver performance for a Ricean faded signal with M=4, L=3, $E_b/N_0 = 13.35$ dB and direct-to-diffuse power ratio=100 with $\gamma = 0.25$ and $\pm 50\%$ estimate error with $\hat{\sigma}_k^2$ a parameter. For comparison, the performance with $\hat{\sigma}_k^2$ modeled as a random variable is also shown (labeled "overall").
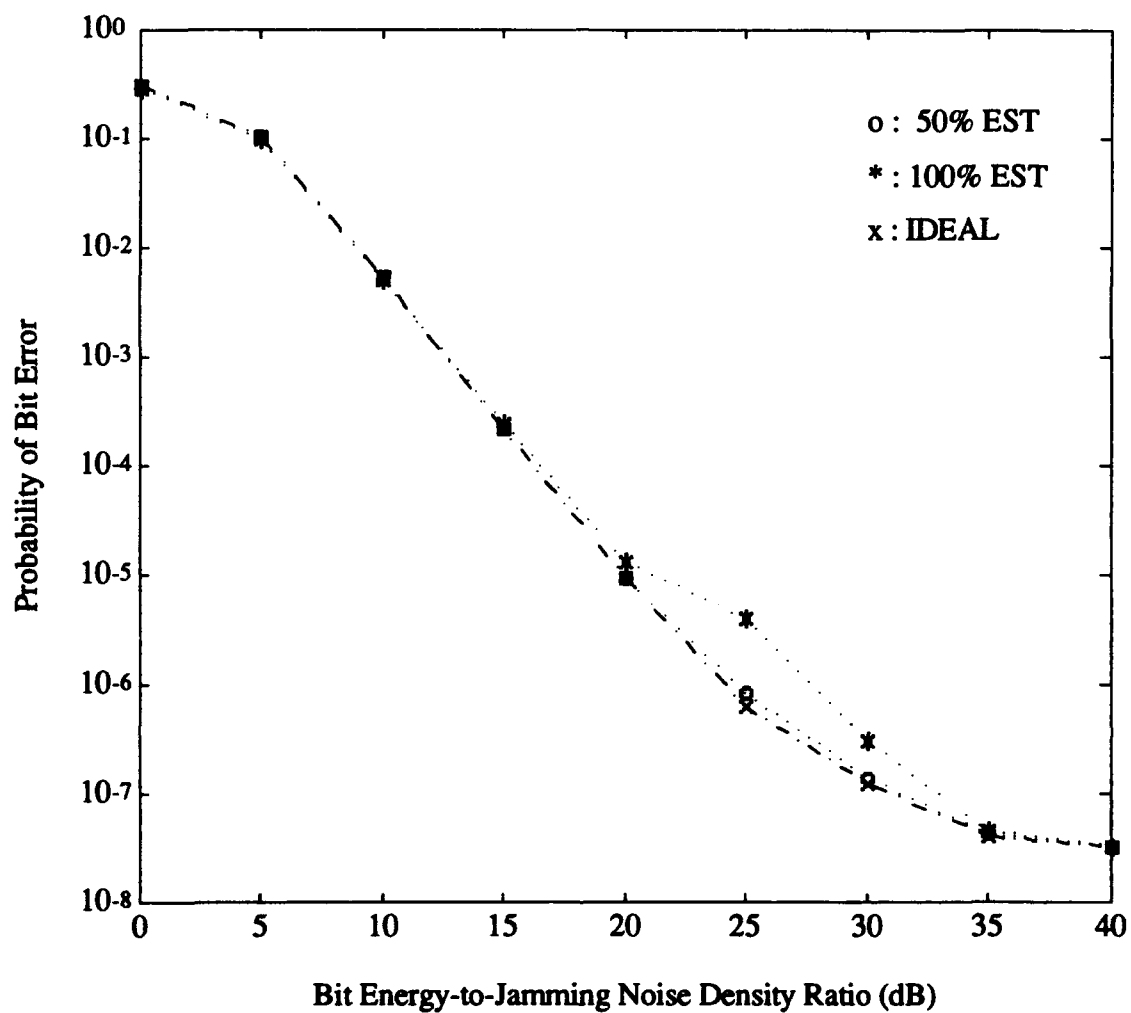
66

Figure 42. Receiver performance for a Ricean faded signal with M=4, L=4, $E_b/N_0 = 13.35$ dB and direct-to-diffuse power ratio=100 with $\gamma = 0.25$ and $\pm 50\%$ estimate error with $\hat{\sigma}_k^2$ a parameter. For comparison, the performance with $\hat{\sigma}_k^2$ modeled as a random variable is also shown (labeled "overall").
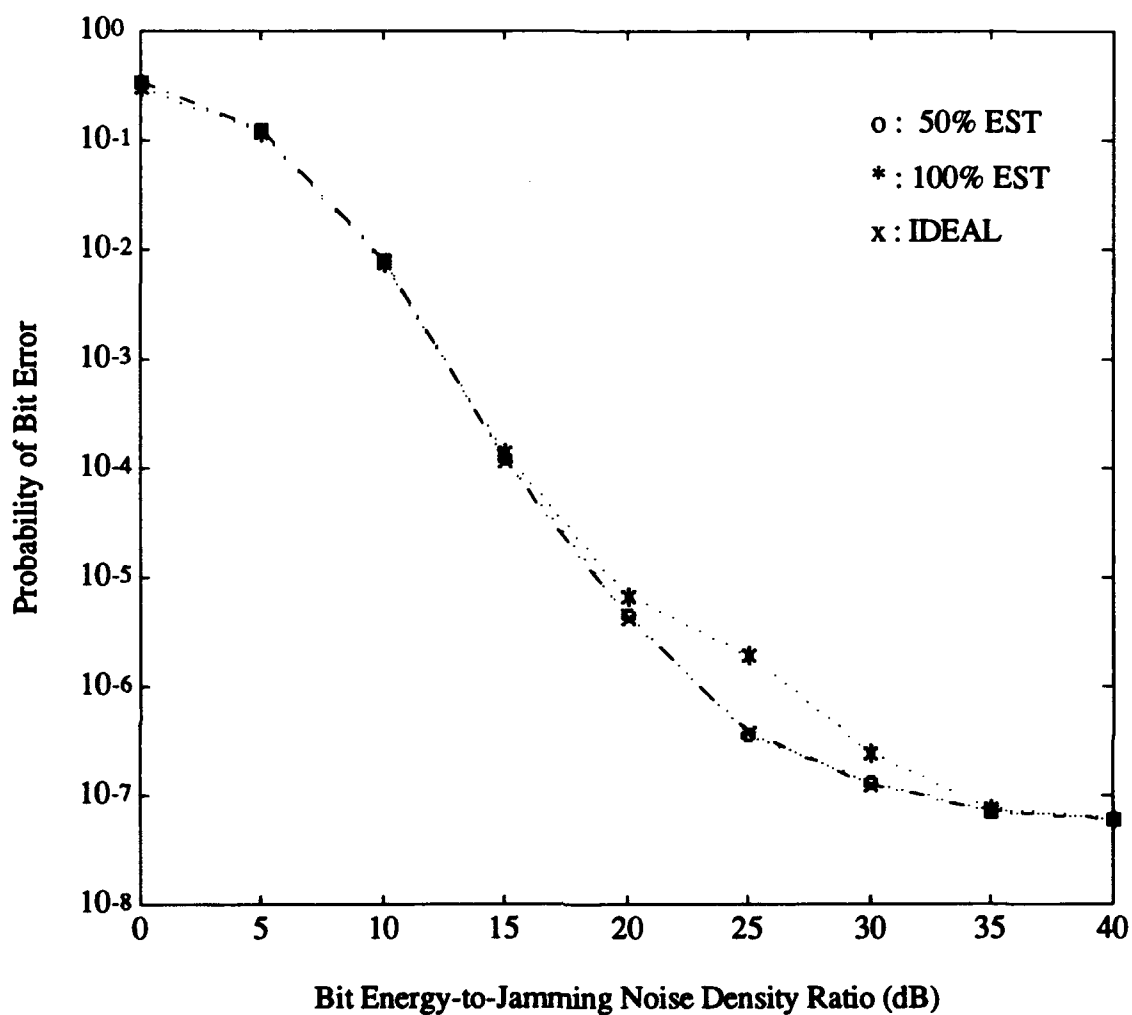
Figure 43. Receiver performance for a Ricean faded signal with M=4, L=3, E_b/N_0 =13.35 dB, direct-to-diffuse power ratio=1 and ±50% estimate error with $\hat{\sigma}_k^2$ a random variable.

68

Figure 44. Receiver performance for a Ricean faded signal with M=4, L=3, E_b/N_0 =13.35 dB, Direct-to-Diffuse power ratio=1 and ±100% estimate error with $\hat{\sigma}_k^2$ a random variable.

Figure 45. Worst case receiver performance comparison for a Ricean faded
signal with M=4, L=3, E_b/N_0 =13.35 dB and direct-to-diffuse
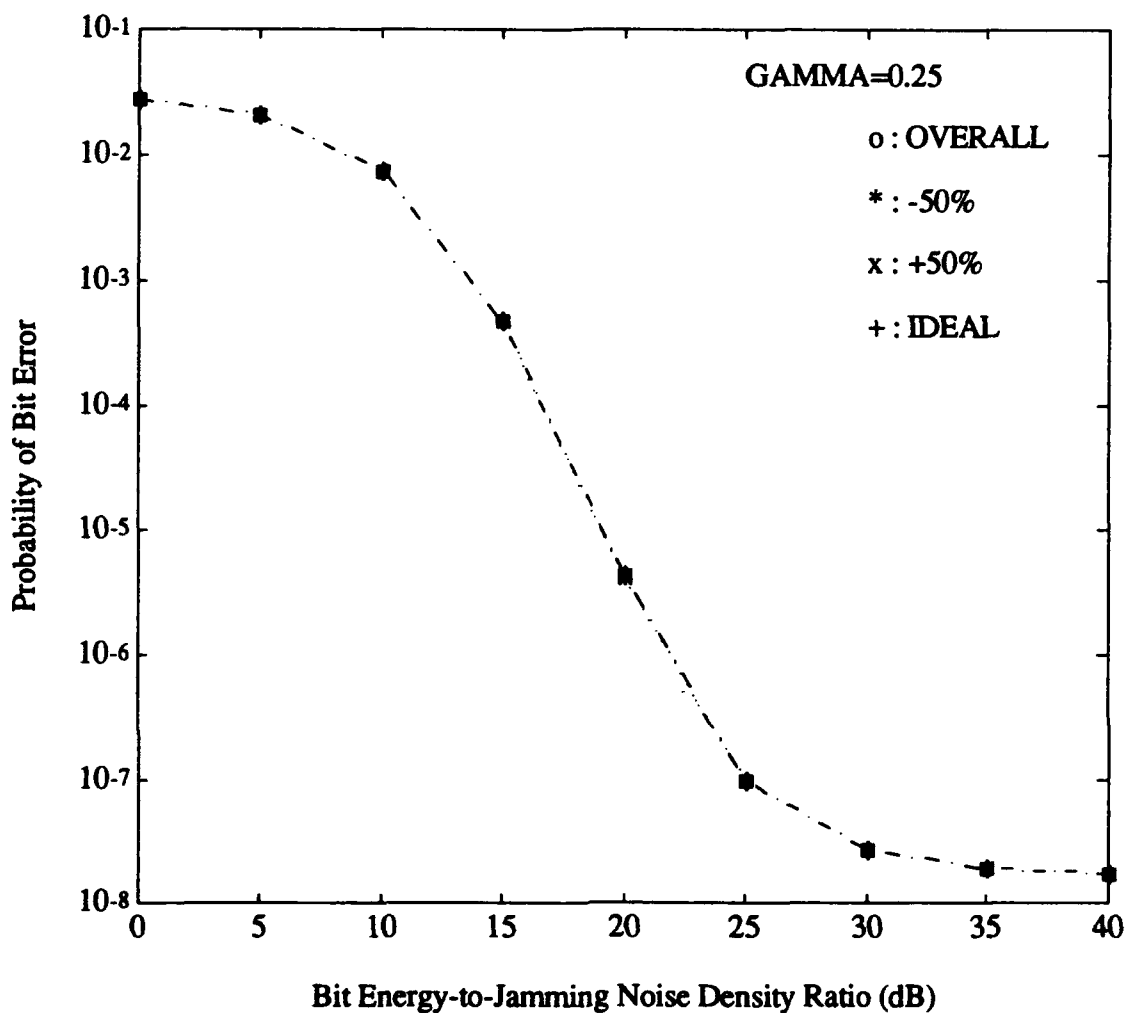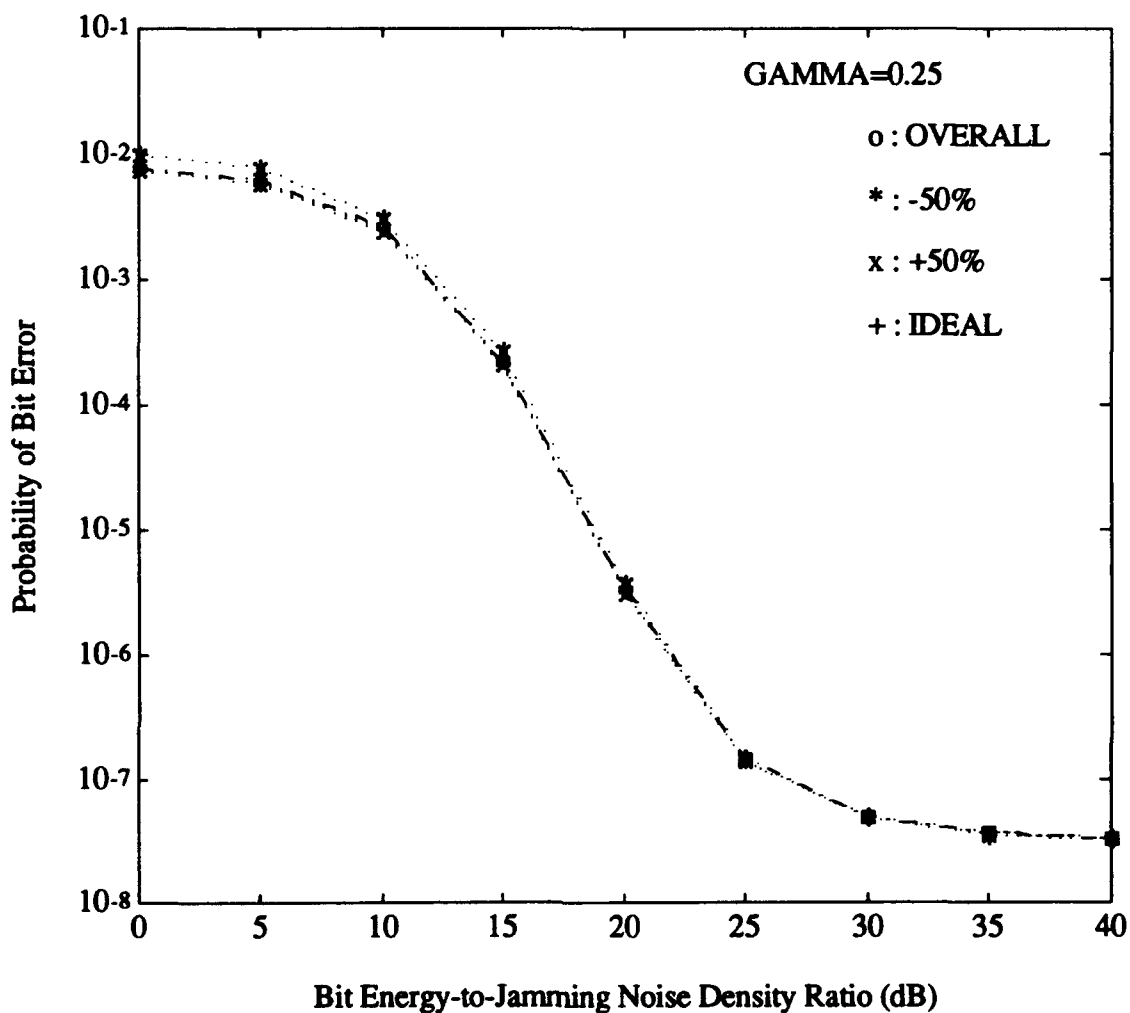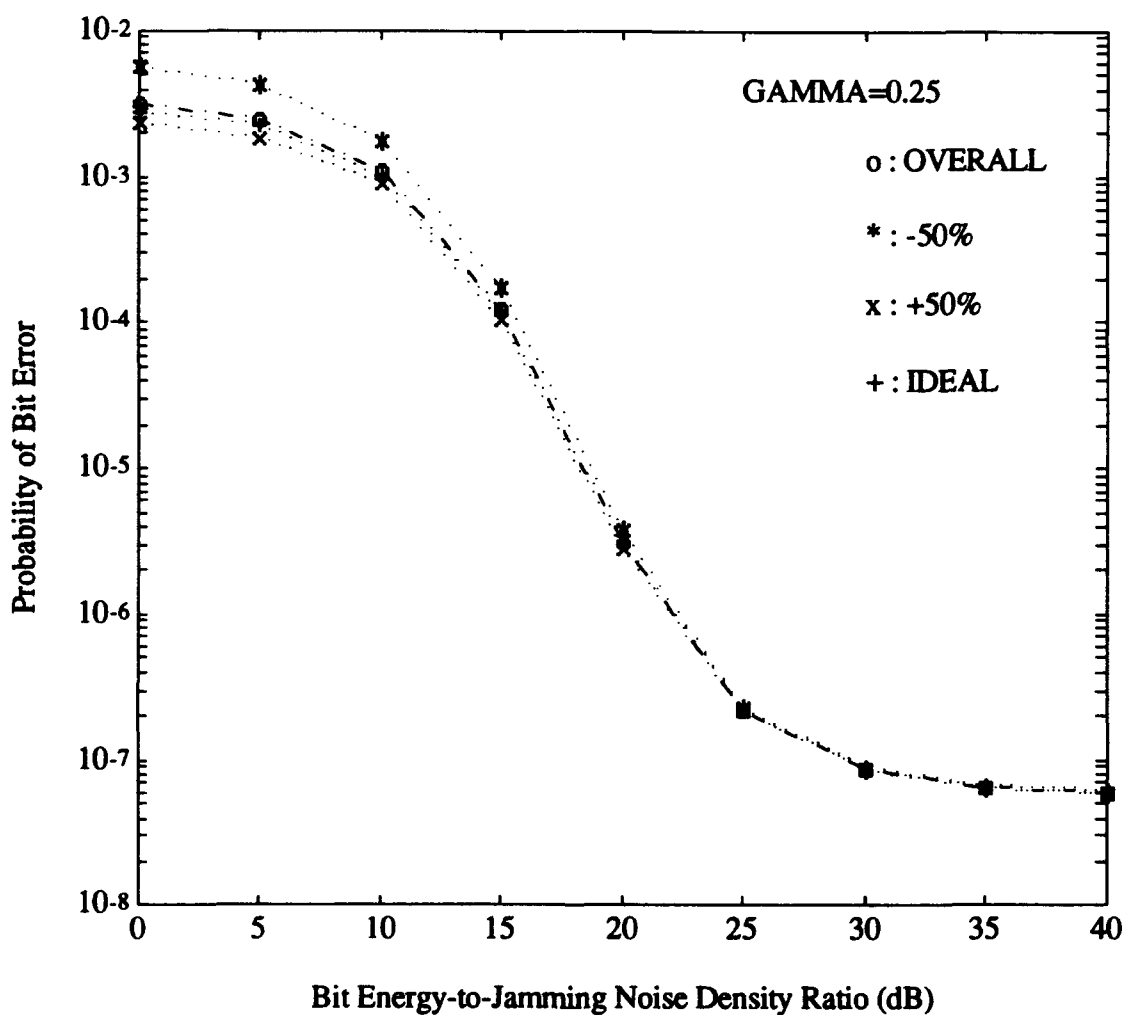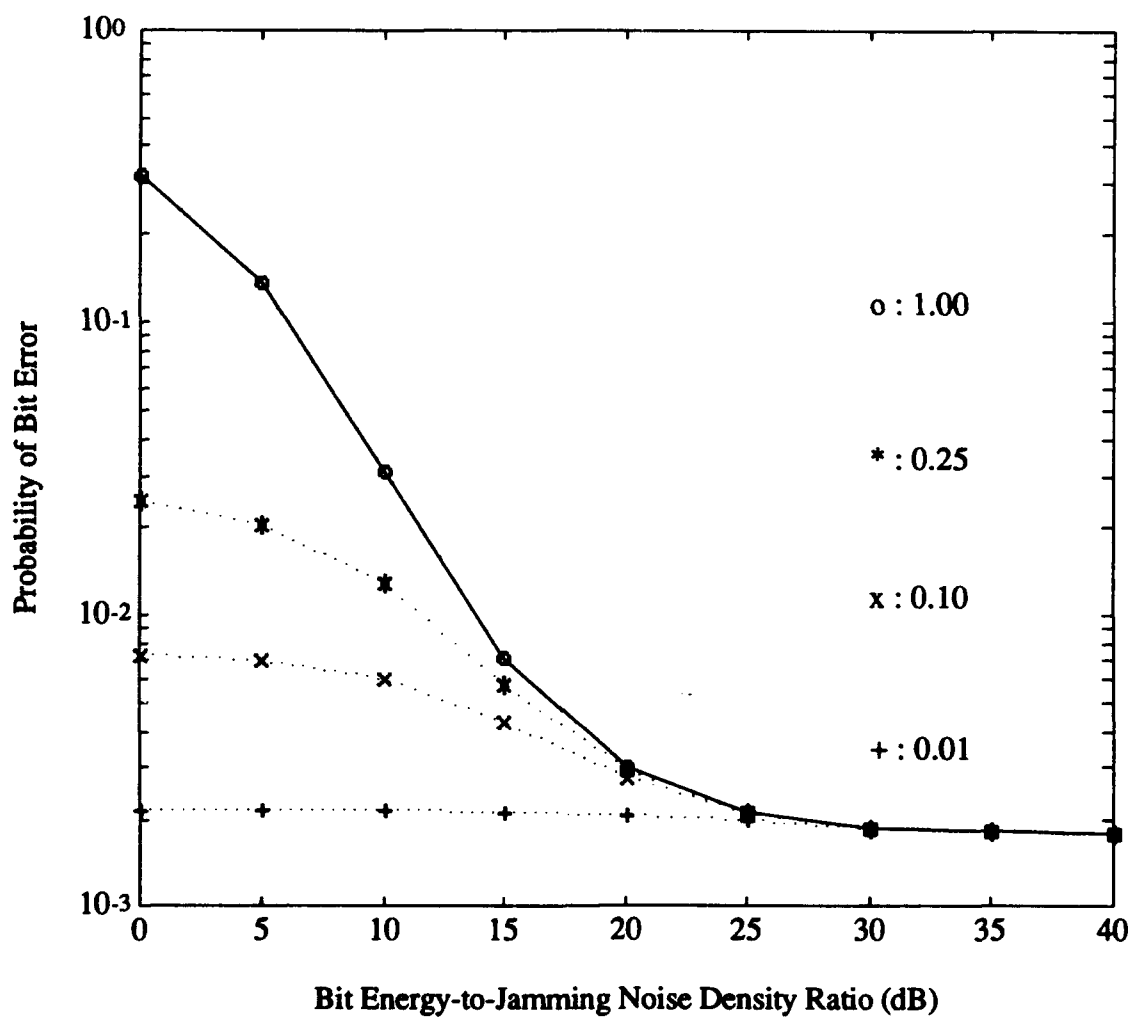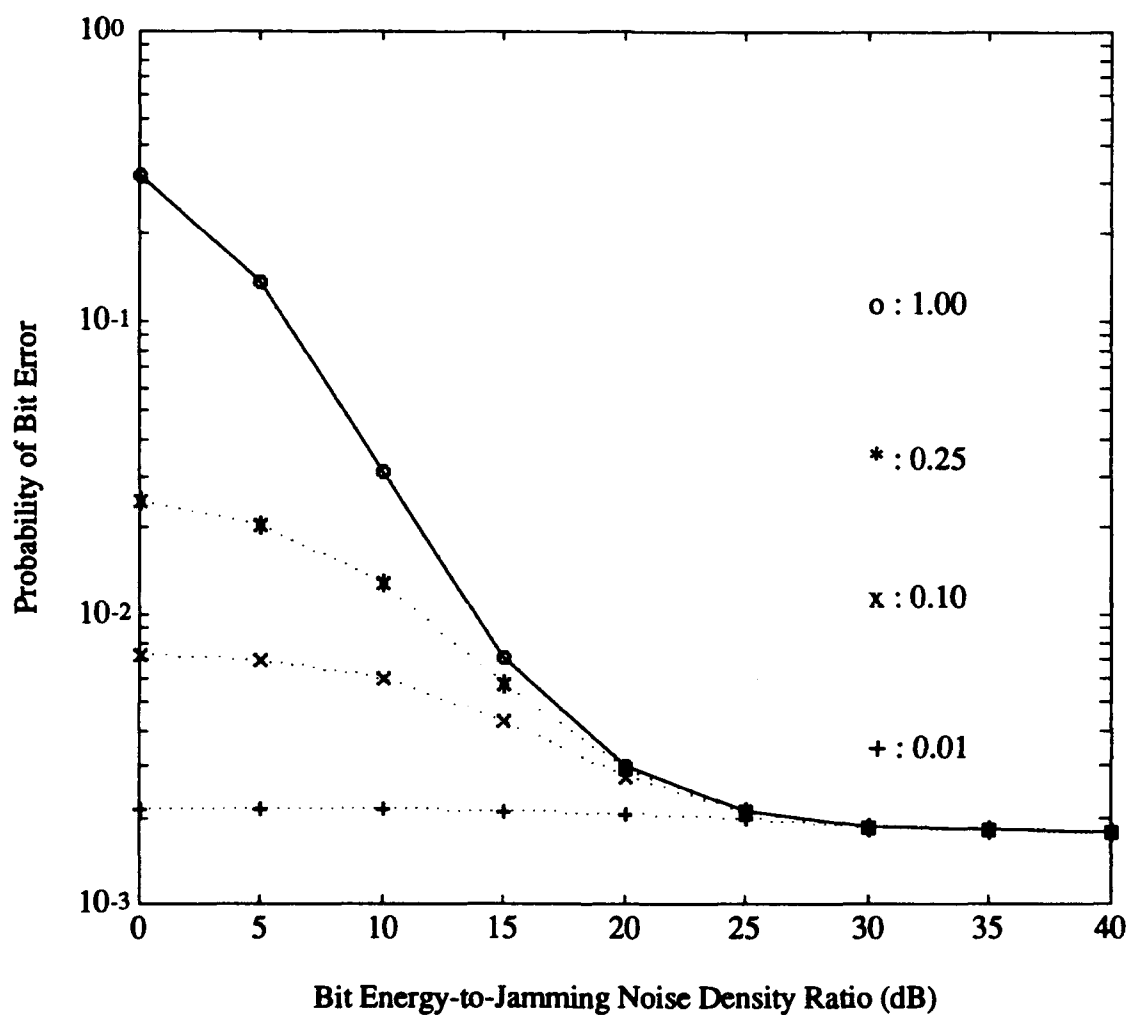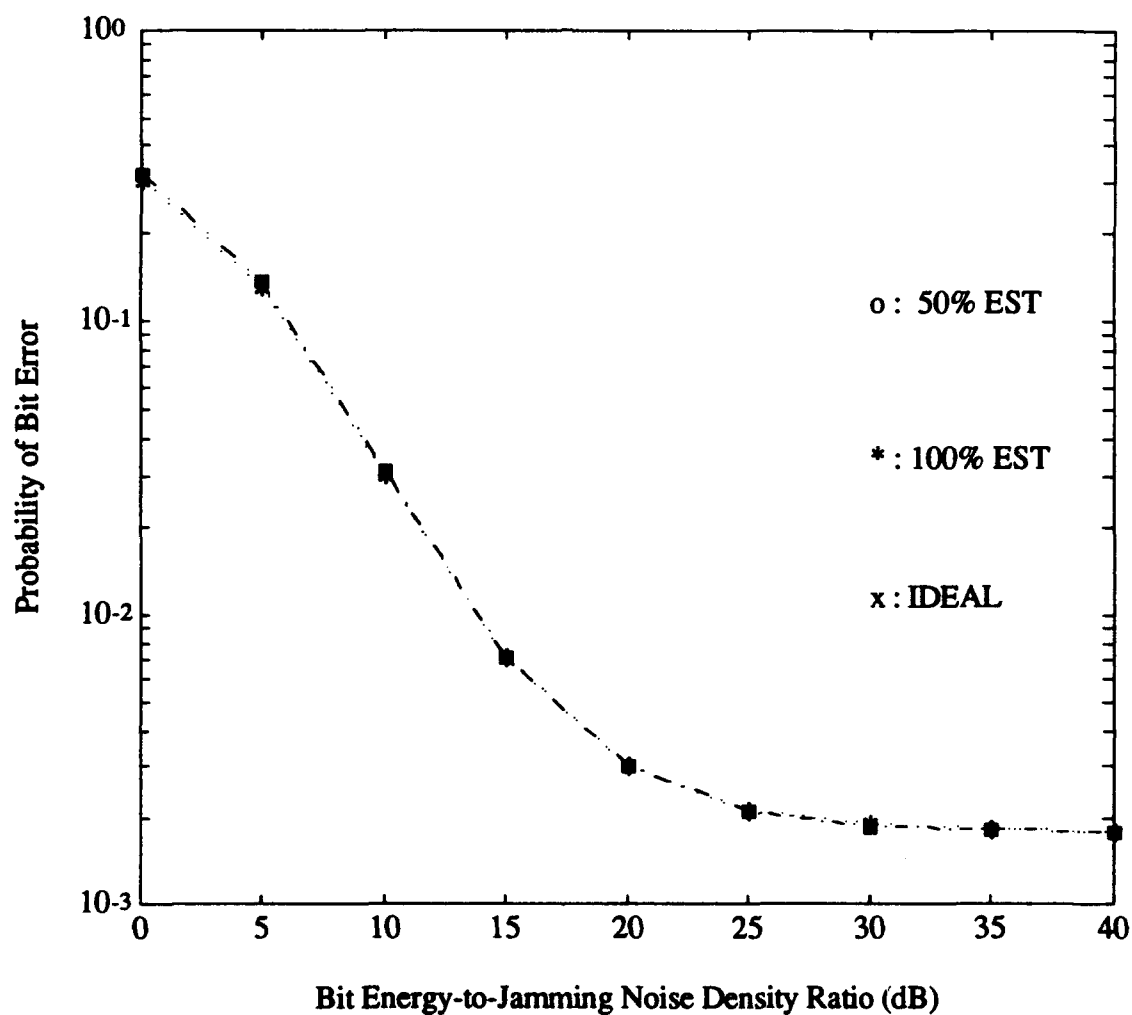power ratio=1 with $\hat{\sigma}_k^2$ a random variable.

V. CONCLUSIONS

Receiver performance for specific fractions of partial-band interference with non-ideal noise normalization having a $\pm 50\%$ error in the noise power estimator is virtually identical to the ideal noise normalization case. The degradation due to partial-band interference increases as the fraction of the spread bandwidth being jammed γ decreases. It is also found that this degradation disappears as diversity increases.

Non-ideal noise-normalized receiver performance for fixed fractions of partial-band interference shows that underestimation of the noise power degrades performance while overestimation gives better performance than for ideal (perfect) noise power estimation. The differences between ideal and non-ideal noise normalization are found for bit energy-to-interference noise density ratios less than about 20 dB when the fraction of partial-band interference is 0.25 and 35 dB when $\gamma = 0.01$. Generalizing, we see that receiver performance will only be affected by noise power estimation error when $E_b / \gamma N_t < 15 \text{dB}$. The performance curves for ideal and non-ideal noise-normalized receivers are identical above this particular bit energy-to-interference noise density ratio. This results is a consequence of the assumption that wideband noise can be measured with a high degree of accuracy.

Since noise normalization has no effect when either all hops are jammed or when all hops are free from interference, noise normalization error has an increasing effect as diversity increases. Even so, the difference between ideal performance and non-ideal noise normalization performance when the noise power estimate error is modeled as a random variable is not great. When the noise

71

power estimate error is taken to be a parameter, underestimation causes the worst performance degradation, but in general overall performance is not significantly different than that obtained with ideal noise normalization. Consequently, we conclude that the noise-normalized receiver is relatively insensitive to noise power measurement error. In this sense, the noise normalized receiver is very robust in a worst case partial-band jamming environment.

It is also found that the robustness of the receiver with regard to noise measurement error is independent of the strength of channel fading.

REFERENCES

[1] D. J. Torrieri, *Principles of Secure Communication Systems, 2nd ed.* Nowwood: Artech House, 1992.

[2] R. Clark Robertson and Tri T. Ha , "Error probabilities of fast frequency-hopped MFSK with noise-normalization combining in a fading channel with partial-band interference," *IEEE Trans. Commun.,* vol. 40, no. 2, pp. 404-412, Feb. 1992.

[3] A.J.Viterbi and I.M.Jacobs, "Advances in coding and modulation for noncoherent channels affected by fading, partial band, and multiple access interference," in *Advances in Communication Systems, Theory and Applications*, vol 4, A.J. Viterbi, Ed. New York :Academic press,1975.

[4] J.S. Lee, L.E. Miller, and Y.K. Kim, "Probability of error analysis of a BFSK frequency-hopping system with diversity under partial-band jar ning interference - part II: Performance of square-law nonlinear combinin$_5$ soft decision receivers," *IEEE Trans. Commun.,*vol . COM-32, pp. 1243-1250, Dec.1984.

[5] J.S. Lee, L.E. Miller, and R.H. French, "The analysis of uncoded performances for certain ECCM receiver design strategies for multi-hops/symbol FH/MFSK waveforms," *IEEE J.Select. Areas Commun.,*vol. SAC-3, pp. 611-620, Sept. 1985.

[6] C.M. Keller and M.B.Pursley, " Diversity combining for channels with fading and partial-band interference," *IEEE J.Select. Areas Commun.,*vol SAC-5, pp.248-260, Feb. 1987.

[7] J.G. Proakis, *Digital Communications,2nd ed.* New York: McGraw-Hill, 1989.

[8] C.M. Keller and M.B.Pursley, " Frequency spacing in MFSK frequency-hopped spread spectrum communications over selective fading channels," in *Proc.17th Conf. Inform. Sci.Syst.,* Johns Hopkins Univ., Baltimore, MD, pp.749-754, Mar. 1983.

[9] A.D. Whalen, *Detection of Signal in Noise,* New York: Academic,1971.

[10] M. Abramowitz and I.A. Stegun, *Handbook of Mathematical Functions,* New York: Dover, 1972.

[11] I.S. Gradshteyn and I.M.Ryzhik, *Table of Integrals, Series and Products, Corrected and Enlarged ed.*, translated and edited by Alan Jeffrey, New York: Academic Press, 1980.

[12] W.C. Lindsey, "Error probabilities for Rician fading multichannel reception of binary and N-ary signals," *IEEE Trans. Infom. Theory*, vol. IT-10, pp. 339-350, Oct. 1964.

[13] R.S.Simon, M.T. Stroot, and G.H. Weiss, "Numerical inversion of Laplace transforms with application to percentage labeled mitoses experiments," *Comput. Biomed. Res.*, vol. 5. pp. 596-607, 1972.

INITIAL DISTRIBUTION LIST

No. Copies

1. Defense Technical Information Center   2
   Cameron Station
   Alexandria, Virginia 22314-6145

2. Library, Code 52   2
   Naval Postgraduate School
   Monterey, California 93943

3. Chairman, Code EC   1
   Department of Electrical and Computer Engineering
   Naval Postgraduate School
   Monterey, California 93943

4. Chairman, Code EW   1
   Electronic Warfare Academic Group
   Naval Postgraduate School
   Monterey, California 93943

5. Professor R. Clark Robertson, Code EC/Rc   3
   Department of Electrical and Computer Engineering
   Naval Postgraduate School
   Monterey, California 93943

6. Professor Donald v. Z. Wadsworth, Code EC/Wd 1
   Department of Electrical and Computer Engineering
   Naval Postgraduate School
   Monterey, California 93943

7. Hidetoshi Iwasaki   3
   c/o Takeda 3-3-4 Nakajujo Kita-ku
   Tokyo, Japan 114